

COMPLEXES FROM COMPLEXES: FINITE ELEMENT COMPLEXES IN THREE DIMENSIONS

LONG CHEN AND XUEHAI HUANG

ABSTRACT. In the field of solving partial differential equations (PDEs), Hilbert complexes have become highly significant. Recent advances focus on creating new complexes using the Bernstein-Gelfand-Gelfand (BGG) framework, as shown by Arnold and Hu [Complexes from complexes. *Found. Comput. Math.*, 2021]. This paper extends their approach to three-dimensional finite element complexes. The finite element Hessian, elasticity, and divdiv complexes are systematically derived by applying techniques such as smooth finite element de Rham complexes, the t - n decomposition, and trace complexes, along with related two-dimensional finite element analogs. Notably, the construction includes two reduction operations to address continuity differences in the BGG diagram, ultimately resulting in a comprehensive and effective framework for constructing finite element complexes, which have various applications in PDE solving.

1. INTRODUCTION

Hilbert complexes are essential in developing robust numerical methods for solving partial differential equations (PDEs) [7, 8, 3, 16]. Arnold and Hu [9] have recently introduced a systematic methodology for creating new complexes by applying the Bernstein-Gelfand-Gelfand (BGG) framework to well-known differential complexes, including the de Rham complex. In this study, we focus on systematically constructing finite element complexes in a three-dimensional setting using the BGG approach.

Let Ω be a domain in \mathbb{R}^3 . The de Rham complex reads as

$$(1) \quad \mathbb{R} \hookrightarrow H^1(\Omega) \xrightarrow{\text{grad}} H(\text{curl}, \Omega) \xrightarrow{\text{curl}} H(\text{div}, \Omega) \xrightarrow{\text{div}} L^2(\Omega) \rightarrow 0,$$

where Sobolev spaces

$$\begin{aligned} H^1(\Omega) &:= \{\phi \in L^2(\Omega) : \text{grad } \phi \in L^2(\Omega; \mathbb{R}^3)\}, \\ H(\text{curl}, \Omega) &:= \{\mathbf{u} \in L^2(\Omega; \mathbb{R}^3) : \text{curl } \mathbf{u} \in L^2(\Omega; \mathbb{R}^3)\}, \\ H(\text{div}, \Omega) &:= \{\mathbf{u} \in L^2(\Omega; \mathbb{R}^3) : \text{div } \mathbf{u} \in L^2(\Omega)\}. \end{aligned}$$

By stacking copies of de Rham complexes to form a BGG diagram, several complexes can be derived from the BGG framework [9], including, but not limited to, the Hessian complex, the elasticity complex, and the divdiv complex. Both the Hessian complex and the divdiv complex are applied in solving the biharmonic equation [25, 15, 44] and the Einstein-Bianchi equation [47]. The space $H^{-1}(\text{div div}, \Omega; \mathbb{S})$ in the divdiv complex can also be used to address elasticity problems [45] and the Reissner-Mindlin plate model [46]. The space $H(\text{div}, \Omega; \mathbb{S})$ in the elasticity complex is crucial for modeling stress in elasticity

2020 *Mathematics Subject Classification.* 65N30; 58J10; 65N12;

The first author was supported by NSF DMS-2012465 and DMS-2309785.

The second author is the corresponding author. The second author was supported by the National Natural Science Foundation of China (Grant No. 12171300) and the Natural Science Foundation of Shanghai (Grant No. 21ZR1480500).

problems [40, 5]. The incompatibility operator inc in the elasticity complex has applications in intrinsic elasticity [29], dislocation theory [49], elastoplasticity [1], and relativity [26, 42]. However, this paper does not present numerical methods for specific partial differential equations. Instead, it focuses on developing a framework for constructing finite element complexes, which may have applications in the areas mentioned above.

Recently, there have been significant developments in the construction of finite element Hessian complexes, elasticity complexes, and divdiv complexes. These constructions have typically been approached on a case-by-case basis in previous works [17, 21, 19, 27, 33, 34, 35, 37]. Our objective is to extend the application of the BGG construction to finite element complexes, thereby unifying these previously scattered results and systematically generating new ones. This has been achieved in our recent work [22], which focused on two-dimensional cases.

However, the transition to three dimensions introduces additional complexities. One significant challenge is the construction of finite element de Rham complexes with varying degrees of smoothness in three dimensions. We have successfully tackled this issue in our recent work [23], which we will briefly summarize below.

We firstly recall the smooth finite elements constructed in [36] by Hu, Lin and Wu. Given an integer vector $\mathbf{r} = (r^v, r^e, r^f)^\top$ with $r^v \geq 2r^e \geq 4r^f \geq 0$ and polynomial degree $k \geq 2r^v + 1$, one can construct a decomposition of the simplicial lattice and design finite elements with C^{r^v} smoothness at vertices, C^{r^e} smoothness on edges, and C^{r^f} smoothness across faces. Therefore the finite element space is H^{r^f+1} -conforming. Such approach can be generalized to arbitrary dimension; see [36] or [23, Appendix A]. It unifies the scattered results [13, 50, 2] in two dimensions (including the well known C^1 Argyris element), [51, 55, 41] in three dimensions, and [56] in four dimensions. Notice that the finite element spaces constructed in [52, 53, 54] are H^m non-conforming while this paper focus on conforming discretization.

The requirement $r^v \geq 2r^e \geq 4r^f \geq 0$ can be relaxed. We call \mathbf{r} a smoothness vector if $r^f \geq -1$, $r^e \geq \max\{2r^f, -1\}$, and $r^v \geq \max\{2r^e, -1\}$. Here -1 means no continuity and thus a lower bound $\mathbf{r} \geq -1$ is imposed. To reflect such requirement, for a smoothness vector \mathbf{r} , define $\mathbf{r} \ominus 1 := \max\{\mathbf{r} - 1, -1\}$. Again through the utilization of a simplicial lattice decomposition, we are enabled to construct scalar finite element space $\mathbb{V}_k^{\text{grad}}(\mathbf{r})$ which is C^{r^f} conforming with $r^f \geq 0$, and space $\mathbb{V}_k^{L^2}(\mathbf{r})$ which admits $r^f = -1$.

Let $\mathbf{r}_0 \geq 0$, $\mathbf{r}_1 = \mathbf{r}_0 - 1$, $\mathbf{r}_2 \geq \mathbf{r}_1 \ominus 1$, $\mathbf{r}_3 \geq \mathbf{r}_2 \ominus 1$. Introduce spaces

$$\begin{aligned} \mathbb{V}_{k+1}^{\text{curl}}(\mathbf{r}_1, \mathbf{r}_2) &:= \{\mathbf{v} \in \mathbb{V}_{k+1}^3(\mathbf{r}_1) \cap H(\text{curl}, \Omega) : \text{curl } \mathbf{v} \in \mathbb{V}_k^{\text{div}}(\mathbf{r}_2)\}, \\ \mathbb{V}_k^{\text{div}}(\mathbf{r}_2, \mathbf{r}_3) &:= \{\mathbf{v} \in \mathbb{V}_k^3(\mathbf{r}_2) \cap H(\text{div}, \Omega) : \text{div } \mathbf{v} \in \mathbb{V}_{k-1}^{L^2}(\mathbf{r}_3)\}. \end{aligned}$$

Assume $(\mathbf{r}_2, \mathbf{r}_3, k)$ is div stable, i.e., $\text{div } \mathbb{V}_k^{\text{div}}(\mathbf{r}_2, \mathbf{r}_3) = \mathbb{V}_{k-1}^{L^2}(\mathbf{r}_3)$, and $k \geq \max\{2r_1^v + 1, 2r_2^v + 1, 2r_3^v + 2, 1\}$. In [23], we construct the finite element de Rham complex as follows:

$$(2) \quad \mathbb{R} \xrightarrow{\subset} \mathbb{V}_{k+2}^{\text{grad}}(\mathbf{r}_0) \xrightarrow{\text{grad}} \mathbb{V}_{k+1}^{\text{curl}}(\mathbf{r}_1, \mathbf{r}_2) \xrightarrow{\text{curl}} \mathbb{V}_k^{\text{div}}(\mathbf{r}_2, \mathbf{r}_3) \xrightarrow{\text{div}} \mathbb{V}_{k-1}^{L^2}(\mathbf{r}_3) \rightarrow 0.$$

And we give finite element descriptions for spaces $\mathbb{V}_{k+1}^{\text{curl}}(\mathbf{r}_1, \mathbf{r}_2)$ and $\mathbb{V}_k^{\text{div}}(\mathbf{r}_2, \mathbf{r}_3)$ in (2). When $r_2^f \geq 0$, (2) transforms into a finite element Stokes complex, given that the space $\mathbb{V}_k^{\text{div}}(\mathbf{r}_2, \mathbf{r}_3) \subset H^1(\Omega; \mathbb{R}^3)$. This enables the discretization of Stokes equation.

The major challenge of extending BGG to the finite element complexes emerges from the mis-match in the continuity of Sobolev spaces, specifically $H^1(\Omega)$, $H(\text{curl}, \Omega)$, and

$H(\text{div}, \Omega)$. This discrepancy can be explained using the following diagram:

$$\begin{array}{ccccccc}
 H^1(\Omega; \mathbb{R}^3) & \xrightarrow{\text{grad}} & H(\text{curl}, \Omega; \mathbb{M}) & \xrightarrow{\text{curl}} & H(\text{div}, \Omega; \mathbb{M}) & \xrightarrow{\text{div}} & L^2(\Omega; \mathbb{R}^3) \rightarrow \mathbf{0} \\
 & \nearrow \iota & & \nearrow \text{mskw} & & \nearrow \text{id} & \\
 H^1(\Omega) & \xrightarrow{\text{grad}} & H(\text{curl}, \Omega) & \xrightarrow{\text{curl}} & H(\text{div}, \Omega) & \xrightarrow{\text{div}} & L^2(\Omega) \rightarrow 0.
 \end{array}$$

- The mapping $\iota : H^1(\Omega) \rightarrow H(\text{curl}, \Omega; \mathbb{M})$, where $\mathbb{M} = \mathbb{R}^{3 \times 3}$ and $\iota v = v\mathbf{I} \in \mathbb{M}$, is well-defined. However, its right inverse $\text{tr} : H(\text{curl}, \Omega; \mathbb{M}) \rightarrow H^1(\Omega)$ is not, as functions in $H(\text{curl}, \Omega)$ possess only the tangential continuity.
- The inclusion $\text{mskw} H(\text{curl}, \Omega) \subset H(\text{div}, \Omega; \mathbb{M})$ is justifiable (refer to Section 2.1), yet its right inverse $\text{vskw} : H(\text{div}, \Omega; \mathbb{M}) \rightarrow H(\text{curl}, \Omega)$ is not attainable.
- The obvious inclusion $H(\text{div}, \Omega) \subset L^2(\Omega, \mathbb{R}^3)$ is not surjective.

In the work of Arnold and Hu [9], the domain Sobolev spaces $H(\text{d}, \Omega)$, where $\text{d} = \text{curl}$ or div , are substituted with H^s Sobolev spaces having matching indices s , as depicted in diagram (4). For finite element spaces that solely conform to $H(\text{curl}, \Omega)$ or $H(\text{div}, \Omega)$, the challenge posed by the mis-match in tangential or normal continuity serves as the primary obstacle to extending the BGG framework to the discrete context.

Our approach involves identifying sub-complexes within the finite element de Rham complex (2) by imposing appropriate subspace restrictions. The $\tilde{\cdot}$ and $\hat{\cdot}$ operations applied to a short exact sequence are thoroughly discussed in Section 2.2. By applying these two reduction operations to suitable smooth finite element de Rham complexes, we are able to construct the finite element Hessian complex, the finite element elasticity complex, and the finite element divdiv complex using the BGG framework. Additionally, we propose an augmentation operation to further extend the constructed complexes to a broader set of smoothness vectors.

However, deriving finite element descriptions for these subspaces, which involve element-wise degrees of freedom (DoFs), presents a more intricate challenge and requires significant effort. We will provide DoFs for these tensor finite element spaces using three key methodologies:

- (1) Smooth finite element de Rham complexes. As previously mentioned and discussed in detail in [23], these complexes offer a fundamental basis for the construction.
- (2) The t - n decomposition approach. Introduced in [24], this approach plays a critical role in the construction of $H(\text{div})$ -conforming elements.
- (3) Trace complexes and two-dimensional (2D) finite element complexes. We employ two trace complexes on each face and draw insights from 2D finite element complexes [22] to guide the construction of DoFs on edges.

The remainder of this paper is structured as follows. We commence with a comprehensive presentation of the BGG framework and the two reduction operations in Section 2, which serves as foundational background. In Section 3, we revisit the smooth finite element de Rham complexes, providing a comprehensive review. Subsequently, Section 4 delves into the construction of face finite elements. The BGG construction of finite element Hessian complexes, elasticity complexes, and divdiv complexes is expounded upon in Section 5. Moving forward, Section 6 focuses on the construction of edge elements. Various bubble polynomial complexes are developed in Appendix A. A visual depiction of the organization can be found in Fig. 1, which provides a clear overview of the various sections.

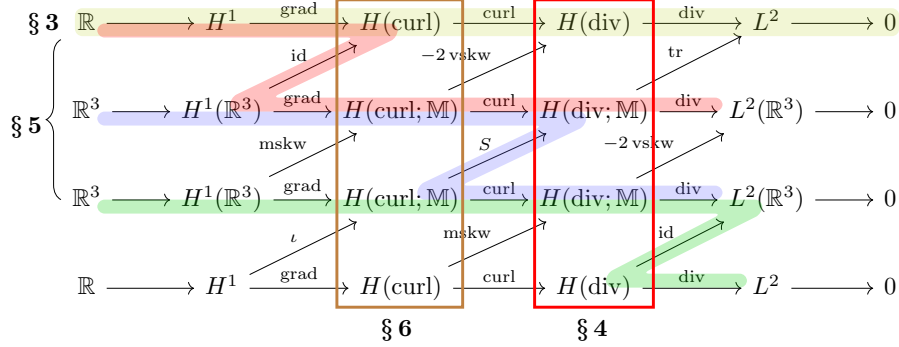


FIGURE 1. Organization of Sections 3 - 6.

2. PRELIMINARY

In this section, we will briefly review the framework developed in [9] for deriving complexes using the Bernstein-Gelfand-Gelfand (BGG) construction [11]. Earlier contributions to this area can be found in works such as [30, 10, 6]. Additionally, we introduce two reduction operations and one augmentation operation applied to a short exact sequence, which effectively broaden the applicability of the BGG framework.

Throughout this paper, we assume that Ω is topologically trivial, ensuring that the de Rham complex (1) is exact. As a result, all derived complexes based on de Rham complexes are also exact [9]. For simplicity, we omit Ω in the notation for spaces. For instance, $H^s = H^s(\Omega)$ represents the standard Sobolev space with real index s .

2.1. Notation. We define the dot product and cross product from the left, denoted as $\mathbf{b} \cdot \mathbf{A}$ and $\mathbf{b} \times \mathbf{A}$, respectively. These operations are applied column-wise to the matrix \mathbf{A} . Conversely, when the vector appears on the right of the matrix, i.e., $\mathbf{A} \cdot \mathbf{b}$ and $\mathbf{A} \times \mathbf{b}$, the operations are defined row-wise. The order of performing row and column products is interchangeable, resulting in the associative rule for triple products:

$$\mathbf{b} \times \mathbf{A} \times \mathbf{c} := (\mathbf{b} \times \mathbf{A}) \times \mathbf{c} = \mathbf{b} \times (\mathbf{A} \times \mathbf{c}).$$

Similar rules apply for $\mathbf{b} \cdot \mathbf{A} \cdot \mathbf{c}$ and $\mathbf{b} \cdot \mathbf{A} \times \mathbf{c}$, allowing parentheses to be omitted.

We treat the Hamilton operator $\nabla = (\partial_1, \partial_2, \partial_3)^\top$ as a column vector. For a scalar function u , $\nabla u = \text{grad } u$ represents the gradient of u . For a vector function $\mathbf{u} = (u_1, u_2, u_3)^\top$, $\text{curl } \mathbf{u} = \nabla \times \mathbf{u}$ and $\text{div } \mathbf{u} = \nabla \cdot \mathbf{u}$ are the standard differential operations. Define $\nabla \mathbf{u} = \nabla \mathbf{u}^\top = (\partial_i u_j)$, which can be understood as the dyadic product of the Hamilton operator ∇ and the column vector \mathbf{u} .

By applying matrix-vector operations to the Hamilton operator ∇ , we obtain column-wise differentiations $\nabla \cdot \mathbf{A}$, $\nabla \times \mathbf{A}$, and row-wise differentiations $\mathbf{A} \cdot \nabla$, $\mathbf{A} \times \nabla$. We introduce the following double differential operators:

$$\text{inc } \mathbf{A} := \nabla \times \mathbf{A} \times \nabla, \quad \text{div div } \mathbf{A} := \nabla \cdot \mathbf{A} \cdot \nabla.$$

In the literature, differential operators for matrices are typically applied row-wise to tensors. To distinguish this from the ∇ notation, we define the operators using letters:

$$\begin{aligned}\text{grad } \mathbf{u} &:= \mathbf{u} \nabla^\top = (\partial_j u_i) = (\nabla \mathbf{u})^\top, \\ \text{curl } \mathbf{A} &:= -\mathbf{A} \times \nabla = (\nabla \times \mathbf{A}^\top)^\top, \\ \text{div } \mathbf{A} &:= \mathbf{A} \cdot \nabla = (\nabla \cdot \mathbf{A}^\top)^\top.\end{aligned}$$

For a given plane F with a normal vector \mathbf{n} , we define the projection matrix and its rotation as

$$\Pi_F := \mathbf{I} - \mathbf{n} \mathbf{n}^\top, \quad \Pi_F^\perp := \mathbf{n} \times \Pi_F.$$

We then introduce the following definitions:

$$\nabla_F := \Pi_F \nabla, \quad \nabla_F^\perp := \Pi_F^\perp \nabla.$$

For a scalar function v , we have:

$$\begin{aligned}\text{grad } {}_F v &= \nabla_F v = \Pi_F (\nabla v) = -\mathbf{n} \times (\mathbf{n} \times \nabla v), \\ \text{curl } {}_F v &= \nabla_F^\perp v = \mathbf{n} \times \nabla v = \mathbf{n} \times \nabla_F v,\end{aligned}$$

where $\text{grad } {}_F v$ is the surface gradient of v , and $\text{curl } {}_F v$ is the surface curl.

For a vector function \mathbf{v} , the surface divergence is defined as:

$$\text{div}_F \mathbf{v} := \nabla_F \cdot \mathbf{v} = \nabla_F \cdot (\Pi_F \mathbf{v}).$$

Additionally, the surface rot operator is defined as:

$$\text{rot}_F \mathbf{v} := \nabla_F^\perp \cdot \mathbf{v} = (\mathbf{n} \times \nabla) \cdot \mathbf{v} = \mathbf{n} \cdot (\nabla \times \mathbf{v}),$$

which represents the normal component of $\nabla \times \mathbf{v}$.

We denote by \mathbb{M} the space of 3×3 matrices, \mathbb{S} the subspace of symmetric matrices, \mathbb{T} the subspace of traceless matrices, and \mathbb{K} the subspace of skew-symmetric matrices. A matrix τ can be decomposed into $\tau = \text{sym } \tau + \text{skw } \tau$ with the symmetric part $\text{sym } \tau := (\tau + \tau^\top)/2$ and the skew-symmetric part $\text{skw } \tau := (\tau - \tau^\top)/2$.

We will use Iverson bracket $[\cdot]$ [39], which extends the Kronecker delta function to a statement P

$$[P] = \begin{cases} 1 & \text{if } P \text{ is true,} \\ 0 & \text{otherwise.} \end{cases}$$

2.2. BGG Construction. We follow [9] to briefly review the BGG construction. A bounded Hilbert complex is a sequence of Hilbert spaces connected by a sequence of linear bounded operators satisfying the property: the composition of two consecutive operators vanishes. Assume we have two bounded Hilbert complexes $(\mathcal{V}_\bullet \otimes \mathbb{E}_\bullet, d_\bullet)$, $(\mathcal{V}_\bullet \otimes \tilde{\mathbb{E}}_\bullet, \tilde{d}_\bullet)$ and bounded linking maps $S_i = \text{id} \otimes s_i : \mathcal{V}_{i+1} \otimes \tilde{\mathbb{E}}_i \rightarrow \mathcal{V}_{i+1} \otimes \mathbb{E}_{i+1}$ for $i = 0, \dots, n-1$

$$(3) \quad \begin{array}{ccccccc} 0 & \longrightarrow & \mathcal{V}_0 \otimes \mathbb{E}_0 & \xrightarrow{d_0} & \mathcal{V}_1 \otimes \mathbb{E}_1 & \xrightarrow{d_1} & \cdots & \xrightarrow{d_J} & \cdots & \xrightarrow{d_{n-1}} & \mathcal{V}_n \otimes \mathbb{E}_n & \longrightarrow & 0 \\ & & & & \nearrow S_0 & & \nearrow S_1 & & \nearrow S_J & & \nearrow S_{n-1} & & \\ 0 & \longrightarrow & \mathcal{V}_1 \otimes \tilde{\mathbb{E}}_0 & \xrightarrow{\tilde{d}_0} & \mathcal{V}_2 \otimes \tilde{\mathbb{E}}_1 & \xrightarrow{\tilde{d}_1} & \cdots & \xrightarrow{\tilde{d}_J} & \cdots & \xrightarrow{\tilde{d}_{n-1}} & \mathcal{V}_{n+1} \otimes \tilde{\mathbb{E}}_n & \longrightarrow & 0, \end{array}$$

in which $s_i : \tilde{\mathbb{E}}_i \rightarrow \mathbb{E}_{i+1}$ is a linear operator between finite-dimensional spaces. The operators in (3) satisfy anti-commutativity: $S_{i+1} \tilde{d}_i = -d_{i+1} S_i$, and J -injectivity/surjectivity

condition: for some particular J with $0 \leq J < n$, s_i is injective for $i = 0, \dots, J$ and is surjective for $i = J, \dots, n-1$. The output complex is

$$0 \rightarrow \mathcal{Y}_0 \xrightarrow{\mathcal{D}_0} \mathcal{Y}_1 \xrightarrow{\mathcal{D}_1} \dots \xrightarrow{\mathcal{D}_{J-1}} \mathcal{Y}_J \xrightarrow{\mathcal{D}_J} \mathcal{Y}_{J+1} \xrightarrow{\mathcal{D}_{J+1}} \dots \xrightarrow{\mathcal{D}_{n-1}} \mathcal{Y}_n \rightarrow 0,$$

where \mathcal{Y}_i is $\mathcal{V}_i \otimes (\mathbb{E}_i / \text{img}(s_{i-1}))$ for $i = 0, \dots, J$ and $\mathcal{V}_{i+1} \otimes \ker(s_i)$ for $i = J+1, \dots, n$, \mathcal{D}_i is the projection of d_i onto \mathcal{Y}_{i+1} for $i = 0, \dots, J-1$, \tilde{d}_i for $i = J+1, \dots, n-1$ and $\tilde{d}_J(S_J)^{-1}d_J$ for $i = J$. By the BGG framework, many new complexes can be generated from old ones.

The following example is presented in [9]. In three dimensions, we stack copies of de Rham complexes to form the diagram

$$(4) \quad \begin{array}{ccccccc} \mathbb{R} & \longrightarrow & H^s & \xrightarrow{\text{grad}} & H^{s-1}(\mathbb{R}^3) & \xrightarrow{\text{curl}} & H^{s-2}(\mathbb{R}^3) & \xrightarrow{\text{div}} & H^{s-3} & \longrightarrow & 0 \\ & & \text{id} & \nearrow & -2 \text{ vskw} & \nearrow & \text{tr} & \nearrow & & & \\ \mathbb{R}^3 & \longrightarrow & H^{s-1}(\mathbb{R}^3) & \xrightarrow{\text{grad}} & H^{s-2}(\mathbb{M}) & \xrightarrow{\text{curl}} & H^{s-3}(\mathbb{M}) & \xrightarrow{\text{div}} & H^{s-4}(\mathbb{R}^3) & \longrightarrow & \mathbf{0} \\ & & \text{mskw} & \nearrow & S & \nearrow & -2 \text{ vskw} & \nearrow & & & \\ \mathbb{R}^3 & \longrightarrow & H^{s-2}(\mathbb{R}^3) & \xrightarrow{\text{grad}} & H^{s-3}(\mathbb{M}) & \xrightarrow{\text{curl}} & H^{s-4}(\mathbb{M}) & \xrightarrow{\text{div}} & H^{s-5}(\mathbb{R}^3) & \longrightarrow & \mathbf{0} \\ & & \iota & \nearrow & \text{mskw} & \nearrow & \text{id} & \nearrow & & & \\ \mathbb{R} & \longrightarrow & H^{s-3} & \xrightarrow{\text{grad}} & H^{s-4}(\mathbb{R}^3) & \xrightarrow{\text{curl}} & H^{s-5}(\mathbb{R}^3) & \xrightarrow{\text{div}} & H^{s-6} & \longrightarrow & 0, \end{array}$$

where $H^s(\mathbb{X}) = H^s \otimes \mathbb{X}$ for $\mathbb{X} = \mathbb{R}^3$ or \mathbb{M} , and operators

$$S\tau = \tau^\top - \text{tr}(\tau)\mathbf{I}, \quad \iota : \mathbb{R} \rightarrow \mathbb{M}, \quad \iota v = v\mathbf{I},$$

$$\text{mskw } \boldsymbol{\omega} := \begin{pmatrix} 0 & -\omega_3 & \omega_2 \\ \omega_3 & 0 & -\omega_1 \\ -\omega_2 & \omega_1 & 0 \end{pmatrix}, \quad \text{vskw} := \text{mskw}^{-1} \circ \text{skw}.$$

Considering operators in the \nearrow direction, the three operators in the diagonal are one-to-one, the lower triangular part is injective, and the upper triangular part is surjective. By direct calculation, the parallelogram formed by the north-east diagonal \nearrow and the horizontal operators is anticommutative.

Then applying the BGG construction, several complexes can be derived from the BGG framework including but not limited to the Hessian complex, the elasticity complex, and the divdiv complex; see the three zigzag paths in Fig. 1.

Recent efforts have led to the individual construction of finite element Hessian complexes, elasticity complexes, and divdiv complexes, as demonstrated in works such as [17, 21, 19, 27, 33, 34, 35, 37]. However, these constructions have been carried out on a case-by-case basis, raising the question: Can the overarching BGG framework be employed to establish a unified foundation for these diverse constructions?

Applying the BGG methodology to finite element complexes is a challenging task. A significant difficulty lies in constructing finite element de Rham complexes with different degrees of smoothness. We have successfully addressed this challenge, as detailed in [23], and will revisit the specific techniques in Section 3.

Another intricate difficulty that arises from the diagram (4) becomes evident when we shift from the Sobolev space H^s to the domain spaces $H(\text{grad})$, $H(\text{curl})$, or $H(\text{div})$

within the diagram:

$$(5) \quad \begin{array}{ccccccccc} \mathbb{R} & \longrightarrow & H^1 & \xrightarrow{\text{grad}} & H(\text{curl}) & \xrightarrow{\text{curl}} & H(\text{div}) & \xrightarrow{\text{div}} & L^2 & \longrightarrow & 0 \\ & & & \text{id} \nearrow & & \text{-2 vskw} \nearrow & & \text{tr} \nearrow & & & \\ \mathbb{R}^3 & \longrightarrow & H^1(\mathbb{R}^3) & \xrightarrow{\text{grad}} & H(\text{curl}; \mathbb{M}) & \xrightarrow{\text{curl}} & H(\text{div}; \mathbb{M}) & \xrightarrow{\text{div}} & L^2(\mathbb{R}^3) & \longrightarrow & \mathbf{0} \\ & & & \text{mskw} \nearrow & & S \nearrow & & \text{-2 vskw} \nearrow & & & \\ \mathbb{R}^3 & \longrightarrow & H^1(\mathbb{R}^3) & \xrightarrow{\text{grad}} & H(\text{curl}; \mathbb{M}) & \xrightarrow{\text{curl}} & H(\text{div}; \mathbb{M}) & \xrightarrow{\text{div}} & L^2(\mathbb{R}^3) & \longrightarrow & \mathbf{0} \\ & & & \iota \nearrow & & \text{mskw} \nearrow & & \text{id} \nearrow & & & \\ \mathbb{R} & \longrightarrow & H^1 & \xrightarrow{\text{grad}} & H(\text{curl}) & \xrightarrow{\text{curl}} & H(\text{div}) & \xrightarrow{\text{div}} & L^2 & \longrightarrow & 0, \end{array}$$

where $H(\text{curl}; \mathbb{M}) = \mathbb{R}^3 \otimes H(\text{curl})$ and $H(\text{div}; \mathbb{M}) = \mathbb{R}^3 \otimes H(\text{div})$. The Hamilton operator ∇ can be employed to represent the differential operators: $\text{grad} = \nabla$, $\text{curl} = \nabla \times$, and $\text{div} = \nabla \cdot$. Symbolically, by substituting ∇ with the outward unit normal vector \mathbf{n} , these operations maintain their respective anticommutative properties. For example,

$$(6) \quad \begin{aligned} (2 \text{ vskw } \boldsymbol{\tau}) \cdot \mathbf{n} &= -\text{tr}(\boldsymbol{\tau} \times \mathbf{n}), \\ (S\boldsymbol{\tau})\mathbf{n} &= -2 \text{ vskw}(\boldsymbol{\tau} \times \mathbf{n}). \end{aligned}$$

Therefore, the operators in the \nearrow direction retain their well-defined nature. To illustrate, consider the operator $S : H(\text{curl}; \mathbb{M}) \rightarrow H(\text{div}; \mathbb{M})$, $S\boldsymbol{\tau} = \boldsymbol{\tau}^\top - \text{tr}(\boldsymbol{\tau})\mathbf{I}$, positioned at the center of (5). Through the utilization of integration by parts and identity (6), it becomes evident that in the distributional sense,

$$\langle \text{div } S\boldsymbol{\tau}, \boldsymbol{\phi} \rangle = (2 \text{ vskw } \text{curl } \boldsymbol{\tau}, \boldsymbol{\phi}), \quad \boldsymbol{\phi} \in C_0^\infty(\Omega; \mathbb{R}^3).$$

Given that $\boldsymbol{\tau} \in H(\text{curl}; \mathbb{M})$, leading to $\text{curl } \boldsymbol{\tau} \in L^2(\mathbb{M})$, we can conclude that $S\boldsymbol{\tau} \in H(\text{div}; \mathbb{M})$.

Nonetheless, the converse direction, i.e., the \swarrow direction, is not well-defined due to inherent continuity mismatches. For instance, all three operators along the diagonal of diagram (5) are clearly not one-to-one, which prevents a straightforward application of the BGG procedure.

In cases where finite element spaces possess sufficient smoothness, the framework corresponds to diagram (4). However, for certain finite element spaces, the situation is better represented by (5) rather than (4). The smoothness discrepancy is the main barrier to extending the BGG construction into the discrete setting. To overcome this issue, we introduce two reduction operations for an exact sequence.

2.3. Two reduction operations. Let $V_i, i = 0, 1, 2$ be Hilbert spaces forming an exact sequence:

$$(7) \quad \ker(d_0) \xrightarrow{c} V_0 \xrightarrow{d_0} V_1 \xrightarrow{d_1} V_2 \rightarrow 0.$$

The exactness implies $\ker(d_1) = \text{img}(d_0)$ and $d_1 V_1 = V_2$. When they are finite-dimensional, the following dimension identity holds:

$$(8) \quad \dim \ker(d_0) - \dim V_0 + \dim V_1 - \dim V_2 = 0.$$

Introduce a subspace $\tilde{V}_2 \subseteq V_2$, and define \tilde{V}_1 as the preimage of \tilde{V}_2 , namely,

$$\tilde{V}_1 = \{v \in V_1 : d_1 v \in \tilde{V}_2\} \subseteq V_1.$$

Since $d_1 d_0 = 0$, the exact sequence remains intact through this construction:

$$(9) \quad \ker(d_0) \xrightarrow{\subset} V_0 \xrightarrow{d_0} \tilde{V}_1 \xrightarrow{d_1} \tilde{V}_2 \rightarrow 0.$$

We shall refer to the process of transitioning from (7) to (9) as a \sim (tilde) operation.

Suppose we have two additional operators, d_2 acting on V_0 and s^* acting on V_1 respectively. In application s^* in the \swarrow direction is the adjoint operator of s used in the BGG diagram. Consider a subspace W contained in $s^*(V_1)$. Define two subspaces in V_0 and V_1 :

$$(10) \quad \widehat{V}_0 = \{u \in V_0 : d_2 u \in W\}, \quad \widehat{V}_1 = \{v \in V_1 : s^* v \in W\}.$$

Assume we have the following triangular commutative diagram

$$(11) \quad \begin{array}{ccc} \widehat{V}_0 & \xrightarrow{d_0} & \widehat{V}_1 \\ d_2 \downarrow & \swarrow s^* & \\ & & W \end{array}.$$

That is $s^* d_0 = d_2$.

Lemma 2.1. *Assume we have the exact sequence (7) and triangular commutative diagram (11), where \widehat{V}_0 and \widehat{V}_1 are defined by (10). Assume $\ker(d_0) \subset \widehat{V}_0$ and $d_1(\widehat{V}_1) = V_2$. Then*

$$(12) \quad \ker(d_0) \xrightarrow{\subset} \widehat{V}_0 \xrightarrow{d_0} \widehat{V}_1 \xrightarrow{d_1} V_2 \rightarrow 0$$

is also an exact sequence.

Proof. As $s^* d_0 = d_2$, $d_0 \widehat{V}_0 \subseteq \widehat{V}_1$ and thus (12) is indeed a complex. To show its exactness, we only have to demonstrate that $\ker(d_1) \cap \widehat{V}_1 = d_0 \widehat{V}_0$. Taking a $\widehat{v} \in \widehat{V}_1$ and $d_1 \widehat{v} = 0$, by the exactness of (7), there exists a $u \in V_0$ s.t. $d_0 u = \widehat{v}$. Recall that $d_2 = s^* d_0$. So $d_2 u = s^* d_0 u = s^* \widehat{v} \in W$, i.e., $u \in \widehat{V}_0$. \square

When $V_i, i = 0, 1, 2$, are finite dimensional, the condition $d_1(\widehat{V}_1) = V_2$ can be verified by dimension count.

Lemma 2.2. *Assume we have the exact sequence (7) with finite-dimensional spaces and triangular commutative diagram (11), where \widehat{V}_0 and \widehat{V}_1 are defined by (10). Assume $W \subseteq s^*(V_1)$ and $\ker(d_0) \subset \widehat{V}_0$. Additionally assume that the equation $\dim V_0 - \dim \widehat{V}_0 = \dim V_1 - \dim \widehat{V}_1$, equivalently $\dim d_2 V_0 - \dim d_2 \widehat{V}_0 = \dim s^* V_1 - \dim s^* \widehat{V}_1$, holds. Then complex (12) is an exact sequence.*

Proof. By the proof of Lemma 2.1, (12) is a complex and $\ker(d_1) \cap \widehat{V}_1 = d_0 \widehat{V}_0$.

For the second part, it is evident that $d_1(\widehat{V}_1) \subseteq V_2$. To prove $d_1(\widehat{V}_1) = V_2$, we count the dimensions:

$$\begin{aligned} \dim d_1(\widehat{V}_1) &= \dim \widehat{V}_1 - \dim d_0(\widehat{V}_0) = \dim \widehat{V}_1 - \dim \widehat{V}_0 + \dim \ker(d_0) \\ &= \dim V_1 - \dim V_0 + \dim \ker(d_0) = \dim V_2, \end{aligned}$$

where in the last step, we have used the dimension identity (8). \square

The procedure described above, which transforms the sequence from (7) to the sequence presented in (12), is referred to as a $\widehat{}$ (hat) operation. This operation specifically modifies the domain and co-domain of the operator d_0 . By combining the hat and tilde operations, it becomes possible to create a further reduced exact sequence:

$$\ker(d_0) \xrightarrow{\subset} \widehat{V}_0 \xrightarrow{d_0} \widehat{\widehat{V}}_1 \xrightarrow{d_1} \widehat{\widehat{V}}_2 \rightarrow 0.$$

Throughout the process, the spaces \widehat{V} , \widetilde{V} , or $\widehat{\widehat{V}}$ can be renamed as needed, depending on the context and the spaces being constructed.

We further introduce an inverse hat operation to enlarge the spaces.

Lemma 2.3. *Assume we have a short exact sequence*

$$\ker(d_0) \xrightarrow{\subset} \widehat{V}_0 \xrightarrow{d_0} \widehat{V}_1 \xrightarrow{d_1} V_2 \rightarrow 0.$$

Let $V_0 \supseteq \widehat{V}_0$ and $V_1 \supseteq \widehat{V}_1$ satisfy

$$d_1 V_1 \subseteq V_2, \quad d_0 V_0 = V_1 \cap \ker(d_1).$$

Then we have the exact sequence

$$\ker(d_0) \xrightarrow{\subset} V_0 \xrightarrow{d_0} V_1 \xrightarrow{d_1} V_2 \rightarrow 0.$$

Proof. It suffices to prove $d_1 V_1 = V_2$ which is from the fact $d_1 \widehat{V}_1 = V_2$ and $V_1 \supseteq \widehat{V}_1$. \square

To illustrate these operations and their interplay, please refer to Fig. 2.

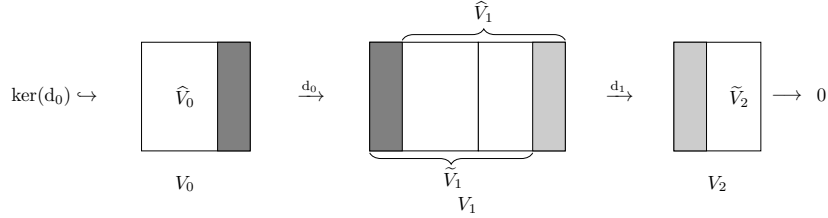


FIGURE 2. Two reduction operations. The $\widetilde{}$ operation reduces the space V_1 to \widetilde{V}_1 and V_2 to \widetilde{V}_2 by removing the sub-spaces marked by the light gray color. The $\widehat{}$ operation reduces the space V_0 to \widehat{V}_0 and V_1 to \widehat{V}_1 by removing the sub-spaces marked by the dark gray color. The inverse hat operation is adding these sub-spaces back.

2.4. Derived complexes. By diagram (4), the surjectivity $\text{tr } H(\text{div}; \mathbb{M}) = L^2$ follows from $\text{div } H^1(\mathbb{R}^3) = L^2$, and $-2 \text{ vskw } H(\text{curl}; \mathbb{M}) = H(\text{div})$ follows from the regular decomposition $H(\text{div}) = H^1(\mathbb{R}^3) + \text{curl } H^1(\mathbb{R}^3)$ [32]. Then applying the hat operation $\widehat{}$ to $V_0 = H^1$ and $V_1 = H(\text{curl})$ with $\widehat{V}_0 = H^2$, $\widehat{V}_1 = H^1(\mathbb{R}^3)$ and $W = H^1(\mathbb{R}^3)$, we obtain

$$(13) \quad \begin{array}{ccccccc} \mathbb{R} & \longrightarrow & H^2 & \xrightarrow{\text{grad}} & H^1(\mathbb{R}^3) & \xrightarrow{\text{curl}} & H(\text{div}) & \xrightarrow{\text{div}} & L^2 & \longrightarrow & 0 \\ & & \text{id} \nearrow & & \text{--}2 \text{ vskw} \nearrow & & \text{tr} \nearrow & & & & \\ \mathbb{R}^3 & \longrightarrow & H^1(\mathbb{R}^3) & \xrightarrow{\text{grad}} & H(\text{curl}; \mathbb{M}) & \xrightarrow{\text{curl}} & H(\text{div}; \mathbb{M}) & \xrightarrow{\text{div}} & L^2(\mathbb{R}^3) & \longrightarrow & \mathbf{0}, \end{array}$$

which leads to the Hessian complex [9, 44]

$$\mathbb{P}_1 \xrightarrow{\subset} H^2 \xrightarrow{\text{hess}} H(\text{curl}; \mathbb{S}) \xrightarrow{\text{curl}} H(\text{div}; \mathbb{T}) \xrightarrow{\text{div}} L^2(\mathbb{R}^3) \rightarrow \mathbf{0},$$

where $H(\text{curl}; \mathbb{S}) = H(\text{curl}; \mathbb{M}) \cap L^2(\mathbb{S})$ and $H(\text{div}; \mathbb{T}) = H(\text{div}; \mathbb{M}) \cap L^2(\mathbb{T})$.

Now we look at the second and third rows of diagram (5). We shall apply the two reductions to construct the BGG diagram

$$(14) \quad \begin{array}{ccccccc} \mathbb{R}^3 & \rightarrow & H^1(\text{curl}) & \xrightarrow{\text{grad}} & \widehat{H}(\text{curl}; \mathbb{M}) & \xrightarrow{\text{curl}} & \widetilde{H}(\text{div}; \mathbb{M}) & \xrightarrow{\text{div}} & L^2(\mathbb{R}^3) & \rightarrow & \mathbf{0} \\ & & \text{mskw} \nearrow & & & \nearrow S & & \nearrow -2 \text{vskw} & & & \\ \mathbb{R}^3 & \rightarrow & H^1(\mathbb{R}^3) & \xrightarrow{\text{grad}} & H(\text{curl}; \mathbb{M}) & \xrightarrow{\text{curl}} & H(\text{div}; \mathbb{M}) & \xrightarrow{\text{div}} & L^2(\mathbb{R}^3) & \rightarrow & \mathbf{0}. \end{array}$$

As we mentioned before $S : H(\text{curl}; \mathbb{M}) \rightarrow H(\text{div}; \mathbb{M})$ is well-defined but $S^{-1} : H(\text{div}; \mathbb{M}) \rightarrow H(\text{curl}; \mathbb{M})$ is not. To fix it, we apply the $\widetilde{}$ operation to reduce space $H(\text{div}; \mathbb{M})$ to $\widetilde{H}(\text{div}; \mathbb{M}) := SH(\text{curl}; \mathbb{M})$. Then $S : H(\text{curl}; \mathbb{M}) \rightarrow \widetilde{H}(\text{div}; \mathbb{M})$ is one-to-one. The div stability $\text{div} \widetilde{H}(\text{div}; \mathbb{M}) = L^2(\mathbb{R}^3)$ holds since $H^1(\mathbb{M}) \subset \widetilde{H}(\text{div}; \mathbb{M})$ and $\text{div} H^1(\mathbb{M}) = L^2(\mathbb{R}^3)$.

To apply the $\widehat{}$ operation, we use $2 \text{vskw grad } \mathbf{u} = \text{curl } \mathbf{u}$ and the triangular diagram

$$\begin{array}{ccc} H^1(\text{curl}) & \xrightarrow{\text{grad}} & \widehat{H}(\text{curl}; \mathbb{M}) \\ \text{curl} \downarrow & \swarrow 2 \text{vskw} & \\ H^1(\mathbb{R}^3) & & \end{array},$$

where

$$H^1(\text{curl}) := \{\mathbf{v} \in H^1(\mathbb{R}^3) : \text{curl } \mathbf{v} \in H^1(\mathbb{R}^3)\},$$

$$\widehat{H}(\text{curl}; \mathbb{M}) := \{\boldsymbol{\tau} \in H(\text{curl}; \mathbb{M}) : \text{vskw } \boldsymbol{\tau} \in H^1(\mathbb{R}^3), \text{curl } \boldsymbol{\tau} \in \widetilde{H}(\text{div}; \mathbb{M})\}.$$

The condition $\text{curl } \widehat{H}(\text{curl}; \mathbb{M}) = \widetilde{H}(\text{div}; \mathbb{M}) \cap \ker(\text{div})$ is again due to the existence of regular potential, i.e. $\text{curl } \widetilde{H}^1(\mathbb{M}) = \widetilde{H}(\text{div}; \mathbb{M}) \cap \ker(\text{div})$ induced from the tilde operation applied to $\text{curl } H^1(\mathbb{M}) = H(\text{div}; \mathbb{M}) \cap \ker(\text{div})$ with

$$\widetilde{H}^1(\mathbb{M}) := \{\boldsymbol{\tau} \in H^1(\mathbb{M}) : \text{curl } \boldsymbol{\tau} \in \widetilde{H}(\text{div}; \mathbb{M})\},$$

and the fact $\widetilde{H}^1(\mathbb{M}) \subset \widehat{H}(\text{curl}; \mathbb{M})$. By Lemma 2.1, the top complex of (14) is exact.

Then by the BGG construction applied to (14), we obtain the elasticity complex

$$(15) \quad \text{RM} \xrightarrow{\subset} H^1(\text{curl}) \xrightarrow{\text{def}} H(\text{inc}^+; \mathbb{S}) \xrightarrow{\text{inc}} H(\text{div}; \mathbb{S}) \xrightarrow{\text{div}} L^2(\mathbb{R}^3) \rightarrow \mathbf{0},$$

where $\text{def } \mathbf{u} = \text{sym grad } \mathbf{u}$, $\text{inc } \boldsymbol{\tau} = \nabla \times \boldsymbol{\tau} \times \nabla$, $\text{RM} = \{\mathbf{a} \times \mathbf{x} + \mathbf{b} : \mathbf{a}, \mathbf{b} \in \mathbb{R}^3\}$ is the space of the linearized rigid body motion, $H(\text{div}; \mathbb{S}) = H(\text{div}; \mathbb{M}) \cap L^2(\mathbb{S})$, and the space

$$H(\text{inc}^+; \mathbb{S}) := H(\text{inc}; \mathbb{S}) \cap H(\text{curl}; \mathbb{S}) = \{\boldsymbol{\tau} \in H(\text{curl}; \mathbb{S}) : \text{inc } \boldsymbol{\tau} \in L^2(\mathbb{S})\}$$

with $H(\text{inc}; \mathbb{S}) = \{\boldsymbol{\tau} \in L^2(\mathbb{S}) : \text{inc } \boldsymbol{\tau} \in L^2(\mathbb{S})\}$. Throughout this paper, we use the script $^+$ to denote extra smoothness. An L^2 function $\boldsymbol{\tau} \in H(\text{inc}; \mathbb{S})$ only requires $\text{inc } \boldsymbol{\tau} \in L^2$, not $\text{curl } \boldsymbol{\tau} \in L^2$. The elasticity complex (15) is slightly smoother than the elasticity complex [30, 7]

$$(16) \quad \text{RM} \xrightarrow{\subset} H^1(\mathbb{R}^3) \xrightarrow{\text{def}} H(\text{inc}; \mathbb{S}) \xrightarrow{\text{inc}} H(\text{div}; \mathbb{S}) \xrightarrow{\text{div}} L^2(\mathbb{R}^3) \rightarrow \mathbf{0}.$$

The complex (16) can be obtained from (15) by an inverse $\widehat{}$ operation. The fact $\text{def } H^1(\mathbb{R}^3) = (H(\text{inc}; \mathbb{S}) \cap \ker(\text{inc}))$ can be derived from the elasticity complex with Sobolev spaces

$$\text{RM} \xrightarrow{\subset} H^1(\mathbb{R}^3) \xrightarrow{\text{def}} L^2(\mathbb{S}) \xrightarrow{\text{inc}} H^{-2}(\mathbb{S}) \xrightarrow{\text{div}} H^{-3}(\mathbb{R}^3) \rightarrow \mathbf{0}$$

derived by the BGG framework in [9], cf. diagram (4).

Similarly by applying the two reduction operations to the third and fourth rows of diagram (5), we obtain

$$\begin{array}{ccccccc} \mathbb{R}^3 & \rightarrow & H^1(\text{div}) & \xrightarrow{\text{grad}} & \widehat{H}(\text{curl}; \mathbb{M}) & \xrightarrow{\text{curl}} & \widetilde{H}(\text{div}; \mathbb{M}) & \xrightarrow{\text{div}} & H(\text{div}) & \rightarrow & \mathbf{0} \\ & & & \nearrow \iota & & \nearrow \text{mskw} & & \nearrow \text{id} & & & \\ \mathbb{R} & \rightarrow & H^1 & \xrightarrow{\text{grad}} & H(\text{curl}) & \xrightarrow{\text{curl}} & H(\text{div}) & \xrightarrow{\text{div}} & L^2 & \rightarrow & 0, \end{array}$$

where

$$\begin{aligned} H^1(\text{div}) &:= \{\mathbf{v} \in H^1(\mathbb{R}^3) : \text{div } \mathbf{v} \in H^1\}, \\ H(\text{div div}^+; \mathbb{S}) &:= \{\boldsymbol{\tau} \in H(\text{div}; \mathbb{S}) : \text{div } \boldsymbol{\tau} \in H(\text{div})\}, \\ \widetilde{H}(\text{div}; \mathbb{M}) &:= H(\text{div div}^+; \mathbb{S}) \oplus \text{mskw } H(\text{curl}), \\ \widehat{H}(\text{curl}; \mathbb{M}) &:= \{\boldsymbol{\tau} \in H(\text{curl}; \mathbb{M}) : \text{tr } \boldsymbol{\tau} \in H^1, \text{curl } \boldsymbol{\tau} \in \widetilde{H}(\text{div}; \mathbb{M})\}. \end{aligned}$$

This leads to the div div complex

$$\text{RT} \xrightarrow{\subset} H^1(\text{div}) \xrightarrow{\text{dev grad}} H(\text{sym curl}^+; \mathbb{T}) \xrightarrow{\text{sym curl}} H(\text{div div}^+; \mathbb{S}) \xrightarrow{\text{div div}} L^2 \rightarrow 0,$$

where $\text{dev } \boldsymbol{\sigma} = \boldsymbol{\sigma} - \text{tr}(\boldsymbol{\sigma})\mathbf{I}/3$, $\text{RT} = \{a\mathbf{x} + \mathbf{b} : a \in \mathbb{R}, \mathbf{b} \in \mathbb{R}^3\}$, and the space

$$H(\text{sym curl}^+; \mathbb{T}) := \{\boldsymbol{\tau} \in H(\text{curl}; \mathbb{T}) : \text{curl } \boldsymbol{\tau} \in \widetilde{H}(\text{div}; \mathbb{M})\}$$

requires additional smoothness on $\boldsymbol{\tau}$ and $\text{curl } \boldsymbol{\tau}$ comparing with the definition of space

$$H(\text{sym curl}; \mathbb{T}) := \{\boldsymbol{\tau} \in L^2(\mathbb{T}) : \text{sym curl } \boldsymbol{\tau} \in L^2(\mathbb{S})\}.$$

The derived div div complex is slightly smoother than the div div complex [9, 44]

$$\text{RT} \xrightarrow{\subset} H^1(\mathbb{R}^3) \xrightarrow{\text{dev grad}} H(\text{sym curl}, \mathbb{T}) \xrightarrow{\text{sym curl}} H(\text{div div}, \mathbb{S}) \xrightarrow{\text{div div}} L^2 \rightarrow 0$$

with $H(\text{div div}, \mathbb{S}) = \{\boldsymbol{\tau} \in L^2(\mathbb{S}) : \text{div div } \boldsymbol{\tau} \in L^2\}$, which again can be obtained by an inverse hat operation.

We would like to highlight that the complexes derived from the BGG framework typically encompass spaces that possess a slightly higher degree of smoothness.

3. SMOOTH FINITE ELEMENT DE RHAM COMPLEXES

In this section we shall review the smooth finite element de Rham complexes developed in [23]. We construct finite element spaces with different smoothness at vertices, edges, and faces which is characterized by a smoothness vector.

An integer vector $\mathbf{r} = (r^v, r^e, r^f)^\top$ is called a smoothness vector if $r^f \geq -1$, $r^e \geq \max\{2r^f, -1\}$ and $r^v \geq \max\{2r^e, -1\}$. Its restriction $(r^v, r^e)^\top$ is a two-dimensional smoothness vector. For a smoothness vector \mathbf{r} and positive integer m , define $\mathbf{r} \ominus m := \max\{\mathbf{r} - m, -1\}$ and $\mathbf{r}_+ = \max\{\mathbf{r}, \mathbf{0}\}$ where max operator is applied component-wise.

3.1. Smooth bubble functions. For edge e , let $r^v \geq 0$ and $k \geq 2r^v + 1$, define edge bubble polynomial space

$$\mathbb{B}_k(e; r^v) := \{u \in \mathbb{P}_k(e) : \partial_t^j u \text{ vanishes at all vertices of } e \text{ for } j = 0, \dots, r^v\},$$

where ∂_t is the tangential derivative along e . This bubble space can be easily characterized as $\mathbb{B}_k(e; r^v) = b_e^{r^v+1} \mathbb{P}_{k-2(r^v+1)}(e)$, where $b_e \in \mathbb{P}_2(e)$ vanishes at two vertices of e .

For triangle f and a smoothness vector $\mathbf{r} = (r^v, r^e)^\top$, define face bubble polynomial space

$$\mathbb{B}_k(f; \begin{pmatrix} r^v \\ r^e \end{pmatrix}) := \{u \in \mathbb{P}_k(f) : \nabla_f^j u \text{ vanishes at all vertices of } f \text{ for } j = 0, \dots, r^v, \\ \text{and } \nabla_f^j u \text{ vanishes on all edges of } f \text{ for } j = 0, \dots, r^e\},$$

where ∇_f is the surface gradient on f . All polynomials defined on e and f can be naturally extended to the whole tetrahedron using the Bernstein basis of polynomials.

For a tetrahedron T and a smoothness vector $\mathbf{r} = (r^v, r^e, r^f)^\top$, define the bubble polynomial space as follows:

$$\mathbb{B}_k(T; \mathbf{r}) := \{u \in \mathbb{P}_k(T) : \nabla^j u \text{ vanishes at all vertices of } T \text{ for } j = 0, \dots, r^v, \\ \nabla^j u \text{ vanishes on all edges of } T \text{ for } j = 0, \dots, r^e, \\ \nabla^j u \text{ vanishes on all faces of } T \text{ for } j = 0, \dots, r^f\}.$$

Note that when $r^f = -1$, the bubble function may not vanish on the boundary of T .

For simplicity of notation, for a three-dimensional smoothness vector $\mathbf{r} = (r^v, r^e, r^f)^\top$, define $\mathbb{B}_k(f; \mathbf{r}) := \mathbb{B}_k(f; (r^v, r^e)^\top)$, which is the face bubble using the restriction of \mathbf{r} on f . Similarly, $\mathbb{B}_k(e; \mathbf{r}) = \mathbb{B}_k(e; r^v)$.

A precise characterization of the bubble polynomial spaces $\mathbb{B}_k(f; \mathbf{r})$ and $\mathbb{B}_k(T; \mathbf{r})$ can be obtained through decompositions of simplicial lattice points (see [22, 23] for more details):

$$\mathbb{B}_k(f; \mathbf{r}) = \mathbb{B}_k(f; \mathbf{r}_+) \oplus_{e \in \Delta_1(T)} [r^e = -1] \mathbb{B}_k(e; \mathbf{r}_+) \oplus [r^v = -1] \mathbb{P}_1(f), \\ \mathbb{B}_k(T; \mathbf{r}) = \mathbb{B}_k(T; \mathbf{r}_+) \oplus_{f \in \Delta_2(T)} [r^f = -1] \mathbb{B}_k(f; \mathbf{r}_+) \oplus_{e \in \Delta_1(T)} [r^e = -1] \mathbb{B}_k(e; \mathbf{r}_+) \\ \oplus [r^v = -1] \mathbb{P}_1(T).$$

For a vector space V , we abbreviate $V \otimes \mathbb{R}^3$ as V^3 . We define the following bubble spaces:

$$\mathbb{B}_k^{\text{curl}}(T; \mathbf{r}) := \{\mathbf{v} \in \mathbb{B}_k^3(T; \mathbf{r}) : \mathbf{v} \times \mathbf{n}|_{\partial T} = \mathbf{0}\}, \\ \mathbb{B}_k^{\text{div}}(T; \mathbf{r}) := \{\mathbf{v} \in \mathbb{B}_k^3(T; \mathbf{r}) : \mathbf{v} \cdot \mathbf{n}|_{\partial T} = 0\}, \\ \mathbb{B}_k^{L^2}(T; \mathbf{r}) := \mathbb{B}_k(T; \mathbf{r}) \cap L_0^2(T).$$

Typically, T will be omitted from the notation, i.e., $\mathbb{B}_k(\mathbf{r}) = \mathbb{B}_k(T; \mathbf{r})$. When $r^f \geq 0$, functions in $\mathbb{B}_k(\mathbf{r})$ vanish on ∂T , thus $\mathbb{B}_k^{\text{curl}}(\mathbf{r}) = \mathbb{B}_k^{\text{div}}(\mathbf{r}) = \mathbb{B}_k^3(\mathbf{r})$. When $r^f = -1$, we have $\mathbb{B}_k^3(\mathbf{r}_+) \subset \mathbb{B}_k^{\text{d}}(\mathbf{r}) \subset \mathbb{B}_k^3(\mathbf{r})$, for $\text{d} = \text{curl}$ or div , as only the tangential or normal components of $\mathbb{B}_k^{\text{d}}(\mathbf{r})$ vanish, respectively.

For each edge e , we choose a tangential vector \mathbf{t}_e and two normal vectors \mathbf{n}_1^e and \mathbf{n}_2^e , abbreviated as \mathbf{t} , \mathbf{n}_1 , and \mathbf{n}_2 . For each face f , we select a normal vector \mathbf{n}_f and two tangential vectors \mathbf{t}_1^f and \mathbf{t}_2^f , abbreviated as \mathbf{n} , \mathbf{t}_1 , and \mathbf{t}_2 when the face f is clear from the context. In a conforming mesh \mathcal{T}_h , \mathbf{n}_1^e , \mathbf{n}_2^e , or \mathbf{n}_f depend on the edge e or the face f , not the element containing them. In expressions such as $\partial_n u$, we use the regular font n rather than the boldface \mathbf{n} .

The bubble spaces $\mathbb{B}_k^{\text{curl}}(T; \mathbf{r})$ and $\mathbb{B}_k^{\text{div}}(T; \mathbf{r})$ have the following decomposition given in [23, 14]

$$(17) \quad \mathbb{B}_k^{\text{curl}}(T; \mathbf{r}) = \mathbb{B}_k^3(T; \mathbf{r}_+) \oplus_{f \in \Delta_2(T)} [r^f = -1] (\mathbb{B}_k(f; \mathbf{r}_+) \otimes \text{span}\{\mathbf{n}_f\}),$$

$$(18) \quad \mathbb{B}_k^{\text{div}}(T; \mathbf{r}) = \mathbb{B}_k^3(T; \mathbf{r}_+) \bigoplus_{f \in \Delta_2(T)} [r^f = -1] (\mathbb{B}_k(f; \mathbf{r}_+) \otimes \text{span}\{\mathbf{t}_1^f, \mathbf{t}_2^f\}) \\ \bigoplus_{e \in \Delta_1(T)} [r^e = -1] (\mathbb{B}_k(e; \mathbf{r}_+) \otimes \text{span}\{\mathbf{t}_e\}).$$

Dimension of $\mathbb{B}_k^{\text{curl}}(T; \mathbf{r})$ and $\mathbb{B}_k^{\text{div}}(T; \mathbf{r})$ can be calculated based on (90).

For an $f \in \Delta_2(T)$ and a smooth vector \mathbf{r} , define bubble spaces on face f

$$\mathbb{B}_k^{\text{div}_f}(f; \mathbf{r}) := \{\mathbf{v} \in \mathbb{B}_k^2(f; \mathbf{r}) : \mathbf{v} \cdot \mathbf{n}|_{\partial f} = 0\} \\ = \mathbb{B}_k^2(f; \mathbf{r}_+) \bigoplus_{e \in \Delta_1(f)} [r^e = -1] (\mathbb{B}_k(e; \mathbf{r}_+) \otimes \text{span}\{\mathbf{t}_e\}), \\ \mathbb{B}_k^{\text{rot}_f}(f; \mathbf{r}) := \{\mathbf{v} \in \mathbb{B}_k^2(f; \mathbf{r}) : \mathbf{v} \cdot \mathbf{t}|_{\partial f} = 0\} \\ = \mathbb{B}_k^2(f; \mathbf{r}_+) \bigoplus_{e \in \Delta_1(f)} [r^e = -1] (\mathbb{B}_k(e; \mathbf{r}_+) \otimes \text{span}\{\mathbf{n}_e\}).$$

3.2. Bubble de Rham complexes. The bubble spaces will form a de Rham complex. As it is not explicitly stated in [22, 23], we present the result below and provide a detailed proof in Appendix.

Lemma 3.1. *Let smoothness vectors $\mathbf{r}_1 \geq -1$, $\mathbf{r}_0 = \mathbf{r}_1 + 1$, and $\mathbf{r}_2 = \mathbf{r}_1 \ominus 1$. Let $f \in \Delta_2(T)$ and $k \geq \max\{2r_1^v - 1, 0\}$. Then the bubble de Rham complexes*

$$0 \xrightarrow{\subset} \mathbb{B}_{k+2}(f; \mathbf{r}_0) \xrightarrow{\text{curl}_f} \mathbb{B}_{k+1}^{\text{div}_f}(f; \mathbf{r}_1) \xrightarrow{\text{div}_f} \mathbb{B}_k(f; \mathbf{r}_2)/\mathbb{R} \rightarrow 0, \\ 0 \xrightarrow{\subset} \mathbb{B}_{k+2}(f; \mathbf{r}_0) \xrightarrow{\text{grad}_f} \mathbb{B}_{k+1}^{\text{rot}_f}(f; \mathbf{r}_1) \xrightarrow{\text{rot}_f} \mathbb{B}_k(f; \mathbf{r}_2)/\mathbb{R} \rightarrow 0$$

are exact.

When move to three dimensions, we require the following condition on a smoothness vector $\mathbf{r} = (r^v, r^e, r^f)^\top$:

$$(19) \quad \begin{cases} r^f \geq 0, & r^e \geq 2r^f + 1 \geq 1, & r^v \geq 2r^e \geq 2, \\ r^f = -1, & \begin{cases} r^e \geq 1, & r^v \geq 2r^e \geq 2, \\ r^e \in \{0, -1\}, & r^v \geq 2r^e + 1. \end{cases} \end{cases}$$

Lemma 3.2 (Theorem 4.5 in [23]). *Let \mathbf{r} be a smoothness vector satisfying (19). Assume $k \geq \max\{2r^v, 1\}$. Then we have the div stability*

$$(20) \quad \text{div } \mathbb{B}_k^{\text{div}}(\mathbf{r}) = \mathbb{B}_{k-1}(\mathbf{r} \ominus 1)/\mathbb{R}.$$

We now present the bubble de Rham complexes.

Lemma 3.3. *Let $\mathbf{r}_0 \geq 0$, $\mathbf{r}_1 = \mathbf{r}_0 - 1$, $\mathbf{r}_2 = \mathbf{r}_1 \ominus 1$, $\mathbf{r}_3 = \mathbf{r}_2 \ominus 1$ be smoothness vectors. Assume \mathbf{r}_2 satisfies (19), and $k \geq \max\{2r_2^v, 1\}$. Then the bubble de Rham complex*

$$0 \xrightarrow{\subset} \mathbb{B}_{k+2}(\mathbf{r}_0) \xrightarrow{\text{grad}} \mathbb{B}_{k+1}^{\text{curl}}(\mathbf{r}_1) \xrightarrow{\text{curl}} \mathbb{B}_k^{\text{div}}(\mathbf{r}_2) \xrightarrow{\text{div}} \mathbb{B}_{k-1}(\mathbf{r}_3)/\mathbb{R} \rightarrow 0$$

is exact.

3.3. Smooth scalar finite elements. Let $\mathbf{r} = (r^v, r^e, r^f)^\top$ be a smoothness vector, and nonnegative integer $k \geq 2r^v + 1$. The shape function space $\mathbb{P}_k(T)$ is determined by the

DoFs

$$(21a) \quad \nabla^j u(\mathbf{v}), \quad j = 0, 1, \dots, r^\vee, \mathbf{v} \in \Delta_0(T),$$

$$(21b) \quad \int_e \frac{\partial^j u}{\partial n_1^i \partial n_2^{j-i}} q \, ds, \quad q \in \mathbb{B}_{k-j}(e; r^\vee - j), 0 \leq i \leq j \leq r^e, e \in \Delta_1(T),$$

$$(21c) \quad \int_f \frac{\partial^j u}{\partial n_f^j} q \, dS, \quad q \in \mathbb{B}_{k-j}(f; \mathbf{r} - j), 0 \leq j \leq r^f, f \in \Delta_2(T),$$

$$(21d) \quad \int_T u q \, dx, \quad q \in \mathbb{B}_k(T; \mathbf{r}).$$

As $b_e \geq 0$, the test function space in (21b) can be changed to $q \in \mathbb{P}_{k-2(r^\vee+1)+j}(e)$.

For the sake of simplifying notation, we use $\text{DoF}_k(\mathbf{r})$ to represent the set of DoFs as defined in (21), and $\text{DoF}_k(s; \mathbf{r})$ for the subset corresponding to the sub-simplex s . The unisolvence can be expressed as:

$$\mathbb{P}_k(T) \text{ is uniquely determined by } \text{DoF}_k(\mathbf{r}).$$

When considering a mesh \mathcal{T}_h , the DoFs (21) define the global C^{r^f} -continuous finite element space as follows:

$$\mathbb{V}_k(\mathcal{T}_h; \mathbf{r}) = \{u \in C^{r^f}(\Omega) : u|_T \in \mathbb{P}_k(T) \text{ for all } T \in \mathcal{T}_h, \\ \text{and all the DoFs (21) are single-valued}\}.$$

In cases where $\mathbb{V}_k(\mathcal{T}_h; \mathbf{r})$ is used as a subspace of $H^1(\Omega)$ or $L^2(\Omega)$, notation $\mathbb{V}_k^{\text{grad}}(\mathcal{T}_h; \mathbf{r})$ or $\mathbb{V}_k^{L^2}(\mathcal{T}_h; \mathbf{r})$ are employed respectively. The reference to the mesh \mathcal{T}_h will subsequently be omitted in the notation to emphasize the dependence on the smoothness vector \mathbf{r} .

3.4. $H(\text{div})$ -conforming finite elements. Let $\mathbf{r}_3 \geq \mathbf{r}_2 \ominus 1$ and positive integer $k \geq \max\{2r_2^\vee + 1, 2r_3^\vee + 2\}$. We define the space

$$\mathbb{V}_k^{\text{div}}(\mathbf{r}_2, \mathbf{r}_3) := \{\mathbf{v} \in \mathbb{V}_k^3(\mathbf{r}_2) \cap H(\text{div}, \Omega) : \text{div } \mathbf{v} \in \mathbb{V}_{k-1}^{L^2}(\mathbf{r}_3)\},$$

abbreviate $\mathbb{V}_k^{\text{div}}(\mathbf{r}_2, \mathbf{r}_2 \ominus 1) = \mathbb{V}_k^3(\mathbf{r}_2) \cap H(\text{div}, \Omega)$ as $\mathbb{V}_k^{\text{div}}(\mathbf{r}_2)$. We construct $\mathbb{V}_k^{\text{div}}(\mathbf{r}_2)$ by using the t - n decomposition approach developed in [24].

In order to have a stable discretization of Stokes equations, it is crucial to have the surjectivity of the div operator in view of Babuška-Brezzi condition [12], which is thus called the div stability; see for example [31]. The div stability $\text{div } \mathbb{V}_k^{\text{div}}(\mathbf{r}_2, \mathbf{r}_3) = \mathbb{V}_{k-1}^{L^2}(\mathbf{r}_3)$ is established under certain restrictions on $(\mathbf{r}_2, \mathbf{r}_3)$ and for sufficiently large values of k .

Lemma 3.4 (Theorem 4.10 in [23]). *Let \mathbf{r}_2 and \mathbf{r}_3 be two smoothness vectors. Assume \mathbf{r}_2 satisfies (19) and $\mathbf{r}_3 \geq \mathbf{r}_2 \ominus 1$. Assume $k \geq \max\{2r_2^\vee + 1, r_2^\vee + 2, 3(r_2^e + 1), 2r_3^\vee + 2, 4r_3^f + 5, (r_3^e + r_3^f + 5)[r_3^\vee = 0]\}$. It holds that*

$$(22) \quad \text{div } \mathbb{V}_k^{\text{div}}(\mathbf{r}_2, \mathbf{r}_3) = \mathbb{V}_{k-1}^{L^2}(\mathbf{r}_3).$$

When (22) holds, we shall call $(\mathbf{r}_2, \mathbf{r}_3, k)$ div stable and we give finite element description of such space $\mathbb{V}_k^{\text{div}}(\mathbf{r}_2, \mathbf{r}_3)$ in [23, Section 4.4]. We emphasize that for continuous div element, i.e., $r^f \geq 0$, the minimal \mathbf{r}_2 satisfying (19) is $\mathbf{r}_2 = (2, 1, 0)^\top$. Consequently $\mathbf{r}_3 = (1, 0, -1)^\top$ and $k \geq 6$. The corresponding Stokes element $\mathbb{V}_k^{\text{div}}((2, 1, 0)^\top) \times \mathbb{V}_{k-1}^{L^2}((1, 0, -1)^\top)$ is firstly constructed by Neilan [43].

3.5. $H(\text{curl})$ -conforming finite elements. Let $\mathbf{r}_2 \geq \mathbf{r}_1 \ominus 1$ be two smoothness vectors. Next we introduce

$$\mathbb{V}_{k+1}^{\text{curl}}(\mathbf{r}_1, \mathbf{r}_2) := \{\mathbf{v} \in \mathbb{V}_{k+1}^3(\mathbf{r}_1) \cap H(\text{curl}, \Omega) : \text{curl } \mathbf{v} \in \mathbb{V}_k^{\text{div}}(\mathbf{r}_2)\},$$

and will abbreviate $\mathbb{V}_{k+1}^{\text{curl}}(\mathbf{r}_1, \mathbf{r}_1 \ominus 1)$ as $\mathbb{V}_{k+1}^{\text{curl}}(\mathbf{r}_1)$. We give finite element description of $\mathbb{V}_{k+1}^{\text{curl}}(\mathbf{r}_1)$, i.e., local DoFs for the shape function space $\mathbb{P}_{k+1}(T; \mathbb{R}^3)$ in [23, Section 5.3].

3.6. Finite element de Rham complexes in three dimensions.

Theorem 3.5 (Theorem 5.9 in [23]). *Let $\mathbf{r}_0 \geq 0, \mathbf{r}_1 = \mathbf{r}_0 - 1, \mathbf{r}_2 \geq \mathbf{r}_1 \ominus 1, \mathbf{r}_3 \geq \mathbf{r}_2 \ominus 1$ be smoothness vectors. Assume $(\mathbf{r}_2, \mathbf{r}_3, k)$ is div stable. Assume $k \geq \max\{2r_1^v + 1, 2r_2^v + 1, r_2^v + 2, 3(r_2^e + 1), 2r_3^v + 2, 4r_3^f + 5, (r_3^e + r_3^f + 5)[r_3^v = 0]\}$. Then the finite element de Rham complex*

$$(23) \quad \mathbb{R} \xrightarrow{C} \mathbb{V}_{k+2}^{\text{grad}}(\mathbf{r}_0) \xrightarrow{\text{grad}} \mathbb{V}_{k+1}^{\text{curl}}(\mathbf{r}_1, \mathbf{r}_2) \xrightarrow{\text{curl}} \mathbb{V}_k^{\text{div}}(\mathbf{r}_2, \mathbf{r}_3) \xrightarrow{\text{div}} \mathbb{V}_{k-1}^{L^2}(\mathbf{r}_3) \rightarrow 0$$

is exact.

We refer to a parameter sequence $(\mathbf{r}_0, \mathbf{r}_1, \mathbf{r}_2, \mathbf{r}_3, k)$ as a valid de Rham parameter sequence if (23) holds with exactness. We also provide the finite element description of the space $\mathbb{V}_{k+1}^{\text{curl}}(\mathbf{r}_1, \mathbf{r}_2)$ in (23) as discussed in [23].

When $r_2^f \geq 0$, (23) transforms into a finite element Stokes complex, as the space $\mathbb{V}_k^{\text{div}}(\mathbf{r}_2, \mathbf{r}_3) \subset H^1(\Omega; \mathbb{R}^3)$. This transformation allows for the discretization of the Stokes equation. Notably, existing works on finite element Stokes complexes [43] and finite element de Rham complexes [28] are specific instances of (23), depending on the selection of different smoothness vectors.

4. FACE ELEMENTS

In this section, our objective is to construct finite elements conforming to $H(\text{div}; \mathbb{X})$ for either $\mathbb{X} = \mathbb{S}$ or \mathbb{T} . We will use the t - n decomposition technique introduced in [24] to construct the finite elements, and we will subsequently leverage the BGG framework to establish the divergence stability property.

4.1. Smooth $H(\text{div}; \mathbb{T})$ and $H(\text{div}; \mathbb{S})$ finite elements. Given a smoothness vector \mathbf{r} with $r^v \geq 0$, we examine the space associated with $\mathbf{r}_+ \geq 0$, leading to the unisolvence condition:

$$(24) \quad \mathbb{P}_k(T) \otimes \mathbb{X} \text{ is uniquely determined by } \text{DoF}_k(\mathbf{r}_+) \otimes \mathbb{X},$$

and its global extension, $\mathbb{V}_k(\mathbf{r}_+) \otimes \mathbb{X}$. For $\boldsymbol{\sigma} \in \mathbb{P}_k(T) \otimes \mathbb{X}$, where $\text{tr}^{\text{div}} \boldsymbol{\sigma} = \boldsymbol{\sigma} \mathbf{n}$, to be $H(\text{div})$ -conforming, $\boldsymbol{\sigma} \mathbf{n}$ must be continuous across the faces of the triangulation. In cases where $r^f = -1$ or $r^e = -1$, we need to adjust the continuity of the element corresponding to \mathbf{r}_+ by transferring the tangential component into the bubble space.

The key lies in an appropriate t - n decomposition of the tensor \mathbb{X} at a sub-simplex s :

$$\mathbb{X} = \mathcal{N}^s(\mathbb{X}) \oplus \mathcal{T}^s(\mathbb{X}),$$

where \mathcal{T}^s and \mathcal{N}^s represent the tangential and normal planes of s , respectively.

For a sub-simplex s , we use the following decomposition of DoFs associated to s (25)

$$\text{DoF}(s; \mathbf{r}_+) \otimes \mathbb{X} = \begin{cases} \text{DoF}(s; \mathbf{r}) \otimes \mathbb{X} & \text{when } r^s \geq 0, \\ \text{DoF}(s; \mathbf{r}_+) \otimes \mathbb{X} & = \begin{cases} \text{DoF}(s; \mathbf{r}_+) \otimes \mathcal{N}^s(\mathbb{X}) & \text{normal trace,} \\ \oplus & \text{when } r^s = -1 \\ \text{DoF}(s; \mathbf{r}_+) \otimes \mathcal{T}^s(\mathbb{X}) & \text{div bubbles.} \end{cases} \end{cases}$$

We relocate the tangential component into the div bubble space and introduce

$$(26) \quad \mathbb{B}_k^{\text{div}}(\mathbf{r}; \mathbb{X}) := (\mathbb{B}_k(\mathbf{r}_+) \otimes \mathbb{X}) \oplus [r^e = -1] \oplus_{e \in \Delta_1(T)} \mathbb{B}_k(e; r_+) \otimes \mathcal{T}^e(\mathbb{X}) \\ \oplus [r^f = -1] \oplus_{f \in \Delta_2(T)} \mathbb{B}_k(f; \mathbf{r}_+) \otimes \mathcal{T}^f(\mathbb{X}).$$

Let $\mathbb{B}_k(\mathbf{r}; \mathbb{X}) := \mathbb{B}_k(\mathbf{r}) \otimes \mathbb{X}$ for $\mathbb{X} = \mathbb{R}^3, \mathbb{M}, \mathbb{S}$, or \mathbb{T} .

Different frames will be employed for distinct sub-simplices. On an edge e , one possible frame is $\{\mathbf{n}_{f_1}, \mathbf{n}_{f_2}, \mathbf{t}_e\}$, where f_1 and f_2 denote the two faces containing e . Another option is $\{\mathbf{n}_1^e, \mathbf{n}_2^e, \mathbf{t}_e\}$, where \mathbf{n}_1^e and \mathbf{n}_2^e represent two orthogonal normal vectors of e . Notably, \mathbf{n}_i^e depends only on e , while \mathbf{n}_{f_i} is contingent on face f_i . On a face f , an orthonormal frame $\{\mathbf{t}_1^f, \mathbf{t}_2^f, \mathbf{n}^f\}$ is utilized, comprising two tangential vectors \mathbf{t}_i^f and a face normal \mathbf{n}^f , both of which depend solely on face f .

Decompositions for \mathbb{T} on edge e and face f are given below and illustrated in Fig. 3

$$\begin{aligned} \mathcal{T}^e(\mathbb{T}) &:= \text{span}\{\mathbf{n}_i^e \otimes \mathbf{t}_e, i = 1, 2\}, \\ \mathcal{N}^e(\mathbb{T}) &:= \text{span}\{\mathbf{t}_e \otimes \mathbf{n}_{f_i}, \mathbf{n}_{f_i} \otimes \mathbf{n}_{f_j} - (\mathbf{n}_{f_i} \cdot \mathbf{n}_{f_j})\mathbf{t}_e \otimes \mathbf{t}_e, i, j = 1, 2\}, \\ \mathcal{T}^f(\mathbb{T}) &:= \text{span}\{\mathbf{n}_f \otimes \mathbf{t}_i^f, i = 1, 2, \mathbf{t}_2^f \otimes \mathbf{t}_1^f, \mathbf{t}_1^f \otimes \mathbf{t}_2^f, \mathbf{t}_2^f \otimes \mathbf{t}_2^f - \mathbf{t}_1^f \otimes \mathbf{t}_1^f\}, \\ \mathcal{N}^f(\mathbb{T}) &:= \text{span}\{\mathbf{n}^f \otimes \mathbf{n}^f - \mathbf{t}_1^f \otimes \mathbf{t}_1^f, \mathbf{t}_i^f \otimes \mathbf{n}^f, i = 1, 2\}. \end{aligned}$$



(a) Decomposition on an edge.

(b) Decomposition on a face.

FIGURE 3. The t - n decompositions of \mathbb{T} on edges and faces. Red blocks are associated to bubbles and green blocks for the normal traces which are redistributed to faces.

The tangential component will be integrated into the div bubble space. As an example, consider a function $b_e \mathbf{n}_1^e \otimes \mathbf{t}_e \in \mathbb{B}_k(e; r^v) \otimes \mathcal{T}^e(\mathbb{T})$. For two faces f that include the edge e , $\mathbf{t}_e \cdot \mathbf{n}_f = 0$. For the other two faces f that do not contain e , the quadratic edge bubble function b_e vanishes on f , i.e., $b_e|_f = 0$. Consequently, $(b_e \mathbf{n}_1^e \otimes \mathbf{t}_e) \mathbf{n}|_{\partial T} = \mathbf{0}$, which falls within $\mathbb{B}_k^{\text{div}}(\mathbf{r}; \mathbb{T})$. A less apparent fact is that $\mathbb{B}_k^{\text{div}}(\mathbf{r}; \mathbb{T})$ defined in (26) encompasses all div bubble polynomials $\mathbb{B}_k(\mathbf{r}; \mathbb{T}) \cap \ker(\text{tr}^{\text{div}})$, which was proved in [24] for $\mathbf{r} = (0, -1, -1)^\top$.

The normal component can be reallocated to each face to enforce the desired normal continuity. Further details will be elucidated in the proof of Lemma 4.1.

Take $\mathbb{P}_k(T; \mathbb{T})$ as the space of shape functions. When $r^f \geq 0$, DoFs are simply tensor product of $\text{DoF}_k(\mathbf{r})$ in (21) and \mathbb{T} . We thus focus on the case $r^f = -1$. The DoFs are

$$(27a) \quad \nabla^i \boldsymbol{\tau}(\mathbf{v}), \quad i = 0, \dots, r^v, \mathbf{v} \in \Delta_0(T),$$

$$(27b) \quad \int_e \frac{\partial^j \boldsymbol{\tau}}{\partial n_1^i \partial n_2^{j-i}} : \mathbf{q} \, ds, \quad \mathbf{q} \in \mathbb{B}_{k-j}(e; r^v - j) \otimes \mathbb{T}, 0 \leq i \leq j \leq r^e, e \in \Delta_1(T),$$

$$(27c) \quad \int_f (\Pi_f \boldsymbol{\tau} \mathbf{n}) \cdot \mathbf{q} \, dS, \quad \mathbf{q} \in (\mathbb{B}_k^2(f; \mathbf{r})/\text{RT}(f)) \oplus \text{RT}(f), f \in \Delta_2(T),$$

$$(27d) \quad \int_f (\mathbf{n}^\top \boldsymbol{\tau} \mathbf{n}) q \, dS, \quad q \in (\mathbb{B}_k(f; \mathbf{r})/\mathbb{P}_0(f)) \oplus \mathbb{P}_0(f), f \in \Delta_2(T),$$

$$(27e) \quad \int_T \boldsymbol{\tau} : \mathbf{q} \, dx, \quad \mathbf{q} \in \mathbb{B}_k^{\text{div}}(\mathbf{r}; \mathbb{T}).$$

Lemma 4.1. *Let \mathbf{r} be a smoothness vector with $r^f = -1, r^v \geq 0$, and let $k \geq 2r^v + 1$. DoFs (27) are unisolvent for $\mathbb{P}_k(T; \mathbb{T})$. Given a triangulation \mathcal{T}_h of Ω , define*

$$\mathbb{V}_k^{\text{div}}(\mathbf{r}; \mathbb{T}) := \{ \boldsymbol{\tau} \in L^2(\Omega; \mathbb{T}) : \boldsymbol{\tau}|_T \in \mathbb{P}_k(T; \mathbb{T}) \text{ for all } T \in \mathcal{T}_h, \\ \text{and all the DoFs (27) are single-valued} \}.$$

Then $\mathbb{V}_k^{\text{div}}(\mathbf{r}; \mathbb{T}) \subset H(\text{div}, \Omega; \mathbb{T})$.

Proof. First consider the case $r^e \geq 0$. The continuous element $\mathbb{V}_k(\mathbf{r}_+) \otimes \mathbb{T}$ is determined by DoFs (27a)-(27b) plus

$$(28) \quad \int_f \boldsymbol{\tau} : \mathbf{q} \, dS, \quad \mathbf{q} \in \mathbb{B}_k(f; \begin{pmatrix} r^v \\ r^e \end{pmatrix}) \otimes \mathbb{T}, f \in \Delta_2(T),$$

$$(29) \quad \int_T \boldsymbol{\tau} : \mathbf{q} \, dx, \quad \mathbf{q} \in \mathbb{B}_k(T; \mathbf{r}_+) \otimes \mathbb{T}.$$

For (28), we decompose $\mathbb{T} = \mathcal{N}^f(\mathbb{T}) \oplus \mathcal{T}^f(\mathbb{T})$ and move $\mathbb{B}_k(f; \mathbf{r}) \otimes \mathcal{T}^f(\mathbb{T})$ into the volume DoFs (27e) by utilizing $\mathbf{q} \in \mathbb{B}_k^{\text{div}}(\mathbf{r}; \mathbb{T})$. For the normal component, we employ the idea of Petrov-Galerkin method. The function $\boldsymbol{\tau}$ is in the trial space containing basis $\mathbf{n}^f \otimes \mathbf{n}^f - \mathbf{t}_1^f \otimes \mathbf{t}_1^f$ for which the test function could be just $\mathbf{n}^f \otimes \mathbf{n}^f$ as $(\mathbf{n}^f \otimes \mathbf{n}^f - \mathbf{t}_1^f \otimes \mathbf{t}_1^f) \mathbf{n}^f = \mathbf{n}^f$, corresponding to DoF (27d). We then combine this with the other two components $\mathbf{t}_i^f \otimes \mathbf{n}$, i.e. DoF (27c), to determine the vector $\boldsymbol{\tau} \mathbf{n}$.

The test function space is further decomposed, e.g. $\mathbb{B}_k(f; \mathbf{r}) = (\mathbb{B}_k(f; \mathbf{r})/\mathbb{P}_0(f)) \oplus \mathbb{P}_0(f)$ so that the moment $\int_f \mathbf{n}^\top \boldsymbol{\tau} \mathbf{n} \, dS$ is included in DoF, which is crucial for the div stability. Similar modification is applied in (27c) to include $\text{RT}(f)$ in the test function space.

Consequently, (28)-(29) are rearranged as

$$\int_f (\Pi_f \boldsymbol{\tau} \mathbf{n}) \cdot \mathbf{q} \, dS, \quad \mathbf{q} \in (\mathbb{B}_k^2(f; \mathbf{r})/\text{RT}(f)) \oplus \text{RT}(f), f \in \Delta_2(T), \\ \int_f (\mathbf{n}^\top \boldsymbol{\tau} \mathbf{n}) q \, dS, \quad q \in (\mathbb{B}_k(f; \mathbf{r})/\mathbb{P}_0(f)) \oplus \mathbb{P}_0(f), f \in \Delta_2(T), \\ \int_f \boldsymbol{\tau} : \mathbf{q} \, dS, \quad \mathbf{q} \in \mathbb{B}_k(f; \mathbf{r}) \otimes \mathcal{T}^f(\mathbb{T}), f \in \Delta_2(T),$$

$$\int_T \boldsymbol{\tau} : \mathbf{q} \, dx, \quad \mathbf{q} \in \mathbb{B}_k(T; \mathbf{r}_+) \otimes \mathbb{T},$$

which are equivalent to (27c)-(27e). The unisolvence then follows from that for tensor product spaces; see (24).

Now let us turn our attention to the case where $r^\vee \geq 0$, $r^e = -1$, $r^f = -1$, and thus $\mathbf{r}_+ = (r^\vee, 0, 0)^\top$. The set of DoFs $\text{DoF}_k(\mathbf{r}_+) \otimes \mathbb{T}$ includes vertex DoF (27a), volume DoF (29), as well as the following edge and face DoFs:

$$(30) \quad \int_e \boldsymbol{\tau} : \mathbf{q} \, ds, \quad \mathbf{q} \in \mathbb{B}_k(e; r^\vee) \otimes \mathbb{T}, \quad e \in \Delta_1(T),$$

$$(31) \quad \int_f \boldsymbol{\tau} : \mathbf{q} \, dS, \quad \mathbf{q} \in \mathbb{B}_k(f; \begin{pmatrix} r^\vee \\ 0 \end{pmatrix}) \otimes \mathbb{T}, \quad f \in \Delta_2(T).$$

As previously mentioned, on each edge e , we employ the frame $\{\mathbf{n}_{f_1}, \mathbf{n}_{f_2}, \mathbf{t}_e\}$, where f_1, f_2 are two faces containing e . The tangential component $\mathbb{B}_k(e; r^\vee) \otimes \mathcal{T}^e(\mathbb{T})$ is moved into the bubble space $\mathbb{B}_k^{\text{div}}(\mathbf{r}; \mathbb{T})$. The normal components will be redistributed to the two faces $f_i, i = 1, 2$, containing e . More precisely, we can first modify the DoF (30) with $\mathbf{q} \in \mathbb{B}_k(e; r^\vee) \otimes \mathcal{N}^e(\mathbb{T})$ to

$$\int_e (\boldsymbol{\tau} \mathbf{n}_{f_i})|_e \cdot \mathbf{q} \quad \text{for } \mathbf{q} \in \mathbb{B}_k^3(e; r^\vee), \quad i = 1, 2.$$

Then redistribute this edge DoF to the face $f_i, i = 1, 2$ containing e :

$$\int_e (\boldsymbol{\tau} \mathbf{n}_{f_i})|_e \cdot \mathbf{q} \rightarrow \int_e (\boldsymbol{\tau} \mathbf{n}_{f_i})|_{f_i} \cdot \mathbf{q} \quad \text{for } \mathbf{q} \in \mathbb{B}_k^3(e; r^\vee), \quad i = 1, 2,$$

so that in (31)

$$\mathbb{B}_k(f; \begin{pmatrix} r^\vee \\ 0 \end{pmatrix}) \oplus_{e \in \Delta_1(f)} \mathbb{B}_k(e; r^\vee) = \mathbb{B}_k(f; \begin{pmatrix} r^\vee \\ -1 \end{pmatrix})$$

for $r^\vee \geq 0, r^e = -1$, which leads to the establishment of (27c)-(27d). Thus, the unisolvence is proven.

The conclusion $\mathbb{V}_k^{\text{div}}(\mathbf{r}; \mathbb{T}) \subset H(\text{div}, \Omega; \mathbb{T})$ is obvious as $\boldsymbol{\tau} \mathbf{n}$ is continuous on each face f due to the single-valued DoFs (27a)-(27d). \square

When $r^\vee = 0$ and $r^e = r^f = -1$, the element $\mathbb{V}_k^{\text{div}}(\mathbf{r}; \mathbb{T})$ exhibits continuity at vertices, which is reminiscent of the Stenberg element [48] designed for $H(\text{div})$ -conforming vector functions. We refer to [24] for an illustration of Stenberg element and the corresponding inf-sup condition.

The construction of an $H(\text{div}; \mathbb{S})$ -conforming element follows a similar approach, albeit with additional complexities introduced by $\mathcal{N}^e(\mathbb{S})$. Decompositions on edge e and f are

$$\mathcal{T}^e(\mathbb{S}) := \text{span}\{\mathbf{t}_e \otimes \mathbf{t}_e\},$$

$$\mathcal{N}^e(\mathbb{S}) := \text{span}\{\text{sym}(\mathbf{t}_e \otimes \mathbf{n}_{f_i}), i = 1, 2\} \oplus \text{span}\{\text{sym}(\mathbf{n}_i^e \otimes \mathbf{n}_j^e), 1 \leq i \leq j \leq 2\},$$

$$\mathcal{T}^f(\mathbb{S}) := \text{span}\{\text{sym}(\mathbf{t}_i^f \otimes \mathbf{t}_j^f), 1 \leq i \leq j \leq 2\},$$

$$\mathcal{N}^f(\mathbb{S}) := \text{span}\{\mathbf{n}^f \otimes \mathbf{n}^f, \text{sym}(\mathbf{t}_i^f \otimes \mathbf{n}^f), i = 1, 2\}.$$

Once again, the tangential component will be incorporated into the bubble space. However, the redistribution of certain normal components to faces might be constrained by symmetry conditions. On an edge e , for instance, the symmetry constraint demands that the normal plane of e must obey $\text{span}\{\text{sym}(\mathbf{n}_i^e \otimes \mathbf{n}_j^e), 1 \leq i \leq j \leq 2\}$, which is a global requirement, indicating that the two normal vectors $\{\mathbf{n}_1^e, \mathbf{n}_2^e\}$ are independent of the elements containing e . We refer to the blue blocks in Fig. 4 for clarification. Conversely, in

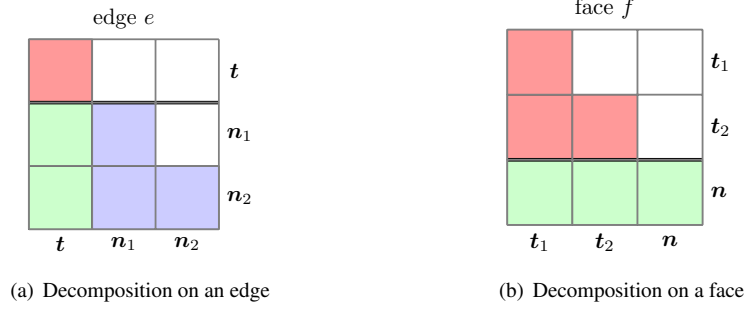


FIGURE 4. The t - n decomposition of \mathbb{S} on edges and faces. Red blocks are associated to bubbles, and green and blue blocks for the normal traces. The green blocks can be redistributed to faces while the blue blocks introduces stronger continuity on the normal plane $\mathcal{N}^e(\mathbb{S})$.

$\mathcal{N}^e(\mathbb{T})$, all the components can be effectively redistributed to faces, as demonstrated by the green blocks in Fig. 4.

Take $\mathbb{P}_k(T; \mathbb{S})$ as the space of shape functions. Again we focus on the case $r^f = -1$. The DoFs are

$$(32a) \quad \nabla^i \tau(\mathbf{v}), \quad i = 0, \dots, r^v, \mathbf{v} \in \Delta_0(T),$$

$$(32b) \quad \int_e \frac{\partial^j \tau}{\partial n_1^i \partial n_2^{j-i}} : \mathbf{q} \, ds, \quad \mathbf{q} \in \mathbb{B}_{k-j}(e; r^v - j) \otimes \mathbb{S}, 0 \leq i \leq j \leq r^e, e \in \Delta_1(T),$$

$$(32c) \quad \int_e (\mathbf{n}_i^\top \tau \mathbf{n}_j) q \, ds, \quad q \in \mathbb{B}_k(e; r^v), 1 \leq i \leq j \leq 2, e \in \Delta_1(T), \text{ if } r^e = -1,$$

$$(32d) \quad \int_f (\Pi_f \tau \mathbf{n}) \cdot \mathbf{q} \, dS, \quad \mathbf{q} \in (\mathbb{B}_k^{\text{div}}(f; \mathbf{r}) / \text{RM}(f)) \oplus \text{RM}(f), f \in \Delta_2(T),$$

$$(32e) \quad \int_f (\mathbf{n}^\top \tau \mathbf{n}) q \, dS, \quad q \in (\mathbb{B}_k(f; \mathbf{r}_+) / \mathbb{P}_1(f)) \oplus \mathbb{P}_1(f), f \in \Delta_2(T),$$

$$(32f) \quad \int_T \tau : \mathbf{q} \, dx, \quad \mathbf{q} \in \mathbb{B}_k^{\text{div}}(\mathbf{r}; \mathbb{S}).$$

Lemma 4.2. *Let \mathbf{r} be a valid smoothness vector with $r^f = -1, r^v \geq 0$, and let $k \geq 2r^v + 1$. DoFs (32) are unisolvent for $\mathbb{P}_k(T; \mathbb{S})$. Given a triangulation \mathcal{T}_h of Ω , define*

$$\mathbb{V}_k^{\text{div}}(\mathbf{r}; \mathbb{S}) := \{ \tau \in L^2(\Omega; \mathbb{S}) : \tau|_T \in \mathbb{P}_k(T; \mathbb{S}) \text{ for all } T \in \mathcal{T}_h, \\ \text{and all the DoFs (32) are single-valued} \}.$$

Then $\mathbb{V}_k^{\text{div}}(\mathbf{r}; \mathbb{S}) \subset H(\text{div}, \Omega; \mathbb{S})$.

Proof. The core approach of the proof aligns with that of Lemma 4.1. We will highlight the differences here. The case where $r^e \geq 0$ remains unchanged. When $r^e = -1$, the components $\mathbf{t}_e \otimes \mathbf{n}_{f_i}$ can be redistributed to faces, resulting in the expression:

$$\mathbb{B}_k^{\text{div}}(f; \mathbf{r}) = \mathbb{B}_k^2(f; \mathbf{r}_+) \oplus \bigoplus_{e \in \Delta_1(f)} \mathbb{B}_k(e, r^v) \mathbf{t}_e,$$

which leads to the form in (32d). The components $\mathbf{n}_i^e \otimes \mathbf{n}_j^e$ cannot be redistributed to faces and are preserved in (32c). Therefore, in (32e), the notation \mathbf{r}_+ is still retained in $\mathbb{B}_k(f; \mathbf{r}_+)$, while in (27d) for $H(\text{div}, \mathbb{T})$ elements, $\mathbb{B}_k(f; \mathbf{r})$ is used. \square

Remark 4.3. When $r^v = 0, r^e = r^f = -1$, if we do not redistribute the tangential-normal component of edge DoFs, cf. [20, 24] for detailed explanation, we can recover the Hu-Zhang element [38]. We prefer redistribution of tangential-normal DoF (32d) as it is more close to the vector face elements. \square

Remark 4.4. The continuity at vertices is enforced due to the constraints – tracelessness conditions in \mathbb{T} or symmetry conditions in \mathbb{S} . This constraint-driven continuity at vertices cannot be relaxed. To elucidate, let v_0, v_1, v_2, v_3 be the four vertices of a tetrahedron T , with corresponding barycentric coordinates $\lambda_0, \lambda_1, \lambda_2, \lambda_3$. Selecting v_0 as the origin, we define $t_{0i} := v_i - v_0$ for $i = 1, 2, 3$, which serve as three basis vectors. For a smooth traceless tensor τ , due to the duality between $\{t_{01}, t_{02}, t_{03}\}$ and $\{\nabla\lambda_1, \nabla\lambda_2, \nabla\lambda_3\}$, we can represent

$$\tau(v_0) = \sum_{i=0}^3 (\tau \nabla \lambda_i)|_{f_i}(v_0) t_{0i}^\top.$$

The traceless property of τ implies

$$\sum_{i=0}^3 t_{0i}^\top (\tau \nabla \lambda_i)|_{f_i}(v_0) = 0,$$

indicating that $(\tau n_1)|_{f_1}, (\tau n_2)|_{f_2}$, and $(\tau n_3)|_{f_3}$ are linearly dependent at vertex v_0 . Consequently, the vertex DoFs in equation (27a) cannot be reallocated to the faces, which underscores the inalterable nature of the constraint $r^v \geq 0$. \square

4.2. Div stability. Due to the similarity, we use $H(\text{div}; \mathbb{S})$ -conforming finite element to illustrate the BGG procedure. Consider the diagram

$$\begin{array}{ccccc} & \mathbb{V}_{k+1}^{\text{div}}(\mathbf{r} + 1; \mathbb{M}) & \xrightarrow{\text{div}} & \mathbb{V}_k^{L^2}(\mathbf{r}; \mathbb{R}^3) & \longrightarrow \mathbf{0} \\ & \nearrow S & & \nearrow -2 \text{vskw} & \\ \mathbb{V}_{k+1}^{\text{curl}}(\mathbf{r} + 1; \mathbb{M}) & \xrightarrow{\text{curl}} & \mathbb{V}_k^{\text{div}}(\mathbf{r}; \mathbb{M}) & \xrightarrow{\text{div}} & \mathbb{V}_{k-1}^{L^2}(\mathbf{r} \ominus 1; \mathbb{R}^3) \longrightarrow \mathbf{0}, \end{array}$$

where $\mathbb{V}_k^{\text{div}}(\mathbf{r}; \mathbb{M}) = \mathbb{R}^3 \otimes \mathbb{V}_k^{\text{div}}(\mathbf{r})$ and $\mathbb{V}_{k+1}^{\text{curl}}(\mathbf{r} + 1; \mathbb{M}) = \mathbb{R}^3 \otimes \mathbb{V}_{k+1}^{\text{curl}}(\mathbf{r} + 1)$. We require that both $(\mathbf{r} + 1, \mathbf{r}, k + 1)$ and $(\mathbf{r}, \mathbf{r} \ominus 1, k)$ are div stable. Then

$$\mathbf{r} + 1 \geq \begin{pmatrix} 2 \\ 1 \\ 0 \end{pmatrix}, \quad \mathbf{r} \geq \begin{pmatrix} 1 \\ 0 \\ -1 \end{pmatrix}, \quad \mathbf{r} \ominus 1 \geq \begin{pmatrix} 0 \\ -1 \\ -1 \end{pmatrix}.$$

In particular $r^e \geq 0$.

Lemma 4.5. *Let \mathbf{r} be a smoothness vector and k large enough satisfying: both $(\mathbf{r} + 1, \mathbf{r}, k + 1)$ and $(\mathbf{r}, \mathbf{r} \ominus 1, k)$ are div stable. Then we have the $(\text{div}; \mathbb{S})$ stability:*

$$\text{div } \mathbb{V}_k^{\text{div}}(\mathbf{r}; \mathbb{S}) = \mathbb{V}_{k-1}^{L^2}(\mathbf{r} \ominus 1; \mathbb{R}^3).$$

Proof. As $\mathbf{r} + 1 \geq 0$, both $\mathbb{V}_{k+1}^{\text{div}}(\mathbf{r} + 1; \mathbb{M}) = \mathbb{V}_{k+1}^{\text{curl}}(\mathbf{r} + 1; \mathbb{M}) = \mathbb{V}_{k+1}^{\text{grad}}(\mathbf{r} + 1) \otimes \mathbb{M}$. Therefore, S is one-to-one.

Given $\mathbf{u} \in \mathbb{V}_k^{L^2}(\mathbf{r}; \mathbb{R}^3)$, since $(\mathbf{r} + 1, \mathbf{r}, k + 1)$ is div stable, we can find $\sigma \in \mathbb{V}_{k+1}^{\text{div}}(\mathbf{r} + 1; \mathbb{M})$ such that $\text{div } \sigma = \mathbf{u}$. Then, by defining $\tau := \text{curl } S^{-1} \sigma$, we have $\tau \in \mathbb{V}_k^{\text{div}}(\mathbf{r}; \mathbb{M})$ and

$$2 \text{vskw } \tau = 2 \text{vskw } \text{curl } (S^{-1} \sigma) = \text{div } S(S^{-1} \sigma) = \mathbf{u}.$$

Thus, $\text{vskw} : \mathbb{V}_k^{\text{div}}(\mathbf{r}; \mathbb{M}) \rightarrow \mathbb{V}_k^{L^2}(\mathbf{r}; \mathbb{R}^3)$ is surjective.

We can apply the BGG construction to conclude that $\text{div} : \mathbb{V}_k^{\text{div}}(\mathbf{r}; \mathbb{M}) \cap \ker(\text{vskw}) \rightarrow \mathbb{V}_{k-1}^{L^2}(\mathbf{r} \ominus 1; \mathbb{R}^3)$ is surjective. Our next step is to establish the relationship

$$(33) \quad \mathbb{V}_k^{\text{div}}(\mathbf{r}; \mathbb{S}) = \mathbb{V}_k^{\text{div}}(\mathbf{r}; \mathbb{M}) \cap \ker(\text{vskw}).$$

Namely, we need to show that the subspace $\mathbb{V}_k^{\text{div}}(\mathbf{r}; \mathbb{M}) \cap \ker(\text{vskw})$ derived via BGG corresponds to the finite element space $\mathbb{V}_k^{\text{div}}(\mathbf{r}; \mathbb{S})$ defined by DoFs (32).

The inclusion $\mathbb{V}_k^{\text{div}}(\mathbf{r}; \mathbb{S}) \subseteq \mathbb{V}_k^{\text{div}}(\mathbf{r}; \mathbb{M}) \cap \ker(\text{vskw})$ is evident. To establish their equality, it suffices to demonstrate that

$$\dim \mathbb{V}_k^{\text{div}}(\mathbf{r}; \mathbb{S}) = \dim(\mathbb{V}_k^{\text{div}}(\mathbf{r}; \mathbb{M}) \cap \ker(\text{vskw})),$$

which is equivalent to showing

$$(34) \quad \dim \mathbb{V}_k^{\text{div}}(\mathbf{r}; \mathbb{M}) - \dim \mathbb{V}_k^{\text{div}}(\mathbf{r}; \mathbb{S}) = \dim \mathbb{V}_k^{L^2}(\mathbf{r}; \mathbb{R}^3),$$

since we have proved that $\text{vskw} : \mathbb{V}_k^{\text{div}}(\mathbf{r}; \mathbb{M}) \rightarrow \mathbb{V}_k^{L^2}(\mathbf{r}; \mathbb{R}^3)$ is surjective.

In the case where $r^f \geq 0$, we have $\mathbb{V}_k^{\text{div}}(\mathbf{r}; \mathbb{X}) = \mathbb{V}_k(\mathbf{r}) \otimes \mathbb{X}$ for $\mathbb{X} = \mathbb{M}, \mathbb{S}$, or \mathbb{R}^3 . Consequently, (34) trivially holds. Let us now consider the case where $r^f = -1$ and $r^e \geq 0$. For the vertex and edge DoFs (32a)-(32b), we find that $\dim \mathbb{M} - \dim \mathbb{S} = \dim \mathbb{R}^3$. The face DoFs (32d)-(32e) remain the same. The only remaining dimension change is within the bubble spaces, and this can be computed as follows:

$$\begin{aligned} & \dim \mathbb{B}_k^{\text{div}}(\mathbf{r}; \mathbb{M}) - \dim \mathbb{B}_k^{\text{div}}(\mathbf{r}; \mathbb{S}) \\ &= \dim \mathbb{B}_k(\mathbf{r}_+; \mathbb{M}) - \dim \mathbb{B}_k(\mathbf{r}_+; \mathbb{S}) \\ & \quad + 4 \dim \mathbb{B}_k(f; \mathbf{r}) \otimes \mathcal{T}^f(\mathbb{M}) - 4 \dim \mathbb{B}_k(f; \mathbf{r}) \otimes \mathcal{T}^f(\mathbb{S}) \\ &= 3(\dim \mathbb{B}_k(\mathbf{r}_+) + 4 \dim \mathbb{B}_k(f; \mathbf{r})) \\ &= \dim \mathbb{B}_k(\mathbf{r}; \mathbb{R}^3), \end{aligned}$$

where $\mathbb{B}_k^{\text{div}}(\mathbf{r}; \mathbb{M}) = \mathbb{R}^3 \otimes \mathbb{B}_k^{\text{div}}(\mathbf{r})$. Hence, (34) holds, and consequently, (33) is confirmed. \square

As $\mathbb{V}_k^{\text{div}}((r^v, 0, -1)^\top; \mathbb{S}) \subset \mathbb{V}_k^{\text{div}}((r^v, -1, -1)^\top; \mathbb{S})$, we also observe the $(\text{div}; \mathbb{S})$ stability for the pair $(r^v, -1, -1)^\top - (r^v - 1, -1, -1)^\top$ when $r^v \geq 1$. The $(\text{div}; \mathbb{S})$ stability for the case with the lowest level of smoothness, i.e., $(0, -1, -1)^\top - (-1, -1, -1)^\top$, has been established in [38], and it appears to be challenging to obtain this result through the BGG construction. Again, cases that can be handled by the BGG construction are slightly smoother.

For the situation where $r^e = -1$, we encounter different variants of $\mathbb{V}_k^{\text{div}}(\mathbf{r}; \mathbb{S})$ elements depending on whether the tangential-normal component is redistributed to faces or not, as discussed in Remark 4.3. Despite these variations, the $(\text{div}; \mathbb{S})$ stability still holds.

Discussion on $(\text{div}; \mathbb{T})$ stability is similar.

Lemma 4.6. *Let \mathbf{r} be a smoothness vector and k large enough satisfying: both $(\mathbf{r} + 1, \mathbf{r}, k + 1)$ and $(\mathbf{r}, \mathbf{r} \ominus 1, k)$ are div stable. Then we have the $(\text{div}; \mathbb{T})$ stability:*

$$\text{div} \mathbb{V}_k^{\text{div}}(\mathbf{r}; \mathbb{T}) = \mathbb{V}_{k-1}^{L^2}(\mathbf{r} \ominus 1; \mathbb{R}^3).$$

Proof. The dimension identity for traceless matrices

$$(35) \quad \dim \mathbb{V}_{k-1}^{\text{div}}(\mathbf{r}; \mathbb{M}) - \dim \mathbb{V}_{k-1}^{\text{div}}(\mathbf{r}; \mathbb{T}) = \dim \mathbb{V}_k^{L^2}(\mathbf{r})$$

holds for smoothness vector \mathbf{r} with $r^v \geq 0$ but without requirement $r^e \geq 0$ as all normal components can be redistributed to faces. \square

We summarize the result below by treating \mathbb{S} and \mathbb{T} together.

Theorem 4.7. *Assume the smoothness vector \mathbf{r} and polynomial degree k satisfy:*

- (1) *Case $r^v \geq 1$ and $r^e \geq 0$: both $(\mathbf{r} + 1, \mathbf{r}, k + 1)$ and $(\mathbf{r}, \mathbf{r} \ominus 1, k)$ are div stable;*
- (2) *Case $\mathbf{r} = (r^v, -1, -1)$ with $r^v \geq 1$: $k \geq \max\{2r^v + 1, 4\}$;*
- (3) *Case $\mathbf{r} = (0, -1, -1)^\top$: $k \geq \begin{cases} 4, & \text{for } \mathbb{X} = \mathbb{S}, \\ 2, & \text{for } \mathbb{X} = \mathbb{T}. \end{cases}$*

Then we have the $(\text{div}; \mathbb{X})$ stability, for $\mathbb{X} = \mathbb{S}$ or \mathbb{T} ,

$$(36) \quad \text{div } \mathbb{V}_k^{\text{div}}(\mathbf{r}; \mathbb{X}) = \mathbb{V}_{k-1}^{L^2}(\mathbf{r} \ominus 1; \mathbb{R}^3).$$

When (36) is satisfied, we will refer to the triple $(\mathbf{r}, \mathbf{r} \ominus 1, k)$ as being $(\text{div}; \mathbb{X})$ stable. The conditions presented in Theorem 4.7 are sufficient to establish this stability, although they might not be necessary in all cases. It is important to note that due to the redistribution of edge DoFs to faces, when $r^v = 0$, for $\mathbb{X} = \mathbb{T}$, the face DoFs (27c)-(27d) include $\mathbb{P}_1^3(f)$ for $k \geq 2$, which is necessary to prove the div stability. On the other hand, for $\mathbb{X} = \mathbb{S}$, $k \geq 4$ is required, since the face DoF (32e) contains a smaller face bubble $\mathbb{B}_k(f; \mathbf{r}_+)$ that demands higher degree of polynomial.

By the same proof, we also have the div stability for the bubble spaces and include the proof in Appendix: Lemma A.3 and Lemma A.5.

Lemma 4.8. *Assume the polynomial degree $k \geq \max\{2r^v + 1, 2\}$, and the smoothness vector \mathbf{r} satisfy either:*

- (1) *$r^v \geq 2r^e + 1$ and $r^e \geq 2(r^f + 1)$, or*
- (2) *$r^v \geq 0$ and $r^e = r^f = -1$.*

Then we have the $(\text{div}; \mathbb{X})$ stability, for $\mathbb{X} = \mathbb{S}$ or \mathbb{T} ,

$$\text{div } \mathbb{B}_k^{\text{div}}(\mathbf{r}; \mathbb{X}) = \mathbb{B}_{k-1}(\mathbf{r} \ominus 1; \mathbb{R}^3)/\text{RX}.$$

Here $\text{RX} = \text{RM}$ for $\mathbb{X} = \mathbb{S}$, and $\text{RX} = \text{RT}$ for $\mathbb{X} = \mathbb{T}$.

4.3. Inequality constraints. We can apply one \sim operation to get the div stability with an inequality constraint on the smoothness vectors.

Corollary 4.9. *Let $(\mathbf{r}_2, \mathbf{r}_2 \ominus 1, k)$ be $(\text{div}; \mathbb{X})$ stable and $\mathbf{r}_3 \geq \mathbf{r}_2 \ominus 1$. Define*

$$\mathbb{V}_k^{\text{div}}(\mathbf{r}_2, \mathbf{r}_3; \mathbb{X}) = \{\boldsymbol{\tau} \in \mathbb{V}_k^{\text{div}}(\mathbf{r}_2; \mathbb{X}) : \text{div } \boldsymbol{\tau} \in \mathbb{V}_{k-1}^{L^2}(\mathbf{r}_3; \mathbb{R}^3)\}.$$

Then we have the $(\text{div}; \mathbb{X})$ stability

$$\text{div } \mathbb{V}_k^{\text{div}}(\mathbf{r}_2, \mathbf{r}_3; \mathbb{X}) = \mathbb{V}_{k-1}^{L^2}(\mathbf{r}_3; \mathbb{R}^3).$$

The subspace $\mathbb{V}_k^{\text{div}}(\mathbf{r}_2, \mathbf{r}_3; \mathbb{X})$ always exists as $\mathbb{V}_{k-1}^{L^2}(\mathbf{r}_3; \mathbb{R}^3) \subseteq \mathbb{V}_{k-1}^{L^2}(\mathbf{r}_2 \ominus 1; \mathbb{R}^3)$. However, the challenge lies in formulating local DoFs for this subspace. In this pursuit, we draw insights from our recent work, as outlined in [23, Section 4.4]. We add DoFs to determine $\text{div } \boldsymbol{\tau}$ first but remove non-free index (white blocks in Fig. 3 and 4) in the t - n decomposition. For example, for face DoFs, we remove component $\partial_n^j(\mathbf{t}_1^\top \boldsymbol{\tau} \mathbf{t}_1)$ from vector $\partial_n^j(\boldsymbol{\tau} \mathbf{t}_1)$ as $\mathbf{t}_1 \otimes \mathbf{t}_1 \notin \mathcal{T}^f(\mathbb{T})$. Similarly remove $\mathbf{t}^\top \boldsymbol{\tau} \mathbf{t}$ from the edge DoF.

To save space, we only write out DoFs for $\mathbb{V}_k^{\text{div}}(\mathbf{r}_2, \mathbf{r}_3; \mathbb{S})$. Take $\mathbb{P}_k(T; \mathbb{S})$ as the space of shape functions with $k \geq \max\{2r_2^v + 1, 2r_3^v + 2\}$. Assume $\mathbf{r}_3 \geq \mathbf{r}_2 \ominus 1, r_2^v \geq 0$ and

$(\mathbf{r}_2, \mathbf{r}_2 \ominus 1, k)$ is $(\text{div}; \mathbb{S})$ stable. The DoFs are

$$(37a) \quad \nabla^i \boldsymbol{\tau}(\mathbf{v}), \quad i = 0, \dots, r_2^v,$$

$$(37b) \quad \nabla^j \text{div } \boldsymbol{\tau}(\mathbf{v}), \quad j = r_2^v, \dots, r_3^v,$$

$$(37c) \quad \int_e (\mathbf{n}_i^\top \boldsymbol{\tau} \mathbf{n}_j) q \, ds, \quad q \in \mathbb{B}_k(e; r_2^v), 1 \leq i \leq j \leq 2, \text{ if } r_2^e = -1,$$

$$(37d) \quad \int_e \frac{\partial^j (\mathbf{t}^\top \boldsymbol{\tau} \mathbf{t})}{\partial n_1^i \partial n_2^{j-i}} q \, ds, \quad q \in \mathbb{B}_{k-j}(e; r_2^v - j), 0 \leq i \leq j \leq r_2^e,$$

$$(37e) \quad \int_e \frac{\partial^j (\mathbf{t}^\top \boldsymbol{\tau} \mathbf{n}_1)}{\partial n_1^i \partial n_2^{j-i}} q \, ds, \quad q \in \mathbb{B}_{k-j}(e; r_2^v - j), 0 \leq i \leq j \leq r_2^e,$$

$$(37f) \quad \int_e \frac{\partial^j (\mathbf{n}_1^\top \boldsymbol{\tau} \mathbf{n}_1)}{\partial n_1^i \partial n_2^{j-i}} q \, ds, \quad q \in \mathbb{B}_{k-j}(e; r_2^v - j), 0 \leq i \leq j \leq r_2^e,$$

$$(37g) \quad \int_e \partial_{n_1}^j (\boldsymbol{\tau} \mathbf{n}_2) \cdot \mathbf{q} \, ds, \quad \mathbf{q} \in \mathbb{B}_{k-j}^3(e; r_2^v - j), 0 \leq j \leq r_2^e,$$

$$(37h) \quad \int_e \frac{\partial^j (\text{div } \boldsymbol{\tau})}{\partial n_1^i \partial n_2^{j-i}} \cdot \mathbf{q} \, ds, \quad \mathbf{q} \in \mathbb{B}_{k-1-j}^3(e; r_3^v - j), 0 \leq i \leq j \leq r_3^e,$$

$$(37i) \quad \int_f (\Pi_f \boldsymbol{\tau} \mathbf{n}) \cdot \mathbf{q} \, dS, \quad \mathbf{q} \in (\mathbb{B}_k^{\text{div}}(f; \mathbf{r}_2) / \text{RM}(f)) \oplus \text{RM}(f),$$

$$(37j) \quad \int_f (\mathbf{n}^\top \boldsymbol{\tau} \mathbf{n}) q \, dS, \quad q \in (\mathbb{B}_k(f; (\mathbf{r}_2)_+) / \mathbb{P}_1(f)) \oplus \mathbb{P}_1(f),$$

$$(37k) \quad \int_f \partial_n^j (\Pi_f \boldsymbol{\tau} \Pi_f) : \mathbf{q} \, dS, \quad \mathbf{q} \in \mathbb{B}_{k-j}(f; \mathbf{r}_2 - j) \otimes \mathbb{S}(f), 0 \leq j \leq r_2^f,$$

$$(37l) \quad \int_f \partial_n^j (\text{div } \boldsymbol{\tau}) \cdot \mathbf{q} \, dS, \quad \mathbf{q} \in \mathbb{B}_{k-1-j}^3(f; \mathbf{r}_3 - j), 0 \leq j \leq r_3^f,$$

$$(37m) \quad \int_T (\text{div } \boldsymbol{\tau}) \cdot \mathbf{q} \, dx, \quad \mathbf{q} \in \mathbb{B}_{k-1}^3(\mathbf{r}_3) / \text{RM},$$

$$(37n) \quad \int_T \boldsymbol{\tau} : \mathbf{q} \, dx, \quad \mathbf{q} \in \mathbb{B}_k^{\text{div}}(\mathbf{r}_2; \mathbb{S}) \cap \ker(\text{div})$$

for each $\mathbf{v} \in \Delta_0(T)$, $e \in \Delta_1(T)$ and $f \in \Delta_2(T)$.

Lemma 4.10. *Let $(\mathbf{r}_2, \mathbf{r}_2 \ominus 1, k)$ be $(\text{div}; \mathbb{S})$ stable and $\mathbf{r}_3 \geq \mathbf{r}_2 \ominus 1$. The DoFs (37) are uni-solvent for $\mathbb{P}_k(T; \mathbb{S})$.*

Proof. The introduced DoFs given by (37b), (37h), and (37l)-(37m) play a crucial role in characterizing the divergence of $\boldsymbol{\tau}$. The total number of these DoFs, along with (37a), is independent of \mathbf{r}_3 , specifically given by the expression:

$$6 \binom{r_2^v + 3}{3} + \dim \mathbb{P}_{k-1}^3(T) - \dim \text{RM} - 3 \binom{r_2^v + 2}{3}.$$

This count remains unaffected by variations in \mathbf{r}_3 . For convenience, we can proceed with $\mathbf{r}_3 = \mathbf{r}_2 \ominus 1$. Then by making comparisons with (32), we deduce that the number of DoFs (37) is equal to $\dim \mathbb{P}_k(T; \mathbb{S})$.

Suppose we have $\boldsymbol{\tau} \in \mathbb{P}_k(T; \mathbb{S})$ satisfying the vanishing conditions for all DoFs (37). It then follows that $\boldsymbol{\tau} \mathbf{n}|_{\partial T} = \mathbf{0}$. By applying integration by parts and utilizing the vanishing

DoFs (37i)-(37j), we deduce the critical relation:

$$\int_T (\operatorname{div} \boldsymbol{\tau}) \cdot \mathbf{q} \, dx = 0, \quad \mathbf{q} \in \text{RM}.$$

This result, combined with DoFs (37b), (37h), and (37l)-(37m), which pertain to the divergence of $\boldsymbol{\tau}$, leads to the conclusion that $\operatorname{div} \boldsymbol{\tau} = \mathbf{0}$.

The situation is somewhat analogous when dealing with edges. By expressing div in the frame $\{\mathbf{t}, \mathbf{n}_1, \mathbf{n}_2\}$, we uncover a representation of $\operatorname{div} \boldsymbol{\tau}$ that encompasses the partial derivatives along tangential (\mathbf{t}) and normal ($\mathbf{n}_1, \mathbf{n}_2$) directions:

$$\operatorname{div} \boldsymbol{\tau} = \partial_t(\boldsymbol{\tau} \mathbf{t}) + \partial_{n_1}(\boldsymbol{\tau} \mathbf{n}_1) + \partial_{n_2}(\boldsymbol{\tau} \mathbf{n}_2).$$

Taking into account (37a)-(37h), it becomes evident that $\nabla^j \boldsymbol{\tau}$ vanishes along edges, where $0 \leq j \leq r_2^e$. A similar reasoning applies to faces, where the decomposition into $\{\mathbf{n}, \mathbf{t}_1, \mathbf{t}_2\}$ aids in expressing

$$\operatorname{div} \boldsymbol{\tau} = \partial_n(\boldsymbol{\tau} \mathbf{n}) + \partial_{t_1}(\boldsymbol{\tau} \mathbf{t}_1) + \partial_{t_2}(\boldsymbol{\tau} \mathbf{t}_2),$$

and highlighting that $\nabla^j \boldsymbol{\tau}$ vanishes along faces for $0 \leq j \leq r_2^f$. This collective analysis demonstrates that $\boldsymbol{\tau} \in \mathbb{B}_k^{\operatorname{div}}(\mathbf{r}_2; \mathbb{S}) \cap \ker(\operatorname{div})$. This observation, coupled with DoF (37n), solidifies the conclusion that $\boldsymbol{\tau} = \mathbf{0}$. \square

Example 4.11. The space $\mathbb{V}_k^{\operatorname{div}}(\mathbf{r}_2, \mathbf{r}_3; \mathbb{S})$ for $\mathbf{r}_2 = \mathbf{r}_3 = (0, -1, -1)^\top$ and $k \geq 4$ has been constructed recently in [35].

4.4. Smooth $H(\operatorname{div} \operatorname{div}^+; \mathbb{S})$ and $H(\operatorname{div} \operatorname{div}; \mathbb{S})$ elements. In this subsection, we proceed to construct various $H(\operatorname{div} \operatorname{div})$ -conforming finite elements characterized by a smoothness vector \mathbf{r} . Define the spaces:

$$H(\operatorname{div} \operatorname{div}; \mathbb{S}) := \{\boldsymbol{\tau} \in L^2(\Omega; \mathbb{S}) : \operatorname{div} \operatorname{div} \boldsymbol{\tau} \in L^2(\Omega)\},$$

$$H(\operatorname{div} \operatorname{div}^+; \mathbb{S}) := \{\boldsymbol{\tau} \in L^2(\Omega; \mathbb{S}) : \operatorname{div} \boldsymbol{\tau} \in H(\operatorname{div}, \Omega)\}.$$

It is evident that the inclusion $H(\operatorname{div} \operatorname{div}^+; \mathbb{S}) \subset H(\operatorname{div} \operatorname{div}; \mathbb{S})$ holds.

We will now proceed to construct finite elements that are $H(\operatorname{div} \operatorname{div}^+; \mathbb{S})$ -conforming. Specifically, when $r^f \geq 1$, we define $\mathbb{V}_k^{\operatorname{div} \operatorname{div}^+}(\mathbf{r}; \mathbb{S})$ as $\mathbb{V}_k(\mathbf{r}) \otimes \mathbb{S}$. For the cases where $r^f = -1$ or $r^f = 0$, we will make use of a recent approach presented in [37] and [20]. The space of shape functions is still $\mathbb{P}_k(T; \mathbb{S})$. By modifying the DoFs (32), which are originally designed for $H(\operatorname{div}; \mathbb{S})$ -conforming finite elements, we ensure that $\operatorname{div} \boldsymbol{\tau}$ belongs to $\mathbb{V}_{k-1}^{\operatorname{div}}(\mathbf{r} \ominus 1)$, satisfying the $H(\operatorname{div}; \mathbb{S})$ -conforming condition.

Take $\mathbb{P}_k(T; \mathbb{S})$ as the shape function space. The DoFs are

$$(38a) \quad \nabla^j \boldsymbol{\tau}(\mathbf{v}), \quad j = 0, 1, \dots, r^v,$$

$$(38b) \quad \int_e \frac{\partial^j \boldsymbol{\tau}}{\partial n_1^i \partial n_2^{j-i}} : \mathbf{q} \, ds, \quad \mathbf{q} \in \mathbb{B}_{k-j}(e; r^v - j) \otimes \mathbb{S}, 0 \leq i \leq j \leq r^e,$$

$$(38c) \quad \int_e (\mathbf{n}_i^\top \boldsymbol{\tau} \mathbf{n}_j) q \, ds, \quad \mathbf{q} \in \mathbb{B}_k(e; r^v), 1 \leq i \leq j \leq 2, \text{ if } r^e = -1,$$

$$(38d) \quad \int_f \boldsymbol{\tau} : \mathbf{q} \, dS, \quad \mathbf{q} \in \mathbb{B}_k(f; \mathbf{r}) \otimes \mathbb{S}, \text{ if } r^f = 0,$$

$$(38e) \quad \int_f (\Pi_f \boldsymbol{\tau} \mathbf{n}) \cdot \mathbf{q} \, dS, \quad \mathbf{q} \in \mathbb{B}_k^{\operatorname{div}}(f; \mathbf{r}) / \text{RM}(f) \oplus \text{RM}(f), \text{ if } r^f = -1,$$

$$(38f) \quad \int_f (\mathbf{n}^\top \boldsymbol{\tau} \mathbf{n}) q \, dS, \quad q \in \mathbb{B}_k(f; \mathbf{r}_+) / \mathbb{P}_1(f) \oplus \mathbb{P}_1(f), \text{ if } r^f = -1,$$

$$(38g) \quad \int_f \mathbf{n}^\top \operatorname{div} \boldsymbol{\tau} \, q \, dS, \quad q \in \mathbb{B}_{k-1}(f; \mathbf{r} \ominus 1),$$

$$(38h) \quad \int_T (\operatorname{div} \boldsymbol{\tau}) \cdot \mathbf{q} \, dx, \quad \mathbf{q} \in \mathbb{B}_{k-1}^{\operatorname{div}}(\mathbf{r} \ominus 1)/\operatorname{RM},$$

$$(38i) \quad \int_T \boldsymbol{\tau} : \mathbf{q} \, dx, \quad \mathbf{q} \in \mathbb{B}_k^{\operatorname{div}}(\mathbf{r}; \mathbb{S}) \cap \ker(\operatorname{div}),$$

for each $v \in \Delta_0(T)$, $e \in \Delta_1(T)$ and $f \in \Delta_2(T)$.

Lemma 4.12. *Let $r^f = -1, 0$. The DoFs (38) are uni-solvent for $\mathbb{P}_k(T; \mathbb{S})$.*

Proof. We first consider the case when $r^f = -1$. If we compare the DoFs (32) for constructing $\mathbb{V}_k^{\operatorname{div}}(\mathbf{r}; \mathbb{S})$ with the DoFs required for $H(\operatorname{div} \operatorname{div}^+; \mathbb{S})$ -conforming finite elements, the primary distinction lies in the volume DoF (32f) for $\mathbb{B}_k^{\operatorname{div}}(\mathbf{r}; \mathbb{S})$. In the new context, this particular DoF is replaced by three alternative DoFs: (38g), (38h), and (38i).

Let $E_0 = \mathbb{B}_k^{\operatorname{div}}(\mathbf{r}; \mathbb{S}) \cap \ker(\operatorname{div})$, and let E_0^\perp denote its L^2 -orthogonal complement of $\mathbb{B}_k^{\operatorname{div}}(\mathbf{r}; \mathbb{S})$. By performing a decomposition of the dual space, we arrive at:

$$(\mathbb{B}_k^{\operatorname{div}}(\mathbf{r}; \mathbb{S}))' = (E_0)' \oplus (E_0^\perp)'.$$

DoF (38i) is exactly a basis of $(E_0)'$. The subspace $\operatorname{div} E_0^\perp$ can be uniquely determined through the DoFs (38g) and (38h), both of which are consistent with the requirements for constructing $H(\operatorname{div})$ -conforming elements.

As we count the dimensions, it is essential to note that $\operatorname{div} \mathbb{B}_k^{\operatorname{div}}(\mathbf{r}; \mathbb{S}) = \mathbb{B}_{k-1}^3(\mathbf{r} \ominus 1)/\operatorname{RM}$. The difference in the number of DoFs between (32f) and the newly introduced DoFs (38g)-(38i) is given by:

$$\dim \mathbb{B}_{k-1}^3(T; \mathbf{r} \ominus 1) - \dim \mathbb{B}_{k-1}^{\operatorname{div}}(T; \mathbf{r} \ominus 1) - 4 \dim \mathbb{B}_{k-1}(f; \mathbf{r} \ominus 1) = 0.$$

So the sum of number of DoFs (38) is equal to $\mathbb{P}_k(T; \mathbb{S})$.

Now, let $\boldsymbol{\tau} \in \mathbb{P}_k(T; \mathbb{S})$ and assume that all the DoFs (38a)-(38i) vanish. Due to the vanishing DoFs (38a)-(38b) and (38g), we can infer that $\operatorname{div} \boldsymbol{\tau} \in \mathbb{B}_{k-1}^{\operatorname{div}}(\mathbf{r} \ominus 1)$. By considering the vanishing DoFs (38d)-(38f) and the integration by parts, we deduce that

$$\int_T (\operatorname{div} \boldsymbol{\tau}) \cdot \mathbf{q} \, dx = 0 \quad \forall \mathbf{q} \in \operatorname{RM},$$

which means $\operatorname{div} \boldsymbol{\tau} \in \mathbb{B}_{k-1}^{\operatorname{div}}(\mathbf{r} \ominus 1)/\operatorname{RM}$. This together with the vanishing DoF (38h) yields $\operatorname{div} \boldsymbol{\tau} = \mathbf{0}$. Finally, utilizing the uniqueness of the DoFs (32) for $H(\operatorname{div}; \mathbb{S})$ -conforming finite elements, we conclude that $\boldsymbol{\tau} = \mathbf{0}$.

This completes the explanation of the construction for $H(\operatorname{div} \operatorname{div}^+; \mathbb{S})$ -conforming finite elements for the case $r^f = -1$. The case for $r^f = 0$ follows a similar logic, with the primary difference being in the structure of the bubble space $\mathbb{B}_k^{\operatorname{div}}(\mathbf{r}; \mathbb{S}) = \mathbb{B}_k(\mathbf{r}) \otimes \mathbb{S}$. \square

When $r^f \geq 1$, $\mathbb{V}_k^{\operatorname{div} \operatorname{div}^+}(\mathbf{r}; \mathbb{S}) = \mathbb{V}_k(\mathbf{r}) \otimes \mathbb{S}$. When $r^f = -1, 0$, define

$$\mathbb{V}_k^{\operatorname{div} \operatorname{div}^+}(\mathbf{r}; \mathbb{S}) = \{\boldsymbol{\tau} \in L^2(\Omega; \mathbb{S}) : \boldsymbol{\tau}|_T \in \mathbb{P}_k(T; \mathbb{S}) \text{ for all } T \in \mathcal{T}_h, \\ \text{and all the DoFs (38) are single-valued}\}.$$

Due to DoFs (38d)-(38g), $\mathbb{V}_k^{\operatorname{div} \operatorname{div}^+}(\mathbf{r}; \mathbb{S}) \subset H(\operatorname{div} \operatorname{div}^+; \mathbb{S})$.

Next we use the following BGG diagram

$$\begin{array}{ccccc} \mathbb{V}_k^{\text{div div}^+}(\mathbf{r}; \mathbb{S}) & \xrightarrow{\text{div}} & \mathbb{V}_{k-1}^{\text{div}}(\mathbf{r} \ominus 1) & \longrightarrow & \mathbf{0} \\ & & \nearrow \text{id} & & \\ \mathbb{V}_{k-1}^{\text{div}}(\mathbf{r} \ominus 1) & \xrightarrow{\text{div}} & \mathbb{V}_{k-2}^{L^2}(\mathbf{r} \ominus 2) & \longrightarrow & \mathbf{0} \end{array}$$

to prove the divdiv stability.

Lemma 4.13. *Assume $(\mathbf{r}, \mathbf{r} \ominus 1, k)$ is $(\text{div}; \mathbb{S})$ stable, and $r^f = -1, 0$. It holds that*

$$(39) \quad \text{div } \mathbb{V}_k^{\text{div div}^+}(\mathbf{r}; \mathbb{S}) = \mathbb{V}_{k-1}^{\text{div}}(\mathbf{r} \ominus 1).$$

Proof. Clearly $\text{div } \mathbb{V}_k^{\text{div div}^+}(\mathbf{r}; \mathbb{S}) \subseteq \mathbb{V}_{k-1}^{\text{div}}(\mathbf{r} \ominus 1)$, then it suffices to count the dimensions. Both $\dim \mathbb{V}_k^{\text{div}}(\mathbf{r}; \mathbb{S}) - \dim \mathbb{V}_k^{\text{div div}^+}(\mathbf{r}; \mathbb{S})$ and $\dim \mathbb{V}_{k-1}^{L^2}(\mathbf{r} \ominus 1; \mathbb{R}^3) - \dim \mathbb{V}_{k-1}^{\text{div}}(\mathbf{r} \ominus 1)$ equal

$$(4|\Delta_3(\mathcal{T}_h)| - |\Delta_2(\mathcal{T}_h)|) \dim \mathbb{B}_{k-1}(f; \mathbf{r} \ominus 1),$$

that is

$$\dim \mathbb{V}_k^{\text{div}}(\mathbf{r}; \mathbb{S}) - \dim \mathbb{V}_k^{\text{div div}^+}(\mathbf{r}; \mathbb{S}) = \dim \mathbb{V}_{k-1}^{L^2}(\mathbf{r} \ominus 1; \mathbb{R}^3) - \dim \mathbb{V}_{k-1}^{\text{div}}(\mathbf{r} \ominus 1).$$

As $\text{div}(\mathbb{V}_k^{\text{div}}(\mathbf{r}; \mathbb{S})) = \mathbb{V}_{k-1}^{L^2}(\mathbf{r} \ominus 1; \mathbb{R}^3)$ and the modification will not change $\ker(\text{div})$, we get $\dim \text{div } \mathbb{V}_k^{\text{div div}^+}(\mathbf{r}; \mathbb{S}) = \dim \mathbb{V}_{k-1}^{\text{div}}(\mathbf{r} \ominus 1)$ and (39) follows. \square

Combined the div stability for $(\mathbf{r} \ominus 1, \mathbf{r} \ominus 2, k-1)$, we conclude the divdiv stability.

Corollary 4.14. *Assume $(\mathbf{r}, \mathbf{r} \ominus 1, k)$ is $(\text{div}; \mathbb{S})$ stable and $(\mathbf{r} \ominus 1, \mathbf{r} \ominus 2, k-1)$ is div stable. Then it holds that*

$$\text{div div } \mathbb{V}_k^{\text{div div}^+}(\mathbf{r}; \mathbb{S}) = \mathbb{V}_{k-2}^{L^2}(\mathbf{r} \ominus 2).$$

Next we modify the DoFs (38) slightly to get an $H(\text{div div}; \mathbb{S})$ -conforming element. Take $\mathbb{P}_k(T; \mathbb{S})$ as the space of shape functions. When $r^f \geq 1$, define $\mathbb{V}_k^{\text{div div}}(\mathbf{r}; \mathbb{S}) := \mathbb{V}_k^{\text{div div}^+}(\mathbf{r}; \mathbb{S}) = \mathbb{V}_k(\mathbf{r}) \otimes \mathbb{S}$. For $r^f = -1, 0$, the degrees of freedom are

$$(40a) \quad \nabla^j \boldsymbol{\tau}(\mathbf{v}), \quad j = 0, 1, \dots, r^v, \mathbf{v} \in \Delta_0(T),$$

$$(40b) \quad \int_e \frac{\partial^j \boldsymbol{\tau}}{\partial n_1^i \partial n_2^{j-i}} : \mathbf{q} \, ds, \quad \mathbf{q} \in \mathbb{P}_{k-2(r^v+1)+j}(e; \mathbb{S}), 0 \leq i \leq j \leq r^e, e \in \Delta_1(T),$$

$$(40c) \quad \int_e (\mathbf{n}_i^\top \boldsymbol{\tau} \mathbf{n}_j) q \, ds, \quad q \in \mathbb{B}_k(e; r^v), 1 \leq i \leq j \leq 2, e \in \Delta_1(T), \text{ if } r^e = -1,$$

$$(40d) \quad \int_f \boldsymbol{\tau} : \mathbf{q} \, dS, \quad \mathbf{q} \in \mathbb{B}_k(f; \mathbf{r}) \otimes \mathbb{S}, f \in \Delta_2(T), \text{ if } r^f = 0,$$

$$(40e) \quad \int_f (\mathbf{n}^\top \boldsymbol{\tau} \mathbf{n}) q \, dS, \quad q \in \mathbb{B}_k(f; \mathbf{r}_+), f \in \Delta_2(T), \text{ if } r^f = -1,$$

$$(40f) \quad \int_f \text{tr}_2^{\text{div div}}(\boldsymbol{\tau}) q \, dS, \quad q \in \mathbb{B}_{k-1}(f; \mathbf{r} \ominus 1), f \in \Delta_2(T),$$

$$(40g) \quad \int_T (\text{div } \boldsymbol{\tau}) \cdot \mathbf{q} \, dx, \quad \mathbf{q} \in \mathbb{B}_{k-1}^{\text{div}}(\mathbf{r} \ominus 1)/\text{RM},$$

$$(40h) \quad \int_T \boldsymbol{\tau} : \mathbf{q} \, dx, \quad \mathbf{q} \in \mathbb{B}_k^{\text{div}}(\mathbf{r}; \mathbb{S}) \cap \ker(\text{div}),$$

$$(40i) \quad \int_f (\Pi_f \boldsymbol{\tau} \mathbf{n}) \cdot \mathbf{q} \, dS, \quad \mathbf{q} \in \mathbb{B}_k^{\text{div}}(f; \mathbf{r}), f \in \Delta_2(T), \text{ if } r^f = -1.$$

The modification is introduced in (40f), where we now enforce the continuity condition:

$$\text{tr}_2^{\text{div div}}(\boldsymbol{\tau}) = \mathbf{n}^\top \text{div } \boldsymbol{\tau} + \text{div}_f(\Pi_f \boldsymbol{\tau} \mathbf{n})$$

instead of enforcing continuity for both $\mathbf{n}^\top \text{div } \boldsymbol{\tau}$ and $\Pi_f \boldsymbol{\tau} \mathbf{n}$. Notably, the face DoF (40i) associated with $\Pi_f \boldsymbol{\tau} \mathbf{n}$ has been moved to the end to signify its role as a local DoF that contributes to the divdiv bubble space. This implies that (40i) can take different values in different elements containing the shared face f .

Defining the space

$$\mathbb{V}_k^{\text{div div}}(\mathbf{r}; \mathbb{S}) = \{ \boldsymbol{\tau} \in L^2(\Omega; \mathbb{S}) : \boldsymbol{\tau}|_T \in \mathbb{P}_k(T; \mathbb{S}) \text{ for all } T \in \mathcal{T}_h, \\ \text{and all the DoFs (40a)-(40h) are single-valued} \},$$

we find that for the case $r^f = 0$, $\mathbb{V}_k^{\text{div div}}(\mathbf{r}; \mathbb{S})$ and $\mathbb{V}_k^{\text{div div}^+}(\mathbf{r}; \mathbb{S})$ are indistinguishable. However, in the scenario where $r^f = -1$, again due to (40i), we can deduce that:

$$\mathbb{V}_k^{\text{div div}^+}(\mathbf{r}; \mathbb{S}) \subset \mathbb{V}_k^{\text{div div}}(\mathbf{r}; \mathbb{S}).$$

Consequently, this inclusion relationship ensures the divdiv stability.

Corollary 4.15. *Assume $(\mathbf{r}, \mathbf{r} \ominus 1, k)$ is $(\text{div}; \mathbb{S})$ stable and $(\mathbf{r} \ominus 1, \mathbf{r} \ominus 2, k - 1)$ is div stable. Then it holds that*

$$\text{div div } \mathbb{V}_k^{\text{div div}}(\mathbf{r}; \mathbb{S}) = \mathbb{V}_{k-2}^{L^2}(\mathbf{r} \ominus 2).$$

In a similar vein to the inequality constraint that ensures $(\text{div}; \mathbb{S})$ stability, we also have a comparable flexibility when it comes to divdiv elements. Consider the scenario where $(\mathbf{r}_2, \mathbf{r}_3, k)$ are $(\text{div}; \mathbb{S})$ stable, where $\mathbf{r}_3 \geq \mathbf{r}_2 \ominus 1$, and further assume that $(\mathbf{r}_3, \mathbf{r}_3 \ominus 1, k - 1)$ exhibit div stability. In such cases, following the sequence

$$\mathbb{V}_k^{\text{div}}(\mathbf{r}_2, \mathbf{r}_3; \mathbb{S}) \xrightarrow{\text{div}} \mathbb{V}_{k-1}^{\text{div}}(\mathbf{r}_3) \xrightarrow{\text{div}} \mathbb{V}_{k-2}^{L^2}(\mathbf{r}_3 \ominus 1) \rightarrow 0,$$

and the approach in Section 4.3, we can similarly define the spaces $\mathbb{V}_k^{\text{div div}^+}(\mathbf{r}_2, \mathbf{r}_3 \ominus 1; \mathbb{S})$ and $\mathbb{V}_k^{\text{div div}}(\mathbf{r}_2, \mathbf{r}_3 \ominus 1; \mathbb{S})$, with the constraint $\mathbf{r}_3 \geq \mathbf{r}_2 \ominus 1$.

Regarding the changes in DoFs, when $r_3^f \geq 0$, $\mathbb{V}_{k-1}^{\text{div}}(\mathbf{r}_3) = \mathbb{V}_{k-1}^{\text{grad}}(\mathbf{r}_3; \mathbb{R}^3)$. This implies that $\mathbb{V}_k^{\text{div div}^+}(\mathbf{r}_2, \mathbf{r}_3 \ominus 1; \mathbb{S}) = \mathbb{V}_k^{\text{div}}(\mathbf{r}_2, \mathbf{r}_3; \mathbb{S})$, and therefore, there is no need to modify the DoFs (37). On the other hand, when $r_3^f = -1$, we partition the DoF (37m) associated with the bubble component of $\text{div } \boldsymbol{\tau}$ into:

$$(41a) \quad \int_f \mathbf{n}^\top \text{div } \boldsymbol{\tau} \, q \, dS, \quad q \in \mathbb{B}_{k-1}(f; \mathbf{r}_3), f \in \Delta_2(T),$$

$$(41b) \quad \int_T (\text{div } \boldsymbol{\tau}) \cdot \mathbf{q} \, dx, \quad \mathbf{q} \in \mathbb{B}_{k-1}^{\text{div}}(\mathbf{r}_3)/\text{RM},$$

while retaining all other DoFs from (37). This gives DoFs for $\mathbb{V}_k^{\text{div div}^+}(\mathbf{r}_2, \mathbf{r}_3 \ominus 1; \mathbb{S})$.

To construct $\mathbb{V}_k^{\text{div div}}(\mathbf{r}_2, \mathbf{r}_3 \ominus 1; \mathbb{S})$, we further replace DoFs (41a) by

$$\int_f \text{tr}_2^{\text{div div}}(\boldsymbol{\tau}) \, q \, dS, \quad q \in \mathbb{B}_{k-1}(f; \mathbf{r}_3), f \in \Delta_2(T)$$

and treat (37i) local. The procedure is the same as before and thus the details are skipped.

Corollary 4.16. *Let $(\mathbf{r}_2, \mathbf{r}_3, k)$ be $(\text{div}; \mathbb{S})$ stable with $\mathbf{r}_3 \geq \mathbf{r}_2 \ominus 1$ and $(\mathbf{r}_3, \mathbf{r}_3 \ominus 1, k-1)$ be div stable. Then it holds that*

$$\text{div div } \mathbb{V}_k^{\text{div div}^+}(\mathbf{r}_2, \mathbf{r}_3 \ominus 1; \mathbb{S}) = \text{div div } \mathbb{V}_k^{\text{div div}}(\mathbf{r}_2, \mathbf{r}_3 \ominus 1; \mathbb{S}) = \mathbb{V}_{k-2}^{L^2}(\mathbf{r}_3 \ominus 1).$$

Example 4.17. The space $\mathbb{V}_k^{\text{div div}^+}(\mathbf{r}_2, \mathbf{r}_3 \ominus 1; \mathbb{S})$ for $\mathbf{r}_2 = \mathbf{r}_3 = (0, -1, -1)^\top$ and $k \geq 4$ has been constructed recently in [35].

For convenience, we introduce the following notation:

$$\begin{aligned} \mathbb{B}_k^{\text{div div}^+}(\mathbf{r}; \mathbb{S}) &= \{ \boldsymbol{\tau} \in \mathbb{P}_k(T; \mathbb{S}) : \text{all the DoFs (38a)-(38g) vanish} \}, \\ \mathbb{B}_k^{\text{div div}}(\mathbf{r}; \mathbb{S}) &= \{ \boldsymbol{\tau} \in \mathbb{P}_k(T; \mathbb{S}) : \text{all the DoFs (40a)-(40f) vanish} \}. \end{aligned}$$

By definition, we have the inclusion relationship:

$$\mathbb{B}_k^{\text{div div}^+}(\mathbf{r}; \mathbb{S}) \subseteq \mathbb{B}_k^{\text{div div}}(\mathbf{r}; \mathbb{S}),$$

since the face DoF (40i) associated with $\Pi_f \boldsymbol{\tau} \mathbf{n}$ is zero in the bubble space $\mathbb{B}_k^{\text{div div}^+}(\mathbf{r}; \mathbb{S})$ and non-zero in $\mathbb{B}_k^{\text{div div}}(\mathbf{r}; \mathbb{S})$.

By the same proof with BGG diagram for the bubble spaces, we conclude the divdiv stability for these bubble spaces and refer to Lemma A.7 for detailed proof.

Lemma 4.18. *Assume \mathbf{r} satisfies the condition in Lemma 4.8, $\mathbf{r} \ominus 1$ satisfies the condition in Lemma 3.2, and $k \geq \max\{2r^v + 1, 3\}$. Then it holds that*

$$\text{div div } \mathbb{B}_k^{\text{div div}^+}(\mathbf{r}; \mathbb{S}) = \text{div div } \mathbb{B}_k^{\text{div div}}(\mathbf{r}; \mathbb{S}) = \mathbb{B}_{k-2}^{L^2}(\mathbf{r} \ominus 2) / \mathbb{P}_1(T).$$

5. FINITE ELEMENT COMPLEXES

In the preceding section, our focus was primarily on the last two columns of the diagram (5), where we established the $(\text{div}; \mathbb{X})$ stability. In this section, we turn our attention to the first three columns of the diagram (5) to derive finite element complexes.

5.1. Finite element Hessian complexes. Let

$$\mathbf{r}_0 \geq (4, 2, 1)^\top, \quad \mathbf{r}_1 = \mathbf{r}_0 - 2, \quad \mathbf{r}_2 = \mathbf{r}_1 \ominus 1, \quad \mathbf{r}_3 = \mathbf{r}_2 \ominus 1, \quad k + 2 \geq 2r_0^v + 1.$$

Assume both $(\mathbf{r}_0, \mathbf{r}_0 - 1, \mathbf{r}_1, \mathbf{r}_2)$ and $(\mathbf{r}_0 - 1, \mathbf{r}_1, \mathbf{r}_2, \mathbf{r}_3)$ are valid de Rham smoothness sequences. As a discretization of (13), we will justify the following BGG diagram (42)

$$\begin{array}{ccccccc} \mathbb{V}_{k+2}^{\text{grad}}(\mathbf{r}_0) & \xrightarrow{\text{grad}} & \mathbb{V}_{k+1}^{\text{curl}}(\mathbf{r}_0 - 1) & \xrightarrow{\text{curl}} & \mathbb{V}_k^{\text{div}}(\mathbf{r}_1) \cap \ker(\text{div}) & \xrightarrow{\text{div}} & 0 \\ & \searrow \text{id} & & \nearrow -2 \text{vskw} & & \nearrow \text{tr} & \\ \mathbb{V}_{k+1}^{\text{grad}}(\mathbf{r}_0 - 1; \mathbb{R}^3) & \xrightarrow{\text{grad}} & \widetilde{\mathbb{V}}_k^{\text{curl}}(\mathbf{r}_1; \mathbb{M}) & \xrightarrow{\text{curl}} & \mathbb{V}_{k-1}^{\text{div}}(\mathbf{r}_2; \mathbb{T}) \cap \ker(\text{div}) & \xrightarrow{\text{div}} & \mathbf{0}, \end{array}$$

where $\widetilde{\mathbb{V}}_k^{\text{curl}}(\mathbf{r}_1; \mathbb{M}) = \{ \boldsymbol{\tau} \in \mathbb{V}_k^{\text{curl}}(\mathbf{r}_1; \mathbb{M}) : \text{curl } \boldsymbol{\tau} \in \mathbb{V}_{k-1}^{\text{div}}(\mathbf{r}_2; \mathbb{T}) \cap \ker(\text{div}) \}$.

Lemma 5.1. *The mapping $\text{vskw} : \widetilde{\mathbb{V}}_k^{\text{curl}}(\mathbf{r}_1; \mathbb{M}) \rightarrow \mathbb{V}_k^{\text{div}}(\mathbf{r}_1) \cap \ker(\text{div})$ is well-defined and surjective.*

Proof. Recall that the parallelogram formed by the north-east diagonal \nearrow and the horizontal operators is anticommutative. By substituting the differential operators with the face normal vector, we derive the following relationship:

$$2(\text{vskw } \boldsymbol{\tau}) \cdot \mathbf{n} = -\text{tr}(\boldsymbol{\tau} \times \mathbf{n}).$$

Since $\boldsymbol{\tau} \times \boldsymbol{n}$ remains continuous for an $H(\text{curl})$ function $\boldsymbol{\tau}$, it follows that $(\text{vskw } \boldsymbol{\tau})\boldsymbol{n}$ also maintains continuity across each face. In other words, $\text{vskw } \boldsymbol{\tau} \in H(\text{div}, \Omega)$. Moreover, due to the traceless property of $\text{curl } \boldsymbol{\tau}$:

$$\text{div } 2(\text{vskw } \boldsymbol{\tau}) = \text{tr } \text{curl } \boldsymbol{\tau} = 0.$$

This implies that $\text{vskw}(\tilde{\mathbb{V}}_k^{\text{curl}}(\boldsymbol{r}_1; \mathbb{M})) \subseteq \mathbb{V}_k^{\text{div}}(\boldsymbol{r}_1) \cap \ker(\text{div})$.

For the surjectivity proof, we select a function $\boldsymbol{u} \in \mathbb{V}_k^{\text{div}}(\boldsymbol{r}_1) \cap \ker(\text{div})$. Since $\text{div } \boldsymbol{u} = 0$, we can find a $\boldsymbol{v} \in \mathbb{V}_{k+1}^{\text{curl}}(\boldsymbol{r}_0 - 1)$ such that $\text{curl } \boldsymbol{v} = \boldsymbol{u}$. Consequently, $\text{grad } \boldsymbol{v} \in \tilde{\mathbb{V}}_k^{\text{curl}}(\boldsymbol{r}_1; \mathbb{M})$ and $2 \text{vskw } \text{grad } \boldsymbol{v} = \text{curl } \boldsymbol{v} = \boldsymbol{u}$. This completes the argument for surjectivity. \square

Define

$$(43) \quad \mathbb{V}_k^{\text{curl}}(\boldsymbol{r}_1; \mathbb{S}) := \tilde{\mathbb{V}}_k^{\text{curl}}(\boldsymbol{r}_1; \mathbb{M}) \cap \ker(\text{vskw}).$$

With this space in place, we can proceed to apply the BGG construction to (42) and subsequently deduce the finite element Hessian complex.

Theorem 5.2. *Let $\boldsymbol{r}_0 \geq 1$, $\boldsymbol{r}_1 = \boldsymbol{r}_0 - 2$, $\boldsymbol{r}_2 = \boldsymbol{r}_1 \ominus 1$, $\boldsymbol{r}_3 = \boldsymbol{r}_2 \ominus 1$ be valid smoothness vectors. Assume $(\boldsymbol{r}_2, \boldsymbol{r}_3, k - 1)$ is $(\text{div}; \mathbb{T})$ stable and $k + 2 \geq 2r_0^v + 1$. Then the finite element Hessian complex*

$$\mathbb{P}_1 \xhookrightarrow{\subset} \mathbb{V}_{k+2}^{\text{grad}}(\boldsymbol{r}_0) \xrightarrow{\text{hess}} \mathbb{V}_k^{\text{curl}}(\boldsymbol{r}_1; \mathbb{S}) \xrightarrow{\text{curl}} \mathbb{V}_{k-1}^{\text{div}}(\boldsymbol{r}_2; \mathbb{T}) \xrightarrow{\text{div}} \mathbb{V}_{k-2}^{L^2}(\boldsymbol{r}_3; \mathbb{R}^3) \rightarrow \mathbf{0}$$

is exact.

While we have established finite element descriptions for several spaces, including $\mathbb{V}_{k+2}^{\text{grad}}(\boldsymbol{r}_0)$, $\mathbb{V}_{k-1}^{\text{div}}(\boldsymbol{r}_2; \mathbb{T})$, and $\mathbb{V}_{k-2}^{L^2}(\boldsymbol{r}_3; \mathbb{R}^3)$, we currently face a challenge in providing a finite element description for $\mathbb{V}_k^{\text{curl}}(\boldsymbol{r}_1; \mathbb{S})$. The DoFs on each element for this space are not easily derived using the BGG construction and will be discussed in Section 6.

Throughout this paper, we will further simplify the notation in examples by presenting only the smoothness vectors and omitting the space notation, which should be clear from the differential operator attached to the space.

Example 5.3. Taking $\boldsymbol{r}_0 = (4, 2, 1)^\top$, $\boldsymbol{r}_1 = \boldsymbol{r}_0 - 2$, $\boldsymbol{r}_2 = \boldsymbol{r}_1 \ominus 1$, $\boldsymbol{r}_3 = \boldsymbol{r}_2 \ominus 1$, and $k \geq 7$, we obtain the first finite element Hessian complex constructed in [33]

$$\mathbb{P}_1 \hookrightarrow \begin{pmatrix} 4 \\ 2 \\ 1 \end{pmatrix} \xrightarrow{\text{hess}} \begin{pmatrix} 2 \\ 0 \\ -1 \end{pmatrix} \xrightarrow{\text{curl}} \begin{pmatrix} 1 \\ -1 \\ -1 \end{pmatrix} \xrightarrow{\text{div}} \begin{pmatrix} 0 \\ -1 \\ -1 \end{pmatrix} \rightarrow \mathbf{0}.$$

Remark 5.4. The macro-element Hessian complex based on the Alfeld split and virtual element Hessian complex with $k \geq 3$ developed in [18] correspond, within our notation, to the following sequence:

$$\mathbb{P}_1 \hookrightarrow \begin{pmatrix} 2 \\ 1 \\ 1 \end{pmatrix} \xrightarrow{\text{hess}} \begin{pmatrix} 0 \\ -1 \\ -1 \end{pmatrix} \xrightarrow{\text{curl}} \begin{pmatrix} 0 \\ -1 \\ -1 \end{pmatrix} \xrightarrow{\text{div}} \begin{pmatrix} -1 \\ -1 \\ -1 \end{pmatrix} \rightarrow \mathbf{0}.$$

This particular complex cannot be derived using our framework due to the fact that $\boldsymbol{r}_0 = (2, 1, 1)^\top$ does not constitute a valid smoothness vector for a C^1 -element. \square

By modifying the smoothness constraint for $\mathbb{V}_k^{\text{curl}}(\boldsymbol{r}_1; \mathbb{S})$ to $\boldsymbol{r}_2 \geq \boldsymbol{r}_1 \ominus 1$ and then introducing the space $\mathbb{V}_k^{\text{curl}}(\boldsymbol{r}_1, \boldsymbol{r}_2; \mathbb{S}) = \{\boldsymbol{\tau} \in \mathbb{V}_k^{\text{curl}}(\boldsymbol{r}_1; \mathbb{S}), \text{curl } \boldsymbol{\tau} \in \mathbb{V}_{k-1}^{\text{div}}(\boldsymbol{r}_2; \mathbb{T})\}$, we can derive finite element Hessian complexes with inequality constraints of the smoothness vectors.

Corollary 5.5. *Let $\mathbf{r}_0 \geq 1$, $\mathbf{r}_1 = \mathbf{r}_0 - 2$, $\mathbf{r}_2 \geq \mathbf{r}_1 \ominus 1$, $\mathbf{r}_3 \geq \mathbf{r}_2 \ominus 1$. Assume $(\mathbf{r}_2, \mathbf{r}_3, k-1)$ is $(\text{div}; \mathbb{T})$ stable and $k \geq \max\{2r_0^v - 1, 2r_2^v + 2, 2r_3^v + 3\}$. Then the finite element Hessian complex*

$$\mathbb{P}_1 \xrightarrow{\subset} \mathbb{V}_{k+2}^{\text{grad}}(\mathbf{r}_0) \xrightarrow{\text{hess}} \mathbb{V}_k^{\text{curl}}(\mathbf{r}_1, \mathbf{r}_2; \mathbb{S}) \xrightarrow{\text{curl}} \mathbb{V}_{k-1}^{\text{div}}(\mathbf{r}_2, \mathbf{r}_3; \mathbb{T}) \xrightarrow{\text{div}} \mathbb{V}_{k-2}^{L^2}(\mathbf{r}_3; \mathbb{R}^3) \rightarrow \mathbf{0}$$

is exact.

By a similar proof, we can obtain the bubble Hessian complex and refer to appendix Section A.3 for the detailed proof.

Proposition 5.6. *Let $\mathbf{r}_0 \geq (4, 2, 1)^\top$, $\mathbf{r}_1 = \mathbf{r}_0 - 2$, $\mathbf{r}_2 = \mathbf{r}_1 \ominus 1$, $\mathbf{r}_3 = \mathbf{r}_2 \ominus 1$. Assume \mathbf{r}_2 satisfy the condition in Lemma 4.8, and $k \geq 2r_2^v + 2$. Then the bubble Hessian complex*

$$0 \xrightarrow{\subset} \mathbb{B}_{k+2}(\mathbf{r}_0) \xrightarrow{\text{hess}} \mathbb{B}_k^{\text{curl}}(\mathbf{r}_1; \mathbb{S}) \xrightarrow{\text{curl}} \mathbb{B}_{k-1}^{\text{div}}(\mathbf{r}_2; \mathbb{T}) \xrightarrow{\text{div}} \mathbb{B}_{k-2}(\mathbf{r}_3; \mathbb{R}^3)/\text{RT} \rightarrow 0$$

is exact, where $\mathbb{B}_k^{\text{curl}}(\mathbf{r}_1; \mathbb{S}) := \{\boldsymbol{\tau} \in \mathbb{B}_k(\mathbf{r}_1; \mathbb{S}) : \boldsymbol{\tau} \times \mathbf{n}|_{\partial T} = 0\}$.

5.2. Finite element elasticity complexes. Let

$$(44) \quad \mathbf{r}_0 \geq (2, 1, 0)^\top, \quad \mathbf{r}_1 = \mathbf{r}_0 - 1, \quad \mathbf{r}_2 = \max\{\mathbf{r}_1 \ominus 2, (0, -1, -1)^\top\}, \quad \mathbf{r}_3 = \mathbf{r}_2 \ominus 1.$$

Assume $(\mathbf{r}_1 \ominus 1, \mathbf{r}_2, k)$ is div-stable, and that $(\mathbf{r}_2, \mathbf{r}_3, k-1)$ exhibits $(\text{div}; \mathbb{S})$ stability.

We first consider a slightly smoother case

$$(45) \quad \mathbf{r}_0 \geq (4, 2, 1)^\top, \quad \mathbf{r}_1 = \mathbf{r}_0 - 1, \quad \mathbf{r}_2 = \mathbf{r}_1 \ominus 2, \quad \mathbf{r}_3 = \mathbf{r}_2 \ominus 1.$$

Evidently $\mathbf{r}_2 = (\mathbf{r}_1 \ominus 1) \ominus 1$. Moreover, by our assumptions, $(\mathbf{r}_2, \mathbf{r}_3, k-1)$ is div-stable. Consequently, the sequence $(\mathbf{r}_1, \mathbf{r}_1 \ominus 1, \mathbf{r}_2, \mathbf{r}_3)$ forms a valid de Rham smoothness sequence:

$$\mathbb{R}^3 \xrightarrow{\subset} \mathbb{V}_{k+1}^{\text{grad}}(\mathbf{r}_1; \mathbb{R}^3) \xrightarrow{\text{grad}} \mathbb{V}_k^{\text{curl}}(\mathbf{r}_1 \ominus 1; \mathbb{M}) \xrightarrow{\text{curl}} \mathbb{V}_{k-1}^{\text{div}}(\mathbf{r}_2; \mathbb{M}) \cap \ker(\text{div}) \xrightarrow{\text{div}} \mathbf{0}.$$

Employing a $\tilde{\sim}$ operation to transfer from \mathbb{M} to \mathbb{S} , we then obtain the exact sequence

$$\mathbb{R}^3 \xrightarrow{\subset} \mathbb{V}_{k+1}^{\text{grad}}(\mathbf{r}_1; \mathbb{R}^3) \xrightarrow{\text{grad}} \tilde{\mathbb{V}}_k^{\text{curl}}(\mathbf{r}_1 \ominus 1; \mathbb{M}) \xrightarrow{\text{curl}} \mathbb{V}_{k-1}^{\text{div}}(\mathbf{r}_2; \mathbb{S}) \cap \ker(\text{div}) \xrightarrow{\text{div}} \mathbf{0},$$

where

$$\tilde{\mathbb{V}}_k^{\text{curl}}(\mathbf{r}_1 \ominus 1; \mathbb{M}) := \{\boldsymbol{\tau} \in \mathbb{V}_k^{\text{curl}}(\mathbf{r}_1 \ominus 1; \mathbb{M}) : \text{curl } \boldsymbol{\tau} \in \mathbb{V}_{k-1}^{\text{div}}(\mathbf{r}_2; \mathbb{S})\}.$$

Lemma 5.7. *Define*

$$(46) \quad \tilde{\mathbb{V}}_k^{\text{div}}(\mathbf{r}_1 \ominus 1; \mathbb{M}) := S(\tilde{\mathbb{V}}_k^{\text{curl}}(\mathbf{r}_1 \ominus 1; \mathbb{M})).$$

It holds

$$\tilde{\mathbb{V}}_k^{\text{div}}(\mathbf{r}_1 \ominus 1; \mathbb{M}) \subseteq \mathbb{V}_k^{\text{div}}(\mathbf{r}_1 \ominus 1; \mathbb{M}) \cap \ker(\text{div}).$$

Proof. By $(S\boldsymbol{\tau})\mathbf{n} = -2 \text{vskw}(\boldsymbol{\tau} \times \mathbf{n})$, $\tilde{\mathbb{V}}_k^{\text{div}}(\mathbf{r}_1 \ominus 1; \mathbb{M}) \subseteq \mathbb{V}_k^{\text{div}}(\mathbf{r}_1 \ominus 1; \mathbb{M})$. And $\text{div } \tilde{\mathbb{V}}_k^{\text{div}}(\mathbf{r}_1 \ominus 1; \mathbb{M}) = \mathbf{0}$ follows from $\text{div}(S\boldsymbol{\tau}) = 2 \text{vskw}(\text{curl } \boldsymbol{\tau})$. \square

It is straightforward to demonstrate that the sequence $(\mathbf{r}_0, \mathbf{r}_1, \mathbf{r}_1 \ominus 1, \mathbf{r}_2)$ is also a valid de Rham smoothness sequence. With the application of a $\tilde{\sim}$ operation to this finite element de Rham complex, an exact sequence holds as follows:

$$\mathbb{R}^3 \xrightarrow{\subset} \mathbb{V}_{k+2}^{\text{grad}}(\mathbf{r}_0; \mathbb{R}^3) \xrightarrow{\text{grad}} \tilde{\mathbb{V}}_{k+1}^{\text{curl}}(\mathbf{r}_1; \mathbb{M}) \xrightarrow{\text{curl}} \tilde{\mathbb{V}}_k^{\text{div}}(\mathbf{r}_1 \ominus 1; \mathbb{M}) \xrightarrow{\text{div}} \mathbf{0},$$

where $\tilde{\mathbb{V}}_k^{\text{div}}(\mathbf{r}_1 \ominus 1; \mathbb{M})$ is defined in (46) and

$$\tilde{\mathbb{V}}_{k+1}^{\text{curl}}(\mathbf{r}_1; \mathbb{M}) := \{\boldsymbol{\tau} \in \mathbb{V}_{k+1}^{\text{curl}}(\mathbf{r}_1; \mathbb{M}) : \text{curl } \boldsymbol{\tau} \in \tilde{\mathbb{V}}_k^{\text{div}}(\mathbf{r}_1 \ominus 1; \mathbb{M})\}.$$

Theorem 5.8. *Let $(\mathbf{r}_0, \mathbf{r}_1, \mathbf{r}_2, \mathbf{r}_3)$ be given by (45). Assume $(\mathbf{r}_1 \ominus 1, \mathbf{r}_2, k)$ is div stable, and $(\mathbf{r}_2, \mathbf{r}_3, k-1)$ is $(\text{div}; \mathbb{S})$ stable. Let $k+2 \geq 2r_0^v + 1$. We have the BGG diagram*

$$\begin{array}{ccccccc} \mathbb{V}_{k+2}^{\text{grad}}(\mathbf{r}_0; \mathbb{R}^3) & \xrightarrow{\text{grad}} & \tilde{\mathbb{V}}_{k+1}^{\text{curl}}(\mathbf{r}_1; \mathbb{M}) & \xrightarrow{\text{curl}} & \tilde{\mathbb{V}}_k^{\text{div}}(\mathbf{r}_1 \ominus 1; \mathbb{M}) & \xrightarrow{\text{div}} & 0 \\ & \searrow \text{mskw} & & \nearrow S & & \searrow -2 \text{vskw} & \\ \mathbb{V}_{k+1}^{\text{grad}}(\mathbf{r}_1; \mathbb{R}^3) & \xrightarrow{\text{grad}} & \tilde{\mathbb{V}}_k^{\text{curl}}(\mathbf{r}_1 \ominus 1; \mathbb{M}) & \xrightarrow{\text{curl}} & \mathbb{V}_{k-1}^{\text{div}}(\mathbf{r}_2; \mathbb{S}) & \xrightarrow{\text{div}} & \mathbb{V}_{k-2}^{L^2}(\mathbf{r}_3; \mathbb{R}^3), \end{array}$$

which leads to the finite element elasticity complex

$$\text{RM} \xrightarrow{\subset} \mathbb{V}_{k+2}^{\text{grad}}(\mathbf{r}_0; \mathbb{R}^3) \xrightarrow{\text{def}} \mathbb{V}_{k+1}^{\text{inc}^+}(\mathbf{r}_1; \mathbb{S}) \xrightarrow{\text{inc}} \mathbb{V}_{k-1}^{\text{div}}(\mathbf{r}_2; \mathbb{S}) \xrightarrow{\text{div}} \mathbb{V}_{k-2}^{L^2}(\mathbf{r}_3; \mathbb{R}^3) \rightarrow \mathbf{0},$$

where $\mathbb{V}_{k+1}^{\text{inc}^+}(\mathbf{r}_1; \mathbb{S}) := \{\boldsymbol{\tau} \in \mathbb{V}_{k+1}^{\text{curl}}(\mathbf{r}_1; \mathbb{M}) : \boldsymbol{\tau} \in \mathbb{S}, \text{curl } \boldsymbol{\tau} \in \tilde{\mathbb{V}}_k^{\text{div}}(\mathbf{r}_1 \ominus 1; \mathbb{M})\}$.

Proof. The bijectiveness of the mapping $S : \tilde{\mathbb{V}}_k^{\text{curl}}(\mathbf{r}_1 \ominus 1; \mathbb{M}) \rightarrow \tilde{\mathbb{V}}_k^{\text{div}}(\mathbf{r}_1 \ominus 1; \mathbb{M})$ is a direct outcome of its definition. As $r_1^f \geq 0$, $\text{vskw } \tilde{\mathbb{V}}_{k+1}^{\text{curl}}(\mathbf{r}_1; \mathbb{M}) \subseteq \mathbb{V}_{k+1}^{\text{grad}}(\mathbf{r}_1; \mathbb{R}^3)$. Therefore $\tilde{\mathbb{V}}_{k+1}^{\text{curl}}(\mathbf{r}_1; \mathbb{M}) / \text{mskw } \mathbb{V}_{k+1}^{\text{grad}}(\mathbf{r}_1; \mathbb{R}^3) = \mathbb{V}_{k+1}^{\text{inc}^+}(\mathbf{r}_1; \mathbb{S})$. We arrive at our desired conclusion by applying the BGG framework. \square

As $r_1^f \geq 0$, $\mathbb{V}_{k+1}^{\text{inc}^+}(\mathbf{r}_1; \mathbb{S}) \subset H^1(\Omega; \mathbb{S})$ and $\mathbb{V}_{k+2}^{\text{grad}}(\mathbf{r}_0; \mathbb{R}^3) \subset H^2(\Omega; \mathbb{R}^3)$. The corresponding continuous version is the elasticity complex that initiates with $H^2(\Omega; \mathbb{R}^3)$:

$$(47) \quad \text{RM} \xrightarrow{\subset} H^2(\Omega; \mathbb{R}^3) \xrightarrow{\text{def}} H^1(\text{inc}, \Omega; \mathbb{S}) \xrightarrow{\text{inc}} H(\text{div}, \Omega; \mathbb{S}) \xrightarrow{\text{div}} L^2(\Omega; \mathbb{R}^3) \rightarrow \mathbf{0}.$$

Here, the space

$$H^1(\text{inc}, \Omega; \mathbb{S}) := \{\boldsymbol{\tau} \in H^1(\Omega; \mathbb{S}) : \text{inc } \boldsymbol{\tau} \in L^2(\Omega; \mathbb{S})\}.$$

Example 5.9. For the case of $k+1 \geq 8$ and $\mathbf{r}_0 = (4, 2, 1)^\top$, we arrive at a discrete elasticity complex (47) originating from a subspace of $H^2(\Omega)$:

$$\text{RM} \xrightarrow{\subset} \begin{pmatrix} 4 \\ 2 \\ 1 \end{pmatrix} \xrightarrow{\text{def}} \begin{pmatrix} 3 \\ 1 \\ 0 \end{pmatrix} \xrightarrow{\text{inc}} \begin{pmatrix} 1 \\ -1 \\ -1 \end{pmatrix} \xrightarrow{\text{div}} \begin{pmatrix} 0 \\ -1 \\ -1 \end{pmatrix} \rightarrow \mathbf{0}.$$

\square

Remark 5.10. It is worth noting that a finite element elasticity complex has been recently established for the Alfeld split of a tetrahedron [27], presenting another discrete counterpart of (47). The discrete elasticity complex introduced in [27] corresponds, within our notation, to the following sequence:

$$\text{RM} \xrightarrow{\subset} \begin{pmatrix} 2 \\ 1 \\ 1 \end{pmatrix} \xrightarrow{\text{def}} \begin{pmatrix} 1 \\ 0 \\ 0 \end{pmatrix} \xrightarrow{\text{inc}} \begin{pmatrix} 0 \\ -1 \\ -1 \end{pmatrix} \xrightarrow{\text{div}} \begin{pmatrix} -1 \\ -1 \\ -1 \end{pmatrix} \rightarrow \mathbf{0}.$$

This particular complex cannot be derived using our framework due to the fact that $\mathbf{r}_0 = (2, 1, 1)^\top$ does not constitute a valid smoothness vector for a C^1 -element. In [27], the space $\mathbb{V}^{\text{grad}}((2, 1, 1)^\top; \mathbb{R}^3)$ is constructed on Alfeld splits of tetrahedra. \square

For $\boldsymbol{\tau} \in \mathbb{V}_{k+1}^{\text{inc}^+}(\mathbf{r}_1; \mathbb{S})$, the super-script $+$ means some additional smoothness more than $\boldsymbol{\tau} \in H(\text{inc})$. To relax the smoothness of $\mathbb{V}_{k+1}^{\text{inc}^+}(\mathbf{r}_1; \mathbb{S})$, we introduce

$$(48) \quad \mathbb{V}_{k+1}^{\text{inc}}(\mathbf{r}_1; \mathbb{S}) := \{\boldsymbol{\tau} \in \mathbb{V}_{k+1}(\mathbf{r}_1) \otimes \mathbb{S} : \text{inc } \boldsymbol{\tau} \in \mathbb{V}_{k-1}^{\text{div}}(\mathbf{r}_2; \mathbb{S})\}.$$

Obviously $\mathbb{V}_{k+1}^{\text{inc}^+}(\mathbf{r}_1; \mathbb{S}) \subseteq \mathbb{V}_{k+1}^{\text{inc}}(\mathbf{r}_1; \mathbb{S})$. By applying an inverse hat operation, we can obtain the finite element elasticity complex for $\mathbf{r}_0 = (r_0^v, r_0^e, 0)^\top$ with $r_0^v \geq 4$ and $r_0^e \geq 1$.

Corollary 5.11. *Let $(\mathbf{r}_0, \mathbf{r}_1, \mathbf{r}_2, \mathbf{r}_3)$ be given by (44) and $\mathbf{r}_0 = (r_0^v, r_0^e, 0)^\top$ with $r_0^v \geq 4$ and $r_0^e \geq 1$. Assume $(\mathbf{r}_1 \ominus 1, \mathbf{r}_2, k)$ is div stable, $(\mathbf{r}_2, \mathbf{r}_3, k-1)$ is $(\text{div}; \mathbb{S})$ stable, and $k+2 \geq 2r_0^v + 1$. We have the finite element elasticity complex*

$$\text{RM} \xrightarrow{\subset} \mathbb{V}_{k+2}^{\text{grad}}(\mathbf{r}_0; \mathbb{R}^3) \xrightarrow{\text{def}} \mathbb{V}_{k+1}^{\text{inc}}(\mathbf{r}_1; \mathbb{S}) \xrightarrow{\text{inc}} \mathbb{V}_{k-1}^{\text{div}}(\mathbf{r}_2; \mathbb{S}) \xrightarrow{\text{div}} \mathbb{V}_{k-2}^{L^2}(\mathbf{r}_3; \mathbb{R}^3) \rightarrow \mathbf{0}.$$

Proof. Let $\hat{\mathbf{r}}_0 = (r_0^v, \max\{r_0^e, 2\}, 1)^\top \geq (4, 2, 1)^\top$ and $\hat{\mathbf{r}}_1 = (r_1^v, \max\{r_1^e, 1\}, 0)^\top$, then $\hat{\mathbf{r}}_1 \ominus 2 = \mathbf{r}_2$. So we can apply the inverse hat operation. To verify $\text{def } \mathbb{V}_{k+2}^{\text{grad}}(\mathbf{r}_0; \mathbb{R}^3) = \mathbb{V}_{k+1}^{\text{inc}}(\mathbf{r}_1; \mathbb{S}) \cap \ker(\text{inc})$, we use the exactness of the elasticity complex (16) and the fact if $\text{def } \mathbf{u} \in \mathbb{V}_{k+1}(\mathbf{r}_1; \mathbb{S})$, then $\mathbf{u} \in \mathbb{V}_{k+2}(\mathbf{r}_0; \mathbb{R}^3)$. \square

Next consider $\mathbf{r}_0 = (3, 1, 0)^\top$.

Lemma 5.12. *Let $\mathbf{r}_0 = (3, 1, 0)^\top$, $\mathbf{r}_1 = (2, 0, -1)^\top$ and $\mathbf{r}_2 = (0, -1, -1)^\top$. The de Rham complex*

$$(49) \quad \mathbb{R}^3 \xrightarrow{\subset} \widehat{\mathbb{V}}_{k+1}^{\text{div}}((\mathbf{r}_1)_+) \xrightarrow{\text{grad}} \widetilde{\mathbb{V}}_k^{\text{curl}}(\mathbf{r}_1 \ominus 1; \mathbb{M}) \xrightarrow{\text{curl}} \mathbb{V}_{k-1}^{\text{div}}(\mathbf{r}_2; \mathbb{S}) \cap \ker(\text{div}) \rightarrow 0$$

is exact, where $\widehat{\mathbb{V}}_{k+1}^{\text{div}}((\mathbf{r}_1)_+) = \mathbb{V}_{k+1}^{\text{grad}}((\mathbf{r}_1)_+; \mathbb{R}^3) \cap \ker(\text{div})$ and $\widetilde{\mathbb{V}}_k^{\text{curl}}(\mathbf{r}_1 \ominus 1; \mathbb{M}) = \{\boldsymbol{\tau} \in \mathbb{V}_k^{\text{curl}}(\mathbf{r}_1 \ominus 1; \mathbb{M}) : \text{tr } \boldsymbol{\tau} = 0, \text{curl } \boldsymbol{\tau} \in \mathbb{V}_{k-1}^{\text{div}}(\mathbf{r}_2; \mathbb{S})\}$.

Proof. We introduce auxiliary smoothness vector $\hat{\mathbf{r}}_1 = (2, 1, 0)^\top \geq (\mathbf{r}_1)_+$ and $\hat{\mathbf{r}}_1 \ominus 2 = \mathbf{r}_2$. We have the finite element de Rham complex and the triangular diagram

$$\begin{array}{ccc} \mathbb{V}_{k+1}^{\text{grad}}(\hat{\mathbf{r}}_1; \mathbb{R}^3) & \xrightarrow{\text{grad}} & \mathbb{V}_k^{\text{curl}}(\hat{\mathbf{r}}_1 - 1; \mathbb{M}) \xrightarrow{\text{curl}} \mathbb{V}_{k-1}^{\text{div}}(\mathbf{r}_2; \mathbb{M}) \cap \ker(\text{div}) \xrightarrow{\text{div}} 0 \\ \text{div} \downarrow & \swarrow \text{tr} & \\ \mathbb{V}_k^{L^2}(\hat{\mathbf{r}}_1 - 1) & & \end{array} .$$

Notice that $(\hat{\mathbf{r}}_1, \hat{\mathbf{r}}_1 - 1)$ is div stable, and thus $\text{tr } \mathbb{V}_k^{\text{curl}}(\hat{\mathbf{r}}_1 - 1; \mathbb{M}) = \mathbb{V}_k^{L^2}(\hat{\mathbf{r}}_1 - 1)$. Applying one hat operation (with $W = \{0\}$) will induce the exact sequence

$$\mathbb{R}^3 \xrightarrow{\subset} \widehat{\mathbb{V}}_{k+1}^{\text{div}}(\hat{\mathbf{r}}_1) \xrightarrow{\text{grad}} \mathbb{V}_k^{\text{curl}}(\hat{\mathbf{r}}_1 - 1; \mathbb{M}) \cap \ker(\text{tr}) \xrightarrow{\text{curl}} \mathbb{V}_{k-1}^{\text{div}}(\mathbf{r}_2; \mathbb{M}) \cap \ker(\text{div}).$$

As $\hat{\mathbf{r}}_1 \geq (\mathbf{r}_1)_+$, $\hat{\mathbf{r}}_1 - 1 \geq \mathbf{r}_1 \ominus 1$, and $(\mathbf{r}_1)_+ - 1 = \mathbf{r}_1 \ominus 1$, applying one inverse hat operation, we get the following exact sequence

$$\mathbb{R}^3 \xrightarrow{\subset} \widehat{\mathbb{V}}_{k+1}^{\text{div}}((\mathbf{r}_1)_+) \xrightarrow{\text{grad}} \mathbb{V}_k^{\text{curl}}(\mathbf{r}_1 \ominus 1; \mathbb{M}) \cap \ker(\text{tr}) \xrightarrow{\text{curl}} \mathbb{V}_{k-1}^{\text{div}}(\mathbf{r}_2; \mathbb{M}) \cap \ker(\text{div}).$$

Apply one more tilde operation \sim to change \mathbb{M} to \mathbb{S} to get complex (49). \square

Lemma 5.13. *Let $\mathbf{r}_0 = (3, 1, 0)^\top$, $\mathbf{r}_1 = (2, 0, -1)^\top$ and $\mathbf{r}_2 = (0, -1, -1)^\top$. The de Rham complex*

$$(50) \quad \mathbb{R}^3 \xrightarrow{\subset} \mathbb{V}_{k+2}^{\text{curl}}(\mathbf{r}_0, (\mathbf{r}_1)_+) \xrightarrow{\text{grad}} \widehat{\mathbb{V}}_{k+1}^{\text{curl}}(\mathbf{r}_1; \mathbb{M}) \xrightarrow{\text{curl}} \widetilde{\mathbb{V}}_k^{\text{div}}(\mathbf{r}_1 \ominus 1; \mathbb{M}) \xrightarrow{\text{div}} \mathbf{0}$$

is exact, where $\widetilde{\mathbb{V}}_k^{\text{div}}(\mathbf{r}_1 \ominus 1; \mathbb{M}) = S(\widetilde{\mathbb{V}}_k^{\text{curl}}(\mathbf{r}_1 \ominus 1; \mathbb{M}))$, and

$$\begin{aligned} \widehat{\mathbb{V}}_{k+1}^{\text{curl}}(\mathbf{r}_1; \mathbb{M}) &:= \{\boldsymbol{\tau} \in \mathbb{V}_{k+1}^{\text{curl}}(\mathbf{r}_1; \mathbb{M}) : \text{vskw } \boldsymbol{\tau} \in \widehat{\mathbb{V}}_{k+1}^{\text{div}}((\mathbf{r}_1)_+), \\ &\quad \text{curl } \boldsymbol{\tau} \in \widetilde{\mathbb{V}}_k^{\text{div}}(\mathbf{r}_1 \ominus 1; \mathbb{M})\}. \end{aligned}$$

Proof. Consider the diagram

$$\begin{array}{ccc}
\mathbb{V}_{k+2}^{\text{curl}}(\mathbf{r}_0) & \xrightarrow{\text{grad}} & \widetilde{\mathbb{V}}_{k+1}^{\text{curl}}(\mathbf{r}_1; \mathbb{M}) \\
\text{curl} \downarrow & \swarrow 2 \text{ vskw} & \\
\mathbb{V}_{k+1}^{\text{div}}(\mathbf{r}_1) \cap \ker(\text{div}) & &
\end{array}
, \quad
\begin{array}{ccc}
\mathbb{V}_{k+2}^{\text{curl}}(\mathbf{r}_0, (\mathbf{r}_1)_+) & \xrightarrow{\text{grad}} & \widehat{\widetilde{\mathbb{V}}}_{k+1}^{\text{curl}}(\mathbf{r}_1; \mathbb{M}) \\
\text{curl} \downarrow & \swarrow 2 \text{ vskw} & \\
\mathbb{V}_{k+1}^{\text{div}}((\mathbf{r}_1)_+) \cap \ker(\text{div}) & &
\end{array}
.$$

As $\mathbf{r}_0 + 1 = (4, 2, 1)^\top$ and $(\mathbf{r}_1, \mathbf{r}_1 \ominus 1)$ is div stable, we have the finite element de Rham complex (23) with valid de Rham smoothness vectors $(\mathbf{r}_0 + 1, \mathbf{r}_0, \mathbf{r}_1, \mathbf{r}_1 \ominus 1)$, and consequently $\text{curl } \mathbb{V}_{k+2}^{\text{curl}}(\mathbf{r}_0) = \mathbb{V}_{k+1}^{\text{div}}(\mathbf{r}_1) \cap \ker(\text{div})$.

Then applying one tilde operation $\widetilde{}$, it follows from $\mathbb{V}_{k+1}^{\text{div}}((\mathbf{r}_1)_+) \cap \ker(\text{div}) \subseteq \mathbb{V}_{k+1}^{\text{div}}(\mathbf{r}_1) \cap \ker(\text{div})$ that $\text{curl } \mathbb{V}_{k+2}^{\text{curl}}(\mathbf{r}_0, (\mathbf{r}_1)_+) = \mathbb{V}_{k+1}^{\text{div}}((\mathbf{r}_1)_+) \cap \ker(\text{div})$. As the curl operators in the diagram are surjective we can apply one hat operation $\widehat{}$, cf. Lemma 2.2 to acquire complex (50).

We use $\mathbf{r}_0 = (3, 1, 0)^\top$ to ensure $(\mathbf{r}_0 + 1, \mathbf{r}_0, \mathbf{r}_1, \mathbf{r}_1 \ominus 1)$ is a de Rham parameter sequence, which is not true for $\mathbf{r}_0 = (2, 1, 0)^\top$ as $\mathbf{r}_0 + 1 = (3, 2, 1)^\top$ is not a valid smoothness vector. \square

We further give characterization of the space $\widehat{\widetilde{\mathbb{V}}}_{k+1}^{\text{curl}}(\mathbf{r}_1; \mathbb{M})$.

Lemma 5.14. *Let $(\mathbf{r}_0, \mathbf{r}_1, \mathbf{r}_2, \mathbf{r}_3)$ be given by (44) and $\mathbf{r}_0 = (3, 1, 0)^\top$. We have*

$$(51) \quad \widehat{\widetilde{\mathbb{V}}}_{k+1}^{\text{curl}}(\mathbf{r}_1; \mathbb{M}) = \mathbb{V}_{k+1}^{\text{inc}^+}(\mathbf{r}_1; \mathbb{S}) \oplus \text{mskw } \widehat{\widetilde{\mathbb{V}}}_{k+1}^{\text{div}}((\mathbf{r}_1)_+),$$

where $\mathbb{V}_{k+1}^{\text{inc}^+}(\mathbf{r}_1; \mathbb{S}) := \{\boldsymbol{\tau} \in \mathbb{V}_{k+1}^{\text{curl}}(\mathbf{r}_1; \mathbb{M}) : \boldsymbol{\tau} \in \mathbb{S}, \text{curl } \boldsymbol{\tau} \in \widehat{\widetilde{\mathbb{V}}}_k^{\text{div}}(\mathbf{r}_1 \ominus 1; \mathbb{M})\}$.

Proof. For $\boldsymbol{\tau} = \text{mskw } \mathbf{v} \in \text{mskw } \widehat{\widetilde{\mathbb{V}}}_{k+1}^{\text{div}}((\mathbf{r}_1)_+)$, it follows

$$\text{curl } \boldsymbol{\tau} = \text{curl } \text{mskw } \mathbf{v} = -S(\text{grad } \mathbf{v}) \in \widehat{\widetilde{\mathbb{V}}}_k^{\text{div}}(\mathbf{r}_1 \ominus 1; \mathbb{M}),$$

and $\text{vskw } \boldsymbol{\tau} = \mathbf{v} \in \widehat{\widetilde{\mathbb{V}}}_{k+1}^{\text{div}}((\mathbf{r}_1)_+)$. We thus have proved

$$\text{mskw } \widehat{\widetilde{\mathbb{V}}}_{k+1}^{\text{div}}((\mathbf{r}_1)_+) \subseteq \widehat{\widetilde{\mathbb{V}}}_{k+1}^{\text{curl}}(\mathbf{r}_1; \mathbb{M}).$$

Then decomposition (51) holds from

$$\boldsymbol{\tau} = \text{sym } \boldsymbol{\tau} + \text{skw } \boldsymbol{\tau} = \text{sym } \boldsymbol{\tau} + \text{mskw}(\text{vskw } \boldsymbol{\tau}).$$

\square

Theorem 5.15. *Let $(\mathbf{r}_0, \mathbf{r}_1, \mathbf{r}_2, \mathbf{r}_3)$ be given by (44) and $\mathbf{r}_0 = (3, 1, 0)^\top$. Let $k + 2 \geq 2r_0^\vee + 1$. We have the BGG diagram*

$$\begin{array}{ccccccc}
\mathbb{V}_{k+2}^{\text{curl}}(\mathbf{r}_0, (\mathbf{r}_1)_+) & \xrightarrow{\text{grad}} & \widehat{\widetilde{\mathbb{V}}}_{k+1}^{\text{curl}}(\mathbf{r}_1; \mathbb{M}) & \xrightarrow{\text{curl}} & \widehat{\widetilde{\mathbb{V}}}_k^{\text{div}}(\mathbf{r}_1 \ominus 1; \mathbb{M}) & \xrightarrow{\text{div}} & 0 \\
& \searrow \text{mskw} & & \searrow S & & \searrow -2 \text{ vskw} & \\
& & & & & & \\
\widehat{\widetilde{\mathbb{V}}}_{k+1}^{\text{div}}((\mathbf{r}_1)_+) & \xrightarrow{\text{grad}} & \widetilde{\mathbb{V}}_k^{\text{curl}}(\mathbf{r}_1 \ominus 1; \mathbb{M}) & \xrightarrow{\text{curl}} & \mathbb{V}_{k-1}^{\text{div}}(\mathbf{r}_2; \mathbb{S}) & \xrightarrow{\text{div}} & \mathbb{V}_{k-2}^{L^2}(\mathbf{r}_3; \mathbb{R}^3),
\end{array}$$

which leads to the finite element elasticity complex

$$\begin{array}{ccccccc}
\text{RM} & \xrightarrow{\subset} & \mathbb{V}_{k+2}^{\text{curl}}(\mathbf{r}_0, (\mathbf{r}_1)_+) & \xrightarrow{\text{def}} & \mathbb{V}_{k+1}^{\text{inc}^+}(\mathbf{r}_1; \mathbb{S}) \\
& & & \xrightarrow{\text{inc}} & \mathbb{V}_{k-1}^{\text{div}}(\mathbf{r}_2; \mathbb{S}) & \xrightarrow{\text{div}} & \mathbb{V}_{k-2}^{L^2}(\mathbf{r}_3; \mathbb{R}^3) \rightarrow \mathbf{0}.
\end{array}$$

Consequently, by applying one inverse hat operation, we have

$$(52) \quad \text{RM} \xrightarrow{\subset} \mathbb{V}_{k+2}^{\text{grad}}(\mathbf{r}_0; \mathbb{R}^3) \xrightarrow{\text{def}} \mathbb{V}_{k+1}^{\text{inc}}(\mathbf{r}_1; \mathbb{S}) \xrightarrow{\text{inc}} \mathbb{V}_{k-1}^{\text{div}}(\mathbf{r}_2; \mathbb{S}) \xrightarrow{\text{div}} \mathbb{V}_{k-2}^{L^2}(\mathbf{r}_3; \mathbb{R}^3) \rightarrow \mathbf{0}.$$

Proof. The bijectiveness of the mapping $S : \widetilde{\mathbb{V}}_k^{\text{curl}}(\mathbf{r}_1 \ominus 1; \mathbb{M}) \rightarrow \widetilde{\mathbb{V}}_k^{\text{div}}(\mathbf{r}_1 \ominus 1; \mathbb{M})$ is a direct outcome of its definition. With complex (50), and the decomposition (51) at our disposal, we arrive at our desired conclusion by applying the BGG framework. \square

After we obtain the complex (52) for the case $\mathbf{r}_0 = (3, 1, 0)^\top$, we can extend to the case $\mathbf{r}_0 = (2, 1, 0)^\top$ by applying one inverse hat operation, as they share the same $\mathbf{r}_2 = (0, -1, -1)^\top$.

Combining all the cases, we conclude the construction of finite element elasticity complexes.

Theorem 5.16. *Let*

$$\mathbf{r}_0 \geq (2, 1, 0)^\top, \mathbf{r}_1 = \mathbf{r}_0 - 1, \mathbf{r}_2 = \max\{\mathbf{r}_1 \ominus 2, (0, -1, -1)^\top\}, \mathbf{r}_3 = \mathbf{r}_2 \ominus 1.$$

Assume $(\mathbf{r}_1 \ominus 1, \mathbf{r}_2, k)$ is div stable, and $(\mathbf{r}_2, \mathbf{r}_3, k-1)$ is $(\text{div}; \mathbb{S})$ stable. Let $k+2 \geq 2r_0^v + 1$. We have the finite element elasticity complex

$$(53) \quad \text{RM} \xrightarrow{\subset} \mathbb{V}_{k+2}^{\text{grad}}(\mathbf{r}_0; \mathbb{R}^3) \xrightarrow{\text{def}} \mathbb{V}_{k+1}^{\text{inc}}(\mathbf{r}_1; \mathbb{S}) \xrightarrow{\text{inc}} \mathbb{V}_{k-1}^{\text{div}}(\mathbf{r}_2; \mathbb{S}) \xrightarrow{\text{div}} \mathbb{V}_{k-2}^{L^2}(\mathbf{r}_3; \mathbb{R}^3) \rightarrow \mathbf{0}.$$

By the exactness of complex (53), we have the dimension identity

$$(54) \quad -6 + \dim \mathbb{V}_{k+2}^{\text{grad}}(\mathbf{r}_0; \mathbb{R}^3) - \dim \mathbb{V}_{k+1}^{\text{inc}}(\mathbf{r}_1; \mathbb{S}) \\ + \dim \mathbb{V}_{k-1}^{\text{div}}(\mathbf{r}_2; \mathbb{S}) - \dim \mathbb{V}_{k-2}^{L^2}(\mathbf{r}_3; \mathbb{R}^3) = 0.$$

So far we have finite element descriptions for spaces $\mathbb{V}_{k+2}^{\text{grad}}(\mathbf{r}_0; \mathbb{R}^3)$, $\mathbb{V}_{k-1}^{\text{div}}(\mathbf{r}_2; \mathbb{S})$, and $\mathbb{V}_{k-2}^{L^2}(\mathbf{r}_3; \mathbb{R}^3)$ but not for $\mathbb{V}_{k+1}^{\text{inc}}(\mathbf{r}_1; \mathbb{S})$ which will be given in Section 6.

Example 5.17. Taking $\mathbf{r}_0 = (3, 1, 0)^\top$, $\mathbf{r}_1 = \mathbf{r}_0 - 1$, $\mathbf{r}_2 = (0, -1, -1)^\top$, $\mathbf{r}_3 = \mathbf{r}_2 \ominus 1$, we have

$$\text{RM} \xrightarrow{\subset} \mathbb{V}_{k+2}^{\text{curl}}\left(\begin{pmatrix} 3 \\ 1 \\ 0 \end{pmatrix}, \begin{pmatrix} 2 \\ 0 \\ 0 \end{pmatrix}\right) \xrightarrow{\text{def}} \mathbb{V}_{k+1}^{\text{inc}^+}\left(\begin{pmatrix} 2 \\ 0 \\ -1 \end{pmatrix}; \mathbb{S}\right) \\ \xrightarrow{\text{inc}} \mathbb{V}_{k-1}^{\text{div}}\left(\begin{pmatrix} 0 \\ -1 \\ -1 \end{pmatrix}; \mathbb{S}\right) \xrightarrow{\text{div}} \mathbb{V}_{k-2}^{L^2}\left(\begin{pmatrix} -1 \\ -1 \\ -1 \end{pmatrix}; \mathbb{R}^3\right) \rightarrow \mathbf{0},$$

which is the finite element discretization of the elasticity complex (15). \square

Example 5.18. Consider the choice $\mathbf{r}_0 = (2, 1, 0)^\top$, $\mathbf{r}_1 = \mathbf{r}_0 - 1$, $\mathbf{r}_2 = (0, -1, -1)^\top$, $\mathbf{r}_3 = \mathbf{r}_2 \ominus 1$ and $k+1 \geq 6$. From the finite element elasticity complex (53) we get a finite element discretization of the elasticity complex (16)

$$\text{RM} \xrightarrow{\subset} \begin{pmatrix} 2 \\ 1 \\ 0 \end{pmatrix} \xrightarrow{\text{def}} \begin{pmatrix} 1 \\ 0 \\ -1 \end{pmatrix} \xrightarrow{\text{inc}} \begin{pmatrix} 0 \\ -1 \\ -1 \end{pmatrix} \xrightarrow{\text{div}} \begin{pmatrix} -1 \\ -1 \\ -1 \end{pmatrix} \rightarrow \mathbf{0}.$$

This sequence presents a variation of the finite element elasticity complex in the work by Chen and Huang [19], where the Hu-Zhang $H(\text{div}; \mathbb{S})$ -conforming element is used. \square

The bubble elasticity complex is shown in the following lemma, whose proof is given in Section A.4.

Proposition 5.19. *Let*

$$\mathbf{r}_0 \geq (2, 1, 0)^\top, \quad \mathbf{r}_1 = \mathbf{r}_0 - 1, \quad \mathbf{r}_2 = \max\{\mathbf{r}_1 \ominus 2, (0, -1, -1)^\top\}, \quad \mathbf{r}_3 = \mathbf{r}_2 \ominus 1.$$

Assume \mathbf{r}_2 satisfies the condition in Lemma 4.8, and $k \geq \max\{2r_2^v + 2, 3\}$. Then the bubble elasticity complex

$$0 \xrightarrow{\subset} \mathbb{B}_{k+2}(\mathbf{r}_0; \mathbb{R}^3) \xrightarrow{\text{def}} \mathbb{B}_{k+1}^{\text{inc}}(\mathbf{r}_1; \mathbb{S}) \xrightarrow{\text{inc}} \mathbb{B}_{k-1}^{\text{div}}(\mathbf{r}_2; \mathbb{S}) \xrightarrow{\text{div}} \mathbb{B}_{k-2}(\mathbf{r}_3; \mathbb{R}^3)/\text{RM} \rightarrow 0$$

is exact.

5.3. Finite element divdiv complexes. Let

$$(55) \quad \mathbf{r}_0 \geq (1, 0, 0)^\top, \quad \mathbf{r}_1 = \mathbf{r}_0 - 1, \quad \mathbf{r}_2 = \max\{\mathbf{r}_1 \ominus 1, (0, -1, -1)^\top\}, \quad \mathbf{r}_3 = \mathbf{r}_2 \ominus 2.$$

Assume both $(\mathbf{r}_2, \mathbf{r}_2 \ominus 1, k)$ and $(\mathbf{r}_2 \ominus 1, \mathbf{r}_3, k - 1)$ are div stable. Consequently both $(\mathbf{r}_0, \mathbf{r}_1, \mathbf{r}_2, \mathbf{r}_2 \ominus 1)$ and $((\mathbf{r}_1)_+, \mathbf{r}_1 \ominus 1, \mathbf{r}_2 \ominus 1, \mathbf{r}_3)$ are valid de Rham smoothness sequences.

Lemma 5.20. *Let $(\mathbf{r}_0, \mathbf{r}_1, \mathbf{r}_2, \mathbf{r}_3)$ be given by (55) and $\mathbf{r}_0 \geq (2, 1, 0)^\top$. Assume $(\mathbf{r}_2, \mathbf{r}_2 \ominus 1, k)$ is div stable. The complex*

$$(56) \quad \mathbb{R}^3 \xrightarrow{\subset} \mathbb{V}_{k+2}^{\text{div}}(\mathbf{r}_0, (\mathbf{r}_1)_+) \xrightarrow{\text{grad}} \widehat{\mathbb{V}}_{k+1}^{\text{curl}}(\mathbf{r}_1; \mathbb{M}) \xrightarrow{\text{curl}} \widetilde{\mathbb{V}}_k^{\text{div}}(\mathbf{r}_2; \mathbb{M}) \xrightarrow{\text{div}} \mathbb{V}_{k-1}^{\text{div}}(\mathbf{r}_2 \ominus 1) \rightarrow \mathbf{0}$$

is exact, where

$$\begin{aligned} \widetilde{\mathbb{V}}_k^{\text{div}}(\mathbf{r}_2; \mathbb{M}) &:= \mathbb{V}_k^{\text{div div}^+}(\mathbf{r}_2; \mathbb{S}) \oplus \text{mskw } \mathbb{V}_k^{\text{curl}}(\mathbf{r}_1 \ominus 1), \\ \widetilde{\mathbb{V}}_{k+1}^{\text{curl}}(\mathbf{r}_1; \mathbb{M}) &:= \{\boldsymbol{\tau} \in \mathbb{V}_{k+1}^{\text{curl}}(\mathbf{r}_1; \mathbb{M}) : \text{curl } \boldsymbol{\tau} \in \widetilde{\mathbb{V}}_k^{\text{div}}(\mathbf{r}_2; \mathbb{M})\}, \\ \widehat{\mathbb{V}}_{k+1}^{\text{curl}}(\mathbf{r}_1; \mathbb{M}) &:= \{\boldsymbol{\tau} \in \widetilde{\mathbb{V}}_{k+1}^{\text{curl}}(\mathbf{r}_1; \mathbb{M}) : \text{tr } \boldsymbol{\tau} \in \mathbb{V}_{k+1}^{\text{grad}}((\mathbf{r}_1)_+)\}. \end{aligned}$$

Proof. By definition, we have the de Rham complex

$$(57) \quad \mathbb{R}^3 \xrightarrow{\subset} \mathbb{V}_{k+2}^{\text{grad}}(\mathbf{r}_0; \mathbb{R}^3) \xrightarrow{\text{grad}} \widetilde{\mathbb{V}}_{k+1}^{\text{curl}}(\mathbf{r}_1; \mathbb{M}) \xrightarrow{\text{curl}} \widetilde{\mathbb{V}}_k^{\text{div}}(\mathbf{r}_2; \mathbb{M}) \xrightarrow{\text{div}} \mathbb{V}_{k-1}^{\text{div}}(\mathbf{r}_2 \ominus 1) \rightarrow \mathbf{0}.$$

When $r_1^f \geq 0$, $(\mathbf{r}_1)_+ = \mathbf{r}_1 = \mathbf{r}_0 - 1$, and complex (56) is exactly complex (57).

Then consider case $r_1^f = -1$ and thus $r_0^f = 0$. We have the diagram

$$\begin{array}{ccc} \mathbb{V}_{k+2}^{\text{div}}(\mathbf{r}_0) & \xrightarrow{\text{grad}} & \widetilde{\mathbb{V}}_{k+1}^{\text{curl}}(\mathbf{r}_1; \mathbb{M}) & \quad & \mathbb{V}_{k+2}^{\text{div}}(\mathbf{r}_0, (\mathbf{r}_1)_+) & \xrightarrow{\text{grad}} & \widehat{\mathbb{V}}_{k+1}^{\text{curl}}(\mathbf{r}_1; \mathbb{M}) \\ \text{div} \downarrow & \swarrow \text{tr} & & & \text{div} \downarrow & \swarrow \text{tr} & \\ \mathbb{V}_{k+1}^{L^2}(\mathbf{r}_1) & & & & \mathbb{V}_{k+1}^{\text{grad}}((\mathbf{r}_1)_+) & & \end{array}.$$

Both div operators are surjective. Then apply Lemma 2.2 to conclude the sequence (56) is exact. We do need the div stability $\text{div } \mathbb{V}_{k+2}^{\text{div}}(\mathbf{r}_0) = \mathbb{V}_{k+1}^{L^2}(\mathbf{r}_1)$. Otherwise the range of div operator is only a sub-space, i.e., $\text{div } \mathbb{V}_{k+2}^{\text{div}}(\mathbf{r}_0) \subset \mathbb{V}_{k+1}^{L^2}(\mathbf{r}_1)$ and how the dimension change in the hat operation is unclear. \square

We construct a finite element divdiv complex by the BGG procedure.

Theorem 5.21. *Let $(\mathbf{r}_0, \mathbf{r}_1, \mathbf{r}_2, \mathbf{r}_3)$ be given by (55) and $\mathbf{r}_0 \geq (2, 1, 0)^\top$. Assume $(\mathbf{r}_2, \mathbf{r}_2 \ominus 1, k)$ and $(\mathbf{r}_2 \ominus 1, \mathbf{r}_3, k - 1)$ are div stable. Then we have the BGG diagram*

$$\begin{array}{ccccccc} \mathbb{V}_{k+2}^{\text{div}}(\mathbf{r}_0, (\mathbf{r}_1)_+) & \xrightarrow{\text{grad}} & \widehat{\mathbb{V}}_{k+1}^{\text{curl}}(\mathbf{r}_1; \mathbb{M}) & \xrightarrow{\text{curl}} & \widetilde{\mathbb{V}}_k^{\text{div}}(\mathbf{r}_2; \mathbb{M}) & \xrightarrow{\text{div}} & \mathbb{V}_{k-1}^{\text{div}}(\mathbf{r}_2 \ominus 1) \rightarrow \mathbf{0} \\ & \searrow \iota & & \nearrow \text{mskw} & & \nearrow \text{id} & \\ \mathbb{V}_{k+1}^{\text{grad}}((\mathbf{r}_1)_+) & \xrightarrow{\text{grad}} & \mathbb{V}_k^{\text{curl}}(\mathbf{r}_1 \ominus 1) & \xrightarrow{\text{curl}} & \mathbb{V}_{k-1}^{\text{div}}(\mathbf{r}_2 \ominus 1) & \xrightarrow{\text{div}} & \mathbb{V}_{k-2}^{L^2}(\mathbf{r}_3) \rightarrow 0, \end{array}$$

which leads to the exact finite element divdiv complex

$$(58) \quad \text{RT} \xrightarrow{\subset} \mathbb{V}_{k+2}^{\text{div}}(\mathbf{r}_0, (\mathbf{r}_1)_+) \xrightarrow{\text{dev grad}} \mathbb{V}_{k+1}^{\text{sym curl}^+}(\mathbf{r}_1; \mathbb{T}) \xrightarrow{\text{sym curl}} \mathbb{V}_k^{\text{div div}^+}(\mathbf{r}_2; \mathbb{S}) \xrightarrow{\text{div div}} \mathbb{V}_{k-2}^{L^2}(\mathbf{r}_3) \rightarrow 0,$$

where

$$\mathbb{V}_{k+1}^{\text{sym curl}^+}(\mathbf{r}_1; \mathbb{T}) := \{\boldsymbol{\tau} \in \mathbb{V}_{k+1}^{\text{curl}}(\mathbf{r}_1; \mathbb{M}) : \text{tr } \boldsymbol{\tau} = 0, \text{curl } \boldsymbol{\tau} \in \widetilde{\mathbb{V}}_k^{\text{div}}(\mathbf{r}_2; \mathbb{M})\}.$$

Proof. By definition of spaces, both ι and mskw are injective. In addition, we have the decomposition

$$\begin{aligned} \widehat{\mathbb{V}}_{k+1}^{\text{curl}}(\mathbf{r}_1; \mathbb{M}) &= \mathbb{V}_{k+1}^{\text{sym curl}^+}(\mathbf{r}_1; \mathbb{T}) \oplus \iota \mathbb{V}_{k+1}^{\text{grad}}((\mathbf{r}_1)_+), \\ \widetilde{\mathbb{V}}_k^{\text{div}}(\mathbf{r}_2; \mathbb{M}) &= \mathbb{V}_k^{\text{div div}^+}(\mathbf{r}_2; \mathbb{S}) \oplus \text{mskw } \mathbb{V}_k^{\text{curl}}(\mathbf{r}_1 \ominus 1). \end{aligned}$$

We conclude the result by employing the BGG framework. \square

Again, the complexes derived from the BGG framework typically include spaces that have a slightly higher degree of smoothness. We can relax the smoothness and define

$$\mathbb{V}_{k+1}^{\text{sym curl}^+}(\mathbf{r}_1; \mathbb{T}) := \{\boldsymbol{\tau} \in \mathbb{V}_{k+1}(\mathbf{r}_1) \otimes \mathbb{T} : \text{sym curl } \boldsymbol{\tau} \in \mathbb{V}_k^{\text{div div}^+}(\mathbf{r}_2; \mathbb{S})\}.$$

Corollary 5.22. *Let $(\mathbf{r}_0, \mathbf{r}_1, \mathbf{r}_2, \mathbf{r}_3)$ be given by (55). Assume both $(\mathbf{r}_2, \mathbf{r}_2 \ominus 1, k)$ and $(\mathbf{r}_2 \ominus 1, \mathbf{r}_3, k - 1)$ are div stable. We have the exact finite element divdiv complex*

$$(59) \quad \text{RT} \xrightarrow{\subset} \mathbb{V}_{k+2}^{\text{grad}}(\mathbf{r}_0; \mathbb{R}^3) \xrightarrow{\text{dev grad}} \mathbb{V}_{k+1}^{\text{sym curl}^+}(\mathbf{r}_1; \mathbb{T}) \xrightarrow{\text{sym curl}} \mathbb{V}_k^{\text{div div}^+}(\mathbf{r}_2; \mathbb{S}) \xrightarrow{\text{div div}} \mathbb{V}_{k-2}^{L^2}(\mathbf{r}_3) \rightarrow 0.$$

Consequently

$$(60) \quad -4 + \dim \mathbb{V}_{k+2}^{\text{grad}}(\mathbf{r}_0; \mathbb{R}^3) - \dim \mathbb{V}_{k+1}^{\text{sym curl}^+}(\mathbf{r}_1; \mathbb{T}) + \dim \mathbb{V}_k^{\text{div div}^+}(\mathbf{r}_2; \mathbb{S}) - \dim \mathbb{V}_{k-2}^{L^2}(\mathbf{r}_3) = 0.$$

Proof. We apply an inverse hat operation to obtain complex (59) for $\mathbf{r}_0 \geq (2, 1, 0)^\top$ and then apply one more inverse hat operation to relax to $\mathbf{r}_0 \geq (1, 0, 0)^\top$ since they share the same \mathbf{r}_2 . \square

We can further enlarge the space $\mathbb{V}_k^{\text{div div}^+}(\mathbf{r}_2; \mathbb{S})$ to $\mathbb{V}_k^{\text{div div}}(\mathbf{r}_2; \mathbb{S})$ and define

$$\mathbb{V}_{k+1}^{\text{sym curl}}(\mathbf{r}_1) := \{\boldsymbol{\tau} \in \mathbb{V}_{k+1}(\mathbf{r}_1) \otimes \mathbb{T} : \text{sym curl } \boldsymbol{\tau} \in \mathbb{V}_k^{\text{div div}}(\mathbf{r}_2; \mathbb{S})\}$$

to get the finite element divdiv complex

$$(61) \quad \text{RT} \xrightarrow{\subset} \mathbb{V}_{k+2}^{\text{grad}}(\mathbf{r}_0; \mathbb{R}^3) \xrightarrow{\text{dev grad}} \mathbb{V}_{k+1}^{\text{sym curl}}(\mathbf{r}_1; \mathbb{T}) \xrightarrow{\text{sym curl}} \mathbb{V}_k^{\text{div div}}(\mathbf{r}_2; \mathbb{S}) \xrightarrow{\text{div div}} \mathbb{V}_{k-2}^{L^2}(\mathbf{r}_3) \rightarrow 0.$$

We can also define

$$\mathbb{V}_{k+1}^{\text{sym curl}^+}(\mathbf{r}_1; \mathbb{T}) := \{\boldsymbol{\tau} \in \mathbb{V}_{k+1}^{\text{curl}}(\mathbf{r}_1; \mathbb{M}) : \text{tr } \boldsymbol{\tau} = 0, \text{sym curl } \boldsymbol{\tau} \in \mathbb{V}_k^{\text{div div}}(\mathbf{r}_2; \mathbb{S})\},$$

and obtain another finite element divdiv complex

$$(62) \quad \text{RT} \xrightarrow{\subset} \mathbb{V}_{k+2}^{\text{div}}(\mathbf{r}_0, (\mathbf{r}_1)_+) \xrightarrow{\text{dev grad}} \mathbb{V}_{k+1}^{\text{sym curl}^+}(\mathbf{r}_1; \mathbb{T}) \xrightarrow{\text{sym curl}} \mathbb{V}_k^{\text{div div}}(\mathbf{r}_2; \mathbb{S}) \xrightarrow{\text{div div}} \mathbb{V}_{k-2}^{L^2}(\mathbf{r}_3) \rightarrow 0.$$

Those variants are summarized in Fig. 5.

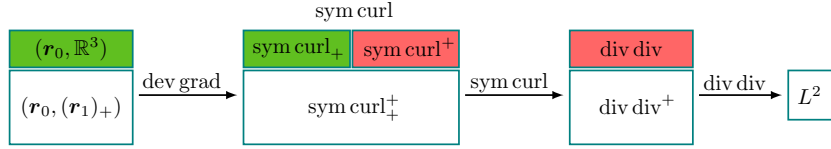


FIGURE 5. Diverse configurations of finite element divdiv complexes. The fundamental finite element divdiv complex (58), depicted by white blocks, is formulated through the BGG framework, with additional smoothness. Then add green blocks to get (59), add red blocks to get (62), and add both to get (61).

Verification of the exactness for the complexes (61) and (62) becomes intricate when the space $\mathbb{V}_k^{\text{div div}}(\mathbf{r}_2; \mathbb{S})$ is introduced. A rigorous proof will be presented subsequently, following the constructive characterization of these spaces.

Example 5.23. We recover the finite element divdiv complex in [34]

$$\text{RT} \xrightarrow{\subset} \begin{pmatrix} 2 \\ 0 \\ 0 \end{pmatrix} \xrightarrow{\text{dev grad}} \begin{pmatrix} 1 \\ -1 \\ -1 \end{pmatrix} \xrightarrow{\text{sym curl}} \begin{pmatrix} 0 \\ -1 \\ -1 \end{pmatrix} \xrightarrow{\text{div div}} \begin{pmatrix} -1 \\ -1 \\ -1 \end{pmatrix} \rightarrow 0.$$

□

Example 5.24. We recover the finite element divdiv complex in [21]

$$\text{RT} \xrightarrow{\subset} \begin{pmatrix} 1 \\ 0 \\ 0 \end{pmatrix} \xrightarrow{\text{dev grad}} \begin{pmatrix} 0 \\ -1 \\ -1 \end{pmatrix} \xrightarrow{\text{sym curl}} \begin{pmatrix} 0 \\ -1 \\ -1 \end{pmatrix} \xrightarrow{\text{div div}} \begin{pmatrix} -1 \\ -1 \\ -1 \end{pmatrix} \rightarrow 0.$$

□

Remark 5.25. Recently in [25] we have constructed $H(\text{div div})$ -conforming element without vertex continuity and the corresponding divdiv complex:

$$\text{RT} \xrightarrow{\subset} \begin{pmatrix} 1 \\ 0 \\ 0 \end{pmatrix} \xrightarrow{\text{dev grad}} \begin{pmatrix} 0 \\ -1 \\ -1 \end{pmatrix} \xrightarrow{\text{sym curl}} \begin{pmatrix} -1 \\ -1 \\ -1 \end{pmatrix} \xrightarrow{\text{div div}} \begin{pmatrix} -1 \\ -1 \\ -1 \end{pmatrix} \rightarrow 0.$$

The construction of $\mathbb{V}_k^{\text{div div}}(-1; \mathbb{S})$ and the div div stability requires careful redistribution of degrees of freedom (DoFs) and appears challenging to derive from the BGG construction. The last space can be further relaxed to the generalized H^2 non-conforming Morley-Wang-Xu elements [52, 53] when div div is understood in the distribution sense; see [25, Section 5.2].

□

The bubble divdiv complex is shown in the following lemma, whose proof is given in Section A.5.

Proposition 5.26. *Let*

$$\mathbf{r}_0 \geq (1, 0, 0)^\top, \quad \mathbf{r}_1 = \mathbf{r}_0 - 1, \quad \mathbf{r}_2 = \max\{\mathbf{r}_1 \ominus 1, (0, -1, -1)^\top\}, \quad \mathbf{r}_3 = \mathbf{r}_2 \ominus 2.$$

Assume \mathbf{r}_2 satisfies the condition in Lemma 4.8, $\mathbf{r}_2 \ominus 1$ satisfies (19), and $k \geq \max\{2r_2^v + 1, 3\}$. We have the following exact bubble divdiv complex

$$\begin{aligned} 0 \xrightarrow{c} \mathbb{B}_{k+2}(\mathbf{r}_0; \mathbb{R}^3) &\xrightarrow{\text{dev grad}} \mathbb{B}_{k+1}^{\text{sym curl}}(\mathbf{r}_1; \mathbb{T}) \\ &\xrightarrow{\text{sym curl}} \mathbb{B}_k^{\text{div div}}(\mathbf{r}_2; \mathbb{S}) \xrightarrow{\text{div div}} \mathbb{B}_{k-2}(\mathbf{r}_3)/\mathbb{P}_1(T) \rightarrow 0. \end{aligned}$$

6. EDGE ELEMENTS

In this section we shall construct finite element spaces for $H(\text{curl}; \mathbb{S})$, $H(\text{inc}; \mathbb{S})$, and $H(\text{sym curl}; \mathbb{T})$ spaces. For $H(\text{curl}; \mathbb{S})$, we use the t - n decomposition approach and for the other two, we use the trace bubble complexes and the knowledge for div elements to determine the face DoFs and the edge traces to determine the edge DoFs.

6.1. $H(\text{curl}; \mathbb{S})$ -conforming elements. When $r^f \geq 0$, it is simply the tensor product:

$$\mathbb{V}_k^{\text{curl}}(\mathbf{r}, \mathbb{S}) := \mathbb{V}_k(\mathbf{r}) \otimes \mathbb{S} \quad \text{when } \mathbf{r} \geq 0.$$

Recall that the Hessian complex starts with an H^2 -conforming element $\mathbb{V}_{k+2}^{\text{hess}}(\mathbf{r} + 2)$, where $\mathbf{r} + 2 \geq (4, 2, 1)^\top$, and consequently, $r^e \geq 0$. Hence, for the remainder of this subsection, we will focus exclusively on the cases where $r^f = -1$ and $r^e \geq 0$.

Since we have $r^v \geq 2r^e \geq 0$, the vertex and edge DoFs take on a tensor product structure: $\text{DoF}_k(s; \mathbf{r}) \otimes \mathbb{S}$, where $s = v$ or e . However, determining the face DoFs requires a different approach. We continue to use the diagram (25), but now with a modified t - n decomposition, as the trace of the curl operator $(\cdot) \times \mathbf{n}$ contains only the tangential component. Consequently, the normal component $\mathbb{B}_k(f; \mathbf{r}) \otimes \text{span}\{\mathbf{n} \otimes \mathbf{n}\}$ contributes to the bubble space.

To clarify this process, we define

$$\mathbb{B}_k^{\text{curl}}(\mathbf{r}; \mathbb{S}) := \mathbb{B}_k(\mathbf{r}_+; \mathbb{S}) \oplus [r^f = -1] \bigoplus_{f \in \Delta_2(T)} (\mathbb{B}_k(f; \mathbf{r}) \otimes \text{span}\{\mathbf{n} \otimes \mathbf{n}\}),$$

and refer to Fig. 6 for an illustration.

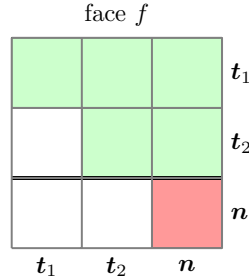


FIGURE 6. A t - n decomposition of \mathbb{S} on a face for $H(\text{curl}; \mathbb{S})$ element. The normal component $\mathbb{B}_k(f; \mathbf{r}) \otimes \text{span}\{\mathbf{n} \otimes \mathbf{n}\}$ (red block) will contribute to the bubble space.

Take $\mathbb{P}_k(T; \mathbb{S})$ as the space of shape functions. Let \mathbf{r} be a smoothness vector with $r^f = -1$ and $r^e \geq 0$. The degrees of freedom are

$$(63a) \quad \nabla^i \boldsymbol{\tau}(\mathbf{v}), \quad i = 0, \dots, r^v, \mathbf{v} \in \Delta_0(T),$$

$$(63b) \quad \int_e \frac{\partial^j \boldsymbol{\tau}}{\partial n_1^i \partial n_2^{j-i}} : \mathbf{q} \, ds, \quad \mathbf{q} \in \mathbb{B}_{k-j}(e; r^v - j) \otimes \mathbb{S}, 0 \leq i \leq j \leq r^e, e \in \Delta_1(T),$$

$$(63c) \quad \int_f (\mathbf{n} \times \boldsymbol{\tau} \times \mathbf{n}) : \mathbf{q} \, dS, \quad \mathbf{q} \in \mathbb{B}_k(f; \mathbf{r}) \otimes \mathbb{S}(f), f \in \Delta_2(T),$$

$$(63d) \quad \int_f (\mathbf{n}^\top \boldsymbol{\tau} \Pi_f) \cdot \mathbf{q} \, dS, \quad \mathbf{q} \in \mathbb{B}_k^2(f; \mathbf{r}), f \in \Delta_2(T),$$

$$(63e) \quad \int_T \boldsymbol{\tau} : \mathbf{q} \, dx, \quad \mathbf{q} \in \mathbb{B}_k^{\text{curl}}(\mathbf{r}; \mathbb{S}),$$

where $\mathbb{S}(f) := \mathcal{T}^f(\mathbb{S}) = \text{span}\{\text{sym}(\mathbf{t}_i^f \otimes \mathbf{t}_j^f), 1 \leq i \leq j \leq 2\}$.

Lemma 6.1. *Let \mathbf{r} be a smoothness vector with $r^f = -1, r^e \geq 0$, and let $k \geq 2r^v + 1$. DoFs (63) are unisolvent for $\mathbb{P}_k(T; \mathbb{S})$. Given a triangulation \mathcal{T}_h of Ω , define*

$$(64) \quad \mathbb{V}_k^{\text{curl}}(\mathbf{r}; \mathbb{S}) := \{\boldsymbol{\tau} \in L^2(\Omega; \mathbb{S}) : \boldsymbol{\tau}|_T \in \mathbb{P}_k(T; \mathbb{S}) \text{ for all } T \in \mathcal{T}_h, \\ \text{and all the DoFs (63) are single-valued}\}.$$

Then $\mathbb{V}_k^{\text{curl}}(\mathbf{r}; \mathbb{S}) \subset H(\text{curl}, \Omega; \mathbb{S})$.

Proof. The unisolvence property can be established by leveraging the unisolvence of the tensor product space $\mathbb{V}_k(\mathbf{r}_+) \otimes \mathbb{S}$ and relocating the face DoF $\int_f \mathbf{n}^\top \boldsymbol{\tau} \mathbf{n} \mathbf{q}$ to $\mathbb{B}_k^{\text{curl}}(\mathbf{r}; \mathbb{S})$. The $H(\text{curl})$ -conformity is a direct consequence of the continuity exhibited by $\boldsymbol{\tau} \times \mathbf{n}$, which arises from the single-valued DoFs (63a)-(63d). \square

Recall that in Section 5.1, we have defined a space $\mathbb{V}_k^{\text{curl}}(\mathbf{r}_1; \mathbb{S}) = \tilde{\mathbb{V}}_k^{\text{curl}}(\mathbf{r}_1; \mathbb{M}) \cap \ker(\text{vskw})$ from the BGG construction. Next we show they are equal.

Lemma 6.2. *Let $\mathbf{r}_1 \geq (2, 0, -1)^\top$. The space defined by (43) is equal to the space $\mathbb{V}_k^{\text{curl}}(\mathbf{r}_1; \mathbb{S})$ defined by (64) when $r_1^f = -1$ and to $\mathbb{V}_k^{\text{curl}}(\mathbf{r}_1, \mathbb{S}) := \mathbb{V}_k(\mathbf{r}_1) \otimes \mathbb{S}$ when $r_1^f \geq 0$.*

Proof. Certainly, we have the inclusion $\mathbb{V}_k^{\text{curl}}(\mathbf{r}_1; \mathbb{S}) \subseteq \tilde{\mathbb{V}}_k^{\text{curl}}(\mathbf{r}_1; \mathbb{M}) \cap \ker(\text{vskw})$. Thus, it is enough to demonstrate the dimension equality:

$$(65) \quad \dim \mathbb{V}_k^{\text{curl}}(\mathbf{r}_1; \mathbb{S}) = \dim(\tilde{\mathbb{V}}_k^{\text{curl}}(\mathbf{r}_1; \mathbb{M}) \cap \ker(\text{vskw})).$$

Let us compare this with $\dim \mathbb{V}_k^{\text{curl}}(\mathbf{r}_1; \mathbb{M})$. Using the definition of the $\tilde{\sim}$ operation and (35), we can express:

$$\begin{aligned} \dim \tilde{\mathbb{V}}_k^{\text{curl}}(\mathbf{r}_1; \mathbb{M}) &= \dim \mathbb{V}_k^{\text{curl}}(\mathbf{r}_1; \mathbb{M}) - (\dim \mathbb{V}_{k-1}^{\text{div}}(\mathbf{r}_2; \mathbb{M}) - \dim \mathbb{V}_{k-1}^{\text{div}}(\mathbf{r}_2; \mathbb{T})) \\ &= \dim \mathbb{V}_k^{\text{curl}}(\mathbf{r}_1; \mathbb{M}) - \dim \mathbb{V}_{k-1}^{L^2}(\mathbf{r}_2). \end{aligned}$$

Also, observe that $\dim \mathbb{V}_k^{\text{div}}(\mathbf{r}_1) \cap \ker(\text{div}) = \dim \mathbb{V}_k^{\text{div}}(\mathbf{r}_1) - \dim \mathbb{V}_{k-1}^{L^2}(\mathbf{r}_2)$. With the surjectiveness of vskw , we can write:

$$(66) \quad \dim(\tilde{\mathbb{V}}_k^{\text{curl}}(\mathbf{r}_1; \mathbb{M}) \cap \ker(\text{vskw})) = \dim \mathbb{V}_k^{\text{curl}}(\mathbf{r}_1; \mathbb{M}) - \dim \mathbb{V}_k^{\text{div}}(\mathbf{r}_1).$$

Now, let us delve into the construction of $\mathbb{V}_k^{\text{curl}}(\mathbf{r}_1; \mathbb{S})$ and exam the dimension reduction as we transition from \mathbb{M} to \mathbb{S} .

When $r_1^f \geq 0$, it is evident that $\dim \mathbb{V}_k^{\text{curl}}(\mathbf{r}_1; \mathbb{S}) = \dim \mathbb{V}_k^{\text{curl}}(\mathbf{r}_1; \mathbb{M}) - \dim \mathbb{V}_k^{\text{div}}(\mathbf{r}_1)$. For the scenario where $r_1^f = -1$, a more intricate analysis is needed. On vertices and edges, since $r_1^v \geq 2r_1^e \geq 0$, the change is a net decrease of 3 DoFs from \mathbb{M} to \mathbb{S} . In the case of faces, referring to Fig. 6, the component $\mathbf{t}_1 \mathbf{t}_2^\top$ goes missing. In terms of the bubble space, transitioning from $\mathbb{B}_k(\mathbf{r}_1; \mathbb{M})$ to $\mathbb{B}_k(\mathbf{r}_1; \mathbb{S})$ incurs a reduction of 3 DoFs. Additionally, for the face bubbles, we observe a reduction of 2 DoFs (namely, the components $\mathbf{t}_1 \mathbf{n}^\top$ and $\mathbf{t}_2 \mathbf{n}^\top$). This reduction perfectly aligns with the dimension decrease required to define $\mathbb{V}_k^{\text{div}}(\mathbf{r}_1)$. Therefore, we have successfully demonstrated that $\dim \mathbb{V}_k^{\text{curl}}(\mathbf{r}_1; \mathbb{S}) = \dim \mathbb{V}_k^{\text{curl}}(\mathbf{r}_1; \mathbb{M}) - \dim \mathbb{V}_k^{\text{div}}(\mathbf{r}_1)$, which implies the validity of (65) by referring back to (66). \square

A finite element description of $\mathbb{V}_k^{\text{curl}}(\mathbf{r}_1, \mathbf{r}_2; \mathbb{S})$ can also be derived by utilizing the DoFs introduced for $\mathbb{V}_{k+1}^{\text{curl}}(\mathbf{r}_1, \mathbf{r}_2)$ in Section 3.5. The main idea involves adding DoFs for $\text{curl } \boldsymbol{\tau} \in \mathbb{V}_{k-1}^{\text{div}}(\mathbf{r}_2; \mathbb{T})$, followed by a careful elimination of redundancies in the DoFs related to derivatives. We omit the lengthy details here.

6.2. $H(\text{inc}; \mathbb{S})$ -conforming elements. We proceed to provide a detailed and explicit characterization of the $H(\text{inc})$ -conforming element space $\mathbb{V}_{k+1}^{\text{inc}}(\mathbf{r}_1; \mathbb{S})$, as defined in (48). Our focus will be primarily on scenarios where $r_1^f = 0$ or $r_1^f = -1$, as the cases with $r_1^f \geq 1$ are simply tensor product $\mathbb{V}_{k+1}^{\text{inc}}(\mathbf{r}_1; \mathbb{S}) = \mathbb{V}_{k+1}(\mathbf{r}_1) \otimes \mathbb{S}$. As $\mathbf{r}_0 \geq (2, 1, 0)^\top$ in the finite element elasticity complex, our subsequent analysis is restricted to $r_1^v \geq 1$ and $r_1^e \geq 0$.

To motivate the edge DoFs, we first recall the trace complexes. For a smooth and symmetric tensor $\boldsymbol{\tau} \in H(\text{inc}, T; \mathbb{S})$, define two trace operators as

$$\begin{aligned} \text{tr}_1^{\text{inc}}(\boldsymbol{\tau}) &= \mathbf{n} \times \boldsymbol{\tau} \times \mathbf{n}, \\ \text{tr}_2^{\text{inc}}(\boldsymbol{\tau}) &= \mathbf{n} \times (\text{curl } \boldsymbol{\tau})^\top \Pi_f + \text{grad}_f(\Pi_f \boldsymbol{\tau} \cdot \mathbf{n}). \end{aligned}$$

In [19, Section 4.2] we have obtained the following trace complexes

$$\begin{array}{ccccccc} \mathbf{a} \times \mathbf{x} + \mathbf{b} & \xrightarrow{\mathcal{C}} & \mathbf{v} & \xrightarrow{\text{def}} & \boldsymbol{\tau} & \xrightarrow{\text{inc}} & \boldsymbol{\sigma} \xrightarrow{\text{div}} \mathbf{p} \\ & & \downarrow & & \downarrow & & \downarrow \\ \mathbf{a}_f \mathbf{x}_f + \mathbf{b}_f & \xrightarrow{\mathcal{C}} & \mathbf{v} \times \mathbf{n} & \xrightarrow{\text{sym curl}_f} & \mathbf{n} \times \boldsymbol{\tau} \times \mathbf{n} & \xrightarrow{\text{div}_f \text{div}_f} & \mathbf{n} \cdot \boldsymbol{\sigma} \cdot \mathbf{n} \longrightarrow 0, \end{array}$$

and

$$\begin{array}{ccccccc} \mathbf{a} \times \mathbf{x} + \mathbf{b} & \xrightarrow{\mathcal{C}} & \mathbf{v} & \xrightarrow{\text{def}} & \boldsymbol{\tau} & \xrightarrow{\text{inc}} & \boldsymbol{\sigma} \xrightarrow{\text{div}} \mathbf{p} \\ & & \downarrow & & \downarrow & & \downarrow \\ \mathbf{a}_f \cdot \mathbf{x}_f + b_f & \xrightarrow{\mathcal{C}} & \mathbf{v} \cdot \mathbf{n} & \xrightarrow{\nabla_f^2} & \text{tr}_2^{\text{inc}}(\boldsymbol{\tau}) & \xrightarrow{\nabla_f^\perp} & \mathbf{n} \cdot \boldsymbol{\sigma} \times \mathbf{n} \longrightarrow \mathbf{0}. \end{array}$$

Take $\mathbb{P}_{k+1}(T; \mathbb{S})$ as the shape function space. Let $(\mathbf{r}_0, \mathbf{r}_1, \mathbf{r}_2, \mathbf{r}_3)$ be given by (44). The degrees of freedom are

$$(67a) \quad \nabla^i \boldsymbol{\tau}(\mathbf{v}), \quad i = 0, \dots, r_1^v,$$

$$(67b) \quad \text{inc } \boldsymbol{\tau}(\mathbf{v}), \quad \text{if } r_1^v = 1,$$

$$(67c) \quad \int_e \frac{\partial^j \boldsymbol{\tau}}{\partial n_1^i \partial n_2^{j-i}} : \mathbf{q} \, ds, \quad \mathbf{q} \in \mathbb{B}_{k+1-j}(e; r_1^v - j) \otimes \mathbb{S}, \quad 0 \leq i \leq j \leq r_1^e,$$

$$(67d) \quad \int_e (\text{curl } \boldsymbol{\tau})^\top \mathbf{t} \cdot \mathbf{q} \, ds, \quad \mathbf{q} \in \mathbb{B}_k^3(e; r_1^v - 1), \quad \text{if } r_1^e = 0,$$

$$\begin{aligned}
(67e) \quad & \int_e (\mathbf{n}_i^\top (\text{inc } \boldsymbol{\tau}) \mathbf{n}_j) q \, ds, \quad \mathbf{q} \in \mathbb{B}_{k-1}(e; r_2^\vee), 1 \leq i \leq j \leq 2, \text{ if } r_2^\varepsilon = -1, \\
(67f) \quad & \int_f (\mathbf{n} \times \boldsymbol{\tau} \times \mathbf{n}) : \mathbf{q} \, dS, \quad \mathbf{q} \in \text{sym curl}_f \mathbb{B}_{k+2}^2(f; \mathbf{r}_0), \\
(67g) \quad & \int_f \text{tr}_2^{\text{inc}}(\boldsymbol{\tau}) : \mathbf{q} \, dS, \quad \mathbf{q} \in \nabla_f^2 \mathbb{B}_{k+2}(f; \mathbf{r}_0), \\
(67h) \quad & \int_f (\boldsymbol{\tau} \mathbf{n}) \cdot \mathbf{q} \, dS, \quad \mathbf{q} \in \mathbb{B}_{k+1}^3(f; \mathbf{r}_1), \text{ if } r_1^f = 0, \\
(67i) \quad & \int_f \Pi_f(\text{inc } \boldsymbol{\tau}) \mathbf{n} \cdot \mathbf{q} \, dS, \quad \mathbf{q} \in \mathbb{B}_{k-1}^{\text{div}}(f; \mathbf{r}_2)/\text{RT}(f), \\
(67j) \quad & \int_f \mathbf{n}^\top (\text{inc } \boldsymbol{\tau}) \mathbf{n} q \, dS, \quad \mathbf{q} \in \mathbb{B}_{k-1}(f; (\mathbf{r}_2)_+)/\mathbb{P}_1(f), \\
(67k) \quad & \int_T \boldsymbol{\tau} : \mathbf{q} \, dx, \quad \mathbf{q} \in \text{def}(\mathbb{B}_{k+2}^3(\mathbf{r}_0)), \\
(67l) \quad & \int_T (\text{inc } \boldsymbol{\tau}) : \mathbf{q} \, dx, \quad \mathbf{q} \in \mathbb{B}_{k-1}^{\text{div}}(\mathbf{r}_2; \mathbb{S}) \cap \ker(\text{div})
\end{aligned}$$

for each $v \in \Delta_0(T)$, $e \in \Delta_1(T)$ and $f \in \Delta_2(T)$.

The motivation behind incorporating DoFs such as (67b), (67e), (67i), (67j), and (67l) lies in their role in enforcing the condition $\text{inc } \boldsymbol{\tau} \in \mathbb{V}_{k-1}^{\text{div}}(\mathbf{r}_2; \mathbb{S})$, which mirrors the purpose of DoFs (32a)-(32f). The inclusion of DoFs (67k)-(67l) serves the distinct purpose of determining the bubble component. By the trace complexes, the face bubble complexes would be

$$\begin{aligned}
\text{tr}_1 : \mathbf{0} &\rightarrow \mathbb{B}_{k+2}^2(f; \mathbf{r}_0) \xrightarrow{\text{sym curl}_f} \mathbb{B}_{k+1}^{\text{div}_f \text{div}_f}(f; \mathbf{r}_1) \xrightarrow{\text{div}_f \text{div}_f} \mathbb{B}_{k-1}(f; \mathbf{r}_2)/\mathbb{P}_1(f) \rightarrow \mathbf{0}, \\
\text{tr}_2 : \mathbf{0} &\rightarrow \mathbb{B}_{k+2}(f; \mathbf{r}_0) \xrightarrow{\text{hess}_f} \mathbb{B}_k^{\text{rot}_f}(f; \mathbf{r}_1 \ominus 1, \mathbb{S}) \xrightarrow{\text{rot}_f} \mathbb{B}_{k-1}^2(f; \mathbf{r}_2)/\text{RM}(f) \rightarrow \mathbf{0}.
\end{aligned}$$

However the face DoFs (67i) and (67j) imply the face bubble complexes are

$$(68) \quad \text{tr}_1 : \mathbf{0} \rightarrow \mathbb{B}_{k+2}^2(f; \mathbf{r}_0) \xrightarrow{\text{sym curl}_f} \mathbb{B}_{k+1}^{\text{div}_f \text{div}_f}(f; \mathbf{r}_1, (\mathbf{r}_2)_+) \xrightarrow{\text{div}_f \text{div}_f} \mathbb{B}_{k-1}(f; (\mathbf{r}_2)_+)/\mathbb{P}_1(f) \rightarrow \mathbf{0},$$

$$(69) \quad \text{tr}_2 : \mathbf{0} \rightarrow \mathbb{B}_{k+2}(f; \mathbf{r}_0) \xrightarrow{\text{hess}_f} \widetilde{\mathbb{B}}_k^{\text{rot}_f}(f; \mathbf{r}_1 \ominus 1, \mathbb{S}) \xrightarrow{\text{rot}_f} \mathbb{B}_{k-1}^{\text{rot}_f}(f; \mathbf{r}_2)/\text{RM}(f) \rightarrow \mathbf{0}.$$

These modifications have been accounted in the face DoFs for $\text{inc } \boldsymbol{\tau}$, without affecting the components stemming from $\mathbb{B}_{k+2}^2(f; \mathbf{r}_0)$ and $\mathbb{B}_{k+2}(f; \mathbf{r}_0)$, as described by DoFs (67f)-(67g). For further insight into the specifics of these two-dimensional bubble polynomial spaces and finite element complexes, we refer to our recent work [22].

In the event that $r_1^\varepsilon = 0$, the inclusion of (67d) is rooted in the aim of enforcing $(\text{curl } \boldsymbol{\tau})^\top \in \mathbb{V}_k^{\text{curl}}(\mathbf{r}_1 \ominus 1; \mathbb{M})$. Conversely, if $r_1^\varepsilon \geq 1$, the same condition is inherently encompassed by (67c), given that $\boldsymbol{\tau}$ exhibits C^1 continuity across edges. A similar rationale underpins the inclusion of (67e), which is exclusively required when $r_2^\varepsilon = -1$. Importantly, all traces of $\boldsymbol{\tau}$ are confined to its tangential component. In instances where $r_1^f = 0$, the introduction of (67h) becomes crucial to ensure the continuous nature of the normal component $\boldsymbol{\tau} \mathbf{n}$.

We present the following lemma for the ease of the dimension count.

Lemma 6.3. *The polynomial elasticity complex*

$$(70) \quad \text{RM} \xrightarrow{\subset} \mathbb{P}_{k+1}(T; \mathbb{R}^3) \xrightarrow{\text{def}} \mathbb{P}_k(T; \mathbb{S}) \xrightarrow{\text{inc}} \mathbb{P}_{k-2}(T; \mathbb{S}) \xrightarrow{\text{div}} \mathbb{P}_{k-3}(T; \mathbb{R}^3) \rightarrow \mathbf{0}$$

is exact for $k \geq 3$. For integer $k \geq 0$,

$$(71) \quad -6 + 3 \binom{k+4}{3} - 6 \binom{k+3}{3} + 6 \binom{k+1}{3} - 3 \binom{k}{3} = 0.$$

Proof. The polynomial elasticity complex is comprehensively presented in [4, (2.6)], or can be systematically derived via polynomial de Rham complexes within the BGG framework; see [19, Section 2.2].

Upon investigating cases where $k \geq 3$, the exactness of (70) implies that (71) can be deduced by taking the alternating sum of the dimensions of the involved spaces. For the instances of $k = 0, 1, 2$, the validity of (71) remains intact and can be readily confirmed through direct verification. \square

Lemma 6.4. *For $r_1^f = 0, -1$, the sum of the number of DoFs (67) equals $\dim \mathbb{P}_{k+1}(T; \mathbb{S})$.*

Proof. At each vertex, when $r_1^v \geq 2$, only DoFs (67a) exist with dimension $6 \binom{r_1^v+3}{3}$. By (71), we have

$$(72) \quad |\text{DoF}_{k+1}^{\text{inc}}(v; \mathbf{r}_1)| = -6 + 3 \binom{r_0^v+3}{3} + 6 \binom{r_2^v+3}{3} - 3 \binom{r_3^v+3}{3}.$$

When $r_1^v = 1$, $(r_0^v, r_1^v, r_2^v, r_3^v) = (2, 1, 0, -1)$, and 6 DoFs (67b) are added. But the sum of number of DoFs (67a)-(67b) is still equal to (72) by direct calculation.

On tetrahedron T , the number of DoFs (67k)-(67l) is

$$(73) \quad |\text{DoF}_{k+1}^{\text{inc}}(T; \mathbf{r}_1)| = 6 + \dim \mathbb{B}_{k+2}^3(\mathbf{r}_0) + \dim \mathbb{B}_{k-1}^{\text{div}}(\mathbf{r}_2; \mathbb{S}) - \dim \mathbb{B}_{k-2}^3(\mathbf{r}_3),$$

as $\text{div } \mathbb{B}_{k-1}^{\text{div}}(\mathbf{r}_2; \mathbb{S}) = \mathbb{B}_{k-2}^3(\mathbf{r}_3)/\text{RM}$.

On each face f , we first consider the case $r_1^f = -1$. By (68)-(69), the number of DoFs (67f)-(67j) is

$$\begin{aligned} & \dim \mathbb{B}_{k+2}^2(f; \mathbf{r}_0) + \dim \mathbb{B}_{k-1}(f; (\mathbf{r}_2)_+) - 3 \\ & + \dim \mathbb{B}_{k+2}(f; \mathbf{r}_0) + \dim \mathbb{B}_{k-1}^{\text{rot}}(f; \mathbf{r}_2) - 3 \\ & = -6 + |\text{DoF}_{k+2}^{\text{grad}}(f; \mathbf{r}_0)| + |\text{DoF}_{k-1}^{\text{div}}(f; \mathbf{r}_2)|. \end{aligned}$$

No DoFs for $\text{DoF}_{k-2}^{\text{grad}}(f; \mathbf{r}_3)$ as $r_3^f = -1$. When $r_1^f = 0$, $r_0^f = 1$, we have one more layer in $\text{DoF}_{k+2}^{\text{grad}}(f; \mathbf{r}_0)$ for $\partial_n \mathbf{v}$: $\mathbb{B}_{k+2-1}^3(f; \mathbf{r}_0 - 1)$ which matches the number of DoF (67h) added for $r_1^f = 0$. So we conclude the the number of face DoFs (67f)-(67j) satisfies

$$(74) \quad \text{DoF}_{k+1}^{\text{inc}}(f; \mathbf{r}_1) = -6 + |\text{DoF}_{k+2}^{\text{grad}}(f; \mathbf{r}_0)| + |\text{DoF}_{k-1}^{\text{div}}(f; \mathbf{r}_2)|.$$

On each edge e , when $r_1^e \geq 2$, only the (67c) exists and its number satisfies

$$(75) \quad \begin{aligned} & 6 + 3 \sum_{j=0}^{r_0^e} (j+1)(k - 2r_1^v - 1 + j) - 6 \sum_{j=0}^{r_1^e} (j+1)(k - 2r_1^v + j) \\ & + 6 \sum_{j=0}^{r_2^e} (j+1)(k - 2r_1^v + 2 + j) - 3 \sum_{j=0}^{r_3^e} (j+1)(k - 2r_1^v + 3 + j). \end{aligned}$$

Let $m = k - 2r_1^v - 1 \geq 0$. We split (75) into terms containing m or not:

$$I_1 = m \left[3 \binom{r_1^e + 3}{2} - 6 \binom{r_1^e + 2}{2} + 6 \binom{r_1^e}{2} - 3 \binom{r_1^e - 1}{2} \right],$$

$$I_2 = 6 + 3 \sum_{j=0}^{r_1^e+1} (j+1)j - 6 \sum_{j=0}^{r_1^e} (j+1)^2 + 6 \sum_{j=0}^{r_1^e-2} (j+1)(j+3) - 3 \sum_{j=0}^{r_1^e-3} (j+1)(j+4).$$

By symbolical calculation, $I_1 = 0$ and $I_2 = 0$ for all integers $r_1^e \geq 2$ even for the boundary case $(r_0^e, r_1^e, r_2^e, r_3^e) = (3, 2, 0, -1)$.

When $r_1^e = 1, r_2^e = -1$, (67e) is added. The added number of DoFs (67e) matches that of (32c) for $\text{DoF}_{k-1}^{\text{div}}(e; \mathbb{S})$. When $r_1^e = 0$, (67d) is further added. Recall that $m = k - 2r_1^v - 1$. By direct calculation, $|\text{DoF}_{k+2}^{\text{grad}}(e; \mathbf{r}_0)| = 9m + 6$. Sum of number of DoFs (67c)-(67d) is

$$6 \dim \mathbb{B}_{k+1}(e; \mathbf{r}_1) + 3 \dim \mathbb{B}_k(e; \mathbf{r}_1 - 1) = 9m + 12 = 6 + |\text{DoF}_{k+2}^{\text{grad}}(e; \mathbf{r}_0)|.$$

So for all cases $r_1^e \geq 0$ the sum of number of edge DoFs (67c)-(67e) satisfies

$$(76) \quad |\text{DoF}_k^{\text{inc}}(e; \mathbf{r}_1)| = 6 + |\text{DoF}_{k+2}^{\text{grad}}(e; \mathbf{r}_0)| + |\text{DoF}_{k-1}^{\text{div}}(e; \mathbf{r}_2)| - |\text{DoF}_{k-2}^{L^2}(e; \mathbf{r}_3)|.$$

Then by the DoFs (21a)-(21d) of spaces $\mathbb{V}_{k+2}(\mathbf{r}_0; \mathbb{R}^3)$ and $\mathbb{V}_{k-2}^{L^2}(\mathbf{r}_3; \mathbb{R}^3)$, Euler's formulae $|\Delta_0| - |\Delta_1| + |\Delta_2| - |\Delta_3| = 1$, and the DoFs (32a) - (32f) of space $\mathbb{V}_{k-1}^{\text{div}}(\mathbf{r}_2; \mathbb{S})$, and identities (72), (76), (74), and (73), the number of DoFs (67) is

$$-6 + \dim \mathbb{P}_{k+2}(T; \mathbb{R}^3) + \dim \mathbb{P}_{k-1}(T; \mathbb{S}) - \dim \mathbb{P}_{k-2}(T; \mathbb{R}^3),$$

which equals $\dim \mathbb{P}_{k+1}(T; \mathbb{S})$ in view of the polynomial elasticity complex (70). \square

Lemma 6.5. *The DoFs (67) are uni-solvent for $\mathbb{P}_{k+1}(T; \mathbb{S})$.*

Proof. By leveraging Lemma 6.4, our objective is to establish $\boldsymbol{\tau} = \mathbf{0}$ when $\boldsymbol{\tau} \in \mathbb{P}_{k+1}(T; \mathbb{S})$ adheres to the condition that all the specified DoFs (67) vanish.

To commence, the vanishing (67a) implies that $\boldsymbol{\tau}(\mathbf{v}) = 0$ and $(\text{curl } \boldsymbol{\tau})^\top(\mathbf{v}) = 0$. This, combined with the vanishing DoFs (67c)-(67d), leads to $\boldsymbol{\tau}|_e = 0$ and $(\text{curl } \boldsymbol{\tau})^\top|_e = 0$. Employing integration by parts further yields:

$$\begin{aligned} \int_f \Pi_f(\text{inc } \boldsymbol{\tau}) \mathbf{n} \cdot \mathbf{q} \, dS &= \int_f \text{rot}_f(\mathbf{n} \times (\text{curl } \boldsymbol{\tau})^\top \Pi_f) \cdot \mathbf{q} \, dS = 0, \quad \mathbf{q} \in \text{RT}(f), \\ \int_f \mathbf{n}^\top(\text{inc } \boldsymbol{\tau}) \mathbf{n} \, q \, dS &= \int_f \text{div}_f \text{div}_f(\mathbf{n} \times \boldsymbol{\tau} \times \mathbf{n}) \, q \, dS = 0, \quad q \in \mathbb{P}_1(f). \end{aligned}$$

More detailed descriptions of edge traces can be found in [19, Lemma 4.8]. This, combined with the nullified DoFs (67a)-(67c), (67e), (67i)-(67j), and (67l), yields $\text{inc } \boldsymbol{\tau} = \mathbf{0}$.

Consequently it implies that $\boldsymbol{\tau} = \text{def}(\mathbf{v})$ for $\mathbf{v} \in \mathbb{P}_{k+2}(T; \mathbb{R}^3)$. Furthermore, the nullification of DoFs (67a) and (67c) leads to $(\nabla^i \mathbf{v})(\mathbf{v}) = \mathbf{0}$ for $\mathbf{v} \in \Delta_0(T)$ and $i = 0, \dots, r_1^v + 1$, and $(\nabla^i \mathbf{v})|_e = \mathbf{0}$ for $e \in \Delta_1(T)$ and $i = 0, \dots, r_1^e + 1$. Similarly, from the nullification of (67f)-(67h), we deduce that $(\nabla^i \mathbf{v})|_f = \mathbf{0}$ for $f \in \Delta_2(T)$ and $i = 0, \dots, r_1^f + 1$.

Combining these outcomes, it is apparent that $\mathbf{v} \in \mathbb{B}_{k+2}^3(\mathbf{r}_0)$. Consequently, $\mathbf{v} = \mathbf{0}$ is deduced from the vanishing DoF (67k). \square

Next we show the constructed $H(\text{inc})$ -conforming finite element space is indeed the space $\mathbb{V}_{k+1}^{\text{inc}}(\mathbf{r}_1; \mathbb{S})$ defined by (48) and used in the finite element elasticity complex (53).

Lemma 6.6. For $r_1^f = -1, 0$, let

$$\mathbb{V}_{k+1}^{\text{inc}}(\mathbf{r}_1; \mathbb{S}) := \{\boldsymbol{\tau} \in L^2(\Omega; \mathbb{S}) : \boldsymbol{\tau}|_T \in \mathbb{P}_{k+1}(T; \mathbb{S}) \text{ for all } T \in \mathcal{T}_h, \\ \text{and all the DoFs (67) are single-valued}\}.$$

Then it is equal to the space $\{\boldsymbol{\tau} \in \mathbb{V}_{k+1}(\mathbf{r}_1) \otimes \mathbb{S} : \text{inc } \boldsymbol{\tau} \in \mathbb{V}_{k-1}^{\text{div}}(\mathbf{r}_2; \mathbb{S})\}$.

Proof. Clearly $\mathbb{V}_{k+1}^{\text{inc}}(\mathbf{r}_1; \mathbb{S}) \subseteq \{\boldsymbol{\tau} \in \mathbb{V}_{k+1}(\mathbf{r}_1) \otimes \mathbb{S} : \text{inc } \boldsymbol{\tau} \in \mathbb{V}_{k-1}^{\text{div}}(\mathbf{r}_2; \mathbb{S})\}$. By (54) and the proof of Lemma 6.4, their dimensions are equal. \square

There exist various variations of the finite element elasticity complexes. To illustrate one of these variations, we construct the space $\mathbb{V}_{k+1}^{\text{inc}^+}(\mathbf{r}_1; \mathbb{S})$. In cases where $r_1^f = -1$, we introduce an additional face degree of freedom:

$$(77) \quad \int_f (\mathbf{n}^\top \boldsymbol{\tau} \Pi_f) \cdot \mathbf{q} \, dS, \quad \mathbf{q} \in \mathbb{B}_{k+1}^2(f; \mathbf{r}_1).$$

Moreover, we modify (67k) to:

$$(78) \quad \int_T \boldsymbol{\tau} : \mathbf{q} \, dx, \quad \mathbf{q} \in \text{def}(\mathbb{B}_{k+2}^{\text{curl}}(\mathbf{r}_0, (\mathbf{r}_1)_+)).$$

Recall that $\mathbf{r}_0 \geq (2, 1, 0)^\top$. For $\mathbf{u} \in \mathbb{V}_{k+2}^{\text{curl}}(\mathbf{r}_0)$, the normal continuity of $\text{curl } \mathbf{u}$ is always maintained. To achieve continuity for all components, we require $\int_f \mathbf{n} \times \text{curl } \mathbf{u} \cdot \mathbf{q} \, dS$ for $\mathbf{q} \in \mathbb{B}_{k+1}^2(f; \mathbf{r}_1)$. This ensures a balance between the added DoFs in (77) and the reduced DoFs from (67k) to (78), maintaining unisolvence in a similar manner.

An advantage of using the space $\mathbb{V}_{k+1}^{\text{inc}^+}(\mathbf{r}_1; \mathbb{S})$ is the reduction in dimension from the space $\mathbb{V}_{k+1}^{\text{inc}}(\mathbf{r}_1; \mathbb{S})$:

$$\dim \mathbb{V}_{k+1}^{\text{inc}}(\mathbf{r}_1; \mathbb{S}) - \dim \mathbb{V}_{k+1}^{\text{inc}^+}(\mathbf{r}_1; \mathbb{S}) = (4|\Delta_3(\mathcal{T}_h)| - |\Delta_2(\mathcal{T}_h)|) \dim \mathbb{B}_{k+1}^2(f; \mathbf{r}_1).$$

A relaxed constraint, $\mathbf{r}_2 \geq \max\{\mathbf{r}_1 \ominus 2, (0, -1, -1)^\top\}$, leads to another variation of the space $\mathbb{V}_{k+1}^{\text{inc}}(\mathbf{r}_1; \mathbb{S})$:

$$\mathbb{V}_{k+1}^{\text{inc}}(\mathbf{r}_1, \mathbf{r}_2; \mathbb{S}) := \{\boldsymbol{\tau} \in \mathbb{V}_{k+1}^{\text{inc}}(\mathbf{r}_1; \mathbb{S}) : \text{inc } \boldsymbol{\tau} \in \mathbb{V}_{k-1}^{\text{div}}(\mathbf{r}_2; \mathbb{S})\}.$$

A finite element description of this space can be derived by first introducing the necessary DoFs to determine $\text{inc } \boldsymbol{\tau}$, and then eliminating any redundant DoFs. Due to the complexity of these variations, we omit the detailed explanation here.

6.3. $H(\text{sym curl}; \mathbb{T})$ -conforming elements. We will now provide a comprehensive description of the $H(\text{sym curl})$ -conforming element space $\mathbb{V}_{k+1}^{\text{sym curl}^+}(\mathbf{r}_1; \mathbb{T})$. When $r_1^f \geq 1$, it is simply $\mathbb{V}_{k+1}(\mathbf{r}_1) \otimes \mathbb{T}$. So our focus is $r_1^f = -1$ or $r_1^f = 0$.

It is important to recall the trace complexes that were previously established in [21]:

$$\begin{array}{ccccccc} \text{RT} & \xrightarrow{\subset} & \mathbf{v} & \xrightarrow{\text{dev grad}} & \boldsymbol{\tau} & \xrightarrow{\text{sym curl}} & \boldsymbol{\sigma} & \xrightarrow{\text{div div}} & p \\ \downarrow & & \downarrow & & \downarrow & & \downarrow & & \\ \mathbb{R} & \xrightarrow{\subset} & \mathbf{v} \cdot \mathbf{n} & \xrightarrow{-\text{curl}_f} & \mathbf{n} \cdot \boldsymbol{\tau} \times \mathbf{n} & \xrightarrow{\text{div}_f} & \mathbf{n} \cdot \boldsymbol{\sigma} \cdot \mathbf{n} & \longrightarrow & 0, \end{array}$$

and

$$\begin{array}{ccccccc}
\text{RT} & \xrightarrow{\subset} & \mathbf{v} & \xrightarrow{\text{dev grad}} & \boldsymbol{\tau} & \xrightarrow{\text{sym curl}} & \boldsymbol{\sigma} & \xrightarrow{\text{div div}} & p \\
\downarrow & & \downarrow & & \downarrow & & \downarrow & & \\
\text{RT}_f & \xrightarrow{\subset} & \Pi_f \mathbf{v} & \xrightarrow{\text{sym curl}_f} & \Pi_f \text{sym}(\boldsymbol{\tau} \times \mathbf{n}) & \xrightarrow{\text{div}_f \text{div}_f} & \text{tr}_2^{\text{div}} \text{div}(\boldsymbol{\sigma}) & \longrightarrow & 0.
\end{array}$$

The trace complexes above play a crucial role in guiding the design of edge and face DoFs to ensure the necessary continuity. As shown in [21, Lemma 6.1], the expression

$$\text{tr}_{2,e}^{\text{div}_f \text{div}_f}(\Pi_f \text{sym}(\boldsymbol{\tau} \times \mathbf{n})\Pi_f) = \mathbf{n}_{f,e}^{\top}(\text{curl } \boldsymbol{\tau})\mathbf{n}_f + \partial_t(\mathbf{t}^{\top} \boldsymbol{\tau} \mathbf{t}),$$

provides the motivation for introducing DoFs involving terms like $\mathbf{n}_2^{\top}(\text{curl } \boldsymbol{\tau})\mathbf{n}_1 + \partial_t(\mathbf{t}^{\top} \boldsymbol{\tau} \mathbf{t})$ on edges. In cases where $r_1^e = 0$, the focus is on enforcing the continuity of $\mathbf{n}_2^{\top}(\text{curl } \boldsymbol{\tau})\mathbf{n}_1$

on edges, which aligns with the requirement $\widehat{\mathbb{V}}_{k+1}^{\text{curl}}(\mathbf{r}_1; \mathbb{M}) \subseteq \text{mskw } \mathbb{V}_k^{\text{curl}}(\mathbf{r}_1 \ominus 1)$. The other edge traces further ensure the continuity of terms like $\mathbf{n}_i^{\top} \boldsymbol{\tau} \mathbf{t}$ on edges.

The shape function space is $\mathbb{P}_{k+1}(T; \mathbb{T})$. The degrees of freedom are

$$(79a) \quad \nabla^i \boldsymbol{\tau}(\mathbf{v}), \quad i = 0, \dots, r_1^{\vee},$$

$$(79b) \quad \text{sym curl } \boldsymbol{\tau}(\mathbf{v}), \quad \text{if } r_1^{\vee} = 0,$$

$$(79c) \quad \int_e \frac{\partial^j \boldsymbol{\tau}}{\partial n_1^i \partial n_2^{j-i}} : \mathbf{q} \, ds, \quad \mathbf{q} \in \mathbb{B}_{k+1-j}(e; r_1^{\vee} - j) \otimes \mathbb{T}, 0 \leq i \leq j \leq r_1^e,$$

$$(79d) \quad \int_e (\mathbf{n}_i^{\top} \boldsymbol{\tau} \mathbf{t}) q \, ds, \quad q \in \mathbb{B}_{k+1}(e; r_1^{\vee}), \text{ if } r_1^e = -1,$$

$$(79e) \quad \int_e (\mathbf{n}_2^{\top}(\text{curl } \boldsymbol{\tau})\mathbf{n}_1 + \partial_t(\mathbf{t}^{\top} \boldsymbol{\tau} \mathbf{t})) q \, ds, \quad q \in \mathbb{B}_k(e; r_1^{\vee} - 1), \text{ if } r_1^e = -1, 0,$$

$$(79f) \quad \int_e (\mathbf{n}_i^{\top}(\text{sym curl } \boldsymbol{\tau})\mathbf{n}_j) q \, ds, \quad q \in \mathbb{B}_k(e; r_2^{\vee}), 1 \leq i \leq j \leq 2, \text{ if } r_2^e = -1,$$

$$(79g) \quad \int_f \boldsymbol{\tau} \mathbf{n} \cdot \mathbf{q} \, dS, \quad \mathbf{q} \in \mathbb{B}_{k+1}^3(f; \mathbf{r}_1), \text{ if } r_1^f = 0,$$

$$(79h) \quad \int_f (\mathbf{n} \cdot \boldsymbol{\tau} \times \mathbf{n}) \cdot \mathbf{q} \, dS, \quad \mathbf{q} \in \text{curl}_f \mathbb{B}_{k+2}(f; \mathbf{r}_0),$$

$$(79i) \quad \int_f \text{div}_f(\mathbf{n} \cdot \boldsymbol{\tau} \times \mathbf{n}) q \, dS, \quad q \in \mathbb{B}_k(f; (\mathbf{r}_2)_+)/\mathbb{R},$$

$$(79j) \quad \int_f \Pi_f \text{sym}(\boldsymbol{\tau} \times \mathbf{n})\Pi_f : \mathbf{q} \, dS, \quad \mathbf{q} \in \text{sym curl}_f \mathbb{B}_{k+2}^2(f; \mathbf{r}_0),$$

$$(79k) \quad \int_f \text{div}_f \text{div}_f(\text{sym}(\boldsymbol{\tau} \times \mathbf{n})) q \, dS, \quad q \in \mathbb{B}_{k-1}(f; \mathbf{r}_2 \ominus 1)/\mathbb{P}_1(f),$$

$$(79l) \quad \int_f \Pi_f(\text{sym curl } \boldsymbol{\tau})\mathbf{n} \cdot \mathbf{q} \, dS, \quad \mathbf{q} \in \mathbb{B}_k^{\text{div}}(f; \mathbf{r}_2),$$

$$(79m) \quad \int_T \boldsymbol{\tau} : \mathbf{q} \, dx, \quad \mathbf{q} \in \text{dev grad}(\mathbb{B}_{k+2}^3(\mathbf{r}_0)),$$

$$(79n) \quad \int_T (\text{sym curl } \boldsymbol{\tau}) : \mathbf{q} \, dx, \quad \mathbf{q} \in \mathbb{B}_k^{\text{div div}^+}(\mathbf{r}_2; \mathbb{S}) \cap \ker(\text{div div})$$

for each $\mathbf{v} \in \Delta_0(T)$, $e \in \Delta_1(T)$ and $f \in \Delta_2(T)$.

Lemma 6.7. *The following polynomial div div complex*

$$(80) \quad \text{RT} \xrightarrow{\subset} \mathbb{P}_{k+2}(T; \mathbb{R}^3) \xrightarrow{\text{dev grad}} \mathbb{P}_{k+1}(T; \mathbb{T}) \xrightarrow{\text{sym curl}} \mathbb{P}_k(T; \mathbb{S}) \xrightarrow{\text{div div}} \mathbb{P}_{k-2}(T) \rightarrow 0$$

is exact. For integer $k \geq 2$,

$$(81) \quad -4 + \dim \mathbb{P}_{k+2}(T; \mathbb{R}^3) - \dim \mathbb{P}_{k+1}(T; \mathbb{T}) + \mathbb{P}_k(T; \mathbb{S}) - \mathbb{P}_{k-2}(T) = 0.$$

And, for all integers $m \geq 0$,

$$(82) \quad -4 + 3 \binom{m+4}{3} - 8 \binom{m+3}{3} + 6 \binom{m+2}{3} - \binom{m}{3} = 0.$$

Proof. A proof of (80) can be found in [21]. A consequence of the exactness of (80) is the dimension identity (81). Identity (82) follows from (81) when $m \geq 3$ and can be verified directly for $m = 0, 1, 2$. \square

Lemma 6.8. *The sum of the number of DoFs (79) equals $\dim \mathbb{P}_{k+1}(T; \mathbb{T})$.*

Proof. At each vertex, when $r_1^v \geq 1$, only DoFs (79a) exists with dimension $8 \binom{r_1^v+3}{3}$. By (82), we have

$$(83) \quad \text{DoF}_{k+1}^{\text{sym curl}^+}(v; \mathbf{r}_1) = -4 + 3 \binom{r_0^v+3}{3} + 6 \binom{r_2^v+3}{3} - \binom{r_3^v+3}{3}.$$

When $r_1^v = 0$, additional 6 DoFs (79b) are added but now $r_2^v = 0, r_3^v = -1$ and so (83) still holds.

On tetrahedron T , the number of DoFs (79m)-(79n) is

$$(84) \quad 4 + \dim \mathbb{B}_{k+2}^3(\mathbf{r}_0) + \dim \mathbb{B}_k^{\text{div div}^+}(\mathbf{r}_2; \mathbb{S}) - \dim \mathbb{B}_{k-2}(\mathbf{r}_3),$$

as $\text{div div } \mathbb{B}_k^{\text{div div}^+}(\mathbf{r}_2; \mathbb{T}) = \mathbb{B}_{k-2}(\mathbf{r}_3)/\text{RT}$.

On each face, we consider $r_1^f = -1$ first. Sum of number of DoFs (79h) and (79j) is $\dim \mathbb{B}_{k+2}^3(f; \mathbf{r}_0) = |\text{DoF}_{k+1}^{\text{grad}}(f; \mathbf{r}_0)|$. Sum of (79i) and (79k) is $\dim \mathbb{B}_k(f; (\mathbf{r}_2)_+) + \dim \mathbb{B}_{k-1}(f; \mathbf{r}_2 \ominus 1) - 4$. Comparing with the face DoFs (38e)-(38g) for $\mathbb{V}_k^{\text{div div}^+}(\mathbf{r}_2; \mathbb{S})$, plus (79l), we conclude the dimension identity

$$(85) \quad |\text{DoF}_{k+1}^{\text{sym curl}^+}(f; \mathbf{r}_1)| = -4 + |\text{DoF}_{k+2}^{\text{grad}}(f; \mathbf{r}_0)| + |\text{DoF}_k^{\text{div div}^+}(f; \mathbf{r}_2)|.$$

When $r_1^f = 0, r_2^f = -1$ and thus no change of $|\text{DoF}_k^{\text{div div}^+}(f; \mathbf{r}_2)|$. But $r_0^f = 1$, one more layer in $\text{DoF}_{k+1}^{\text{grad}}(f; \mathbf{r}_0)$ is added for $\partial_n \mathbf{v}$: $\dim \mathbb{B}_{k+2-1}^3(f; \mathbf{r}_0 - 1)$ which matches the number of DoF (79g) added for $r_1^f = 0$. So (85) holds for both $r_1^f = -1, 0$. No face DoFs for $\mathbb{V}_{k-2}^{L^2}(f; \mathbf{r}_3)$ as $r_3^f = -1$.

On each edge, we separate into three cases.

\square When $r_1^e \geq 1$, only (79c) exists. We write out the dimension of edge DoFs for spaces in the divdiv complex

$$(86) \quad 4 + 3 \sum_{j=0}^{r_0^e} (j+1)(k - 2r_1^v - 1 + j) - 8 \sum_{j=0}^{r_1^e} (j+1)(k - 2r_1^v + j) + 6 \sum_{j=0}^{r_2^e} (j+1)(k - 2r_1^v + 1 + j) - \sum_{j=0}^{r_3^e} (j+1)(k - 2r_1^v + 3 + j).$$

Let $m = k - 2r_1^v - 1 \geq 0$. We split (86) into terms containing m or not:

$$\begin{aligned} I_1 &= m \left[3 \binom{r_1^e + 3}{2} - 8 \binom{r_1^e + 2}{2} + 6 \binom{r_1^e + 1}{2} - \binom{r_1^e - 1}{2} \right], \\ I_2 &= 4 + 3 \sum_{j=0}^{r_0^e} (j+1)j - 8 \sum_{j=0}^{r_1^e} (j+1)^2 + 6 \sum_{j=0}^{r_2^e} (j+1)(j+2) - \sum_{j=0}^{r_3^e} (j+1)(j+4). \end{aligned}$$

By symbolical calculation, $I_1 = 0$ and $I_2 = 0$ for all integers $r_1^e \geq 1$ even for the case $(r_0^e, r_1^e, r_2^e, r_3^e) = (2, 1, 0, -1)$.

[2] When $r_1^e = 0, r_2^e = -1, r_3^e = -1$, in (86) the last two terms disappeared. DoFs (79e) and (79f) are added for $\text{DoF}_{k+1}^{\text{sym curl}^+}(e; \mathbf{r}_1)$. The number of DoFs (79f) is $|\text{DoF}_k^{\text{div div}^+}(e; \mathbf{r}_2)|$.

Recall that $m = k - 2r_1^v - 1$. By direct calculation, $|\text{DoF}_{k+2}^{\text{grad}}(e; \mathbf{r}_0)| = 9m + 6$. Sum of number of DoFs (79c) and (79e) is $8 \dim \mathbb{B}_{k+1}(e; r_1^v) + \dim \mathbb{B}_k(e; r_1^v - 1) = 9m + 10$. Therefore we conclude

$$(87) \quad |\text{DoF}_{k+1}^{\text{sym curl}^+}(e; \mathbf{r}_1)| = 4 + |\text{DoF}_{k+2}^{\text{grad}}(e; \mathbf{r}_0)| + |\text{DoF}_k^{\text{div div}^+}(e; \mathbf{r}_2)|.$$

No $|\text{DoF}_{k-2}^{L^2}(e; \mathbf{r}_3)|$ is in (87) as $r_3^e = -1$.

[3] When $r_1^e = -1, r_2^e = -1, r_0^e = 0$, (79c) is further removed. Now (79d), (79e), and (79f) are present. The number of DoFs (79f) is still $|\text{DoF}_k^{\text{div div}^+}(e; \mathbf{r}_2)|$. The number of DoFs (79d)-(79e) is

$$2 \dim \mathbb{B}_{k+1}(e; r_1^v) + \dim \mathbb{B}_k(e; r_1^v - 1) = 3m + 1 = 4 + |\text{DoF}_{k+2}^{\text{grad}}(e; \mathbf{r}_0)|.$$

So (87) still holds.

In summary, for all cases the number of DoFs (79c)-(79f) at an edge satisfies

$$(88) \quad |\text{DoF}_{k+1}^{\text{sym curl}^+}(e; \mathbf{r}_1)| = 4 + |\text{DoF}_{k+2}^{\text{grad}}(e; \mathbf{r}_0)| + |\text{DoF}_k^{\text{div div}^+}(e; \mathbf{r}_2)| - |\text{DoF}_{k-2}^{L^2}(e; \mathbf{r}_3)|.$$

Then combining (83), (88), (85), and (84), by the DoFs of spaces $\mathbb{V}_{k+2}(\mathbf{r}_1 + 1; \mathbb{R}^3)$, $\mathbb{V}_k^{\text{div div}^+}(\mathbf{r}_2; \mathbb{S})$ and $\mathbb{V}_{k-2}^{L^2}(\mathbf{r}_3)$ and the Euler's formulae $|\Delta_0(T)| - |\Delta_1(T)| + |\Delta_2(T)| - |\Delta_3(T)| = 1$, the number of DoFs (79a)-(79n) is

$$-4 + \dim \mathbb{P}_{k+2}(T; \mathbb{R}^3) + \dim \mathbb{P}_k(T; \mathbb{S}) - \dim \mathbb{P}_{k-2}(T),$$

which equals $\dim \mathbb{P}_{k+1}(T; \mathbb{T})$ in view of (81). \square

Lemma 6.9. *The DoFs (79) are uni-solvent for $\mathbb{P}_{k+1}(T; \mathbb{T})$.*

Proof. In light of Lemma 6.8, we only need to prove $\boldsymbol{\tau} = \mathbf{0}$ for $\boldsymbol{\tau} \in \mathbb{P}_{k+1}(T; \mathbb{T})$ that all the specified DoFs (79) are nullified.

The vanishing DoF (79c) implies

$$\int_e \frac{\partial^j (\text{sym curl } \boldsymbol{\tau})}{\partial n_1^i \partial n_2^{j-i}} : \mathbf{q} \, ds = 0, \quad \mathbf{q} \in \mathbb{B}_{k-j}(e; r_2^v - j) \otimes \mathbb{S}, 0 \leq i \leq j \leq r_2^e.$$

The vanishing DoF (79e) implies

$$\int_e \text{tr}_2^{\text{div}_f \text{div}_f} (\Pi_f \text{sym}(\boldsymbol{\tau} \times \mathbf{n}) \Pi_f) \mathbf{q} \, ds = 0, \quad \mathbf{q} \in \mathbb{B}_k(e; r_1^v - 1), \text{ if } r_1^e = -1, 0.$$

Detailed expressions for these formulations are provided in [21, Lemma 6.1].

Applying the integration by parts, it follows from the vanishing DoFs (79c)-(79e) that

$$\int_f \operatorname{div}_f(\mathbf{n} \cdot \boldsymbol{\tau} \times \mathbf{n}) \, dS = 0,$$

$$\int_f \operatorname{div}_f \operatorname{div}_f(\operatorname{sym}(\boldsymbol{\tau} \times \mathbf{n})) \, q \, dS = 0, \quad q \in \mathbb{P}_1(f).$$

Using the identities

$$\operatorname{tr}_2^{\operatorname{div} \operatorname{div}}(\operatorname{sym} \operatorname{curl} \boldsymbol{\tau}) = \operatorname{div}_f \operatorname{div}_f \operatorname{sym}(\boldsymbol{\tau} \times \mathbf{n}),$$

$$\operatorname{tr}_2^{\operatorname{div} \operatorname{div}}(\operatorname{sym} \operatorname{curl} \boldsymbol{\tau}) = (\operatorname{div} \operatorname{sym} \operatorname{curl} \boldsymbol{\tau}) \cdot \mathbf{n} + \operatorname{div}_f(\Pi_f(\operatorname{sym} \operatorname{curl} \boldsymbol{\tau})\mathbf{n}),$$

the linear combination of DoFs (79k) and (79l) implies the continuity of $(\operatorname{div} \operatorname{sym} \operatorname{curl} \boldsymbol{\tau}) \cdot \mathbf{n}$, i.e., $\operatorname{sym} \operatorname{curl} \boldsymbol{\tau} \in H(\operatorname{div}, \Omega; \mathbb{S})$.

This, combined with the vanishing (79a)-(79c),(79e)-(79f),(79i),(79k)-(79l), and (79n), lead us to the conclusion that $\operatorname{sym} \operatorname{curl} \boldsymbol{\tau} = \mathbf{0}$. As a result, we find that $\boldsymbol{\tau} = \operatorname{dev} \operatorname{grad} \mathbf{v}$ where $\mathbf{v} \in \mathbb{P}_{k+2}(T; \mathbb{R}^3)$.

Then the vanishing DoFs (79a) and (79c)-(79e) imply $(\nabla^i \mathbf{v})(\mathbf{v}) = \mathbf{0}$ for $\mathbf{v} \in \Delta_0(T)$ and $i = 0, \dots, r_0^v$, and $(\nabla^i \mathbf{v})|_e = \mathbf{0}$ for $e \in \Delta_1(T)$ and $i = 0, \dots, r_0^e$. By the vanishing DoFs (79h) and (79j), we get $(\nabla^i \mathbf{v})|_f = \mathbf{0}$ for $f \in \Delta_2(T)$ and $i = 0, \dots, r_0^f$. Combining these results indicates $\mathbf{v} \in \mathbb{B}_{k+2}^3(\mathbf{r}_0)$. Therefore $\mathbf{v} = \mathbf{0}$ holds from the vanishing DoF (79m). \square

Lemma 6.10. *For $r_1^f = -1, 0$, define*

$$\mathbb{V}_{k+1}^{\operatorname{sym} \operatorname{curl}^+}(\mathbf{r}_1; \mathbb{T}) := \{\boldsymbol{\tau} \in L^2(\Omega; \mathbb{T}) : \boldsymbol{\tau}|_T \in \mathbb{P}_{k+1}(T; \mathbb{T}) \text{ for all } T \in \mathcal{T}_h,$$

and all the DoFs (79) are single-valued\}.

Then it is equal to the space $\{\boldsymbol{\tau} \in \mathbb{V}_{k+1}(\mathbf{r}_1) \otimes \mathbb{T} : \operatorname{sym} \operatorname{curl} \boldsymbol{\tau} \in \mathbb{V}_k^{\operatorname{div} \operatorname{div}^+}(\mathbf{r}_2; \mathbb{S})\}$.

Proof. Clearly $\mathbb{V}_{k+1}^{\operatorname{sym} \operatorname{curl}^+}(\mathbf{r}_1; \mathbb{T}) \subseteq \{\boldsymbol{\tau} \in \mathbb{V}_{k+1}(\mathbf{r}_1) \otimes \mathbb{T} : \operatorname{sym} \operatorname{curl} \boldsymbol{\tau} \in \mathbb{V}_k^{\operatorname{div} \operatorname{div}^+}(\mathbf{r}_2; \mathbb{S})\}$. By (60) and the proof of Lemma 6.8, their dimensions are equal. \square

To construct the space $\mathbb{V}_{k+1}^{\operatorname{sym} \operatorname{curl}}(\mathbf{r}_1; \mathbb{T})$, we will modify the DoFs (79). The changes involve removing the DoF (79l), and extending the DoF (79n) to a more general form:

$$(89) \quad \int_T (\operatorname{sym} \operatorname{curl} \boldsymbol{\tau}) : \mathbf{q} \, dx, \quad \mathbf{q} \in \mathbb{B}_k^{\operatorname{div} \operatorname{div}}(\mathbf{r}_2; \mathbb{S}) \cap \ker(\operatorname{div} \operatorname{div}).$$

These modifications maintain the sum of DoFs unchanged, as determined by the bubble space definition. The unisolvence of the modified DoFs can be proven in a manner similar to the original ones.

For the case when $r_1^f = -1$ or 0 , we need to redefine the space as follows:

$$\mathbb{V}_{k+1}^{\operatorname{sym} \operatorname{curl}}(\mathbf{r}_1; \mathbb{T}) := \{\boldsymbol{\tau} \in L^2(\Omega; \mathbb{T}) : \boldsymbol{\tau}|_T \in \mathbb{P}_{k+1}(T; \mathbb{T}) \text{ for all } T \in \mathcal{T}_h, \text{ and}$$

all DoFs (79a)-(79m), removing (79l) adding (89), are single-valued\}

By this construction, we ensure that $\operatorname{sym} \operatorname{curl} \mathbb{V}_{k+1}^{\operatorname{sym} \operatorname{curl}}(\mathbf{r}_1; \mathbb{T}) \subset \mathbb{V}_{k+1}^{\operatorname{div} \operatorname{div}}(\mathbf{r}_2; \mathbb{S})$. Thus, we obtain the complex (61). To establish its exactness, we verify the dimension identity:

$$-4 + \dim \mathbb{V}_{k+2}^{\operatorname{grad}}(\mathbf{r}_0) - \dim \mathbb{V}_{k+1}^{\operatorname{sym} \operatorname{curl}}(\mathbf{r}_1; \mathbb{T})$$

$$+ \dim \mathbb{V}_k^{\operatorname{div} \operatorname{div}}(\mathbf{r}_2; \mathbb{S}) - \dim \mathbb{V}_{k-2}^{L^2}(\mathbf{r}_3) = 0,$$

which can be derived from (60) by notifying

$$\begin{aligned} & \dim \mathbb{V}_{k+1}^{\text{sym curl}}(\mathbf{r}_1; \mathbb{T}) - \dim \mathbb{V}_{k+1}^{\text{sym curl}^+}(\mathbf{r}_1; \mathbb{T}) \\ &= \dim \mathbb{V}_k^{\text{div div}}(\mathbf{r}_2; \mathbb{S}) - \dim \mathbb{V}_k^{\text{div div}^+}(\mathbf{r}_2; \mathbb{S}) \\ &= (4|\Delta_3(\mathcal{T}_h)| - |\Delta_2(\mathcal{T}_h)|) \dim \mathbb{B}_k^{\text{div}}(f; \mathbf{r}_2). \end{aligned}$$

The removed DoF (791) will contribute to the bubble functions.

Remark 6.11. When considering the div div^+ element, one can explore various variants such as the Hu-Zhang type element (cf. Remark 4.3). This may lead to an increase in the number of edge DoFs for $\mathbb{V}_k^{\text{div div}^+}(\mathbf{r}_2)$ when $r_2^e = -1$. However, the modifications introduced will not affect the dimension count for edge DoFs, as the added edge DoFs will correspond to $|\text{DoF}_k^{\text{div div}^+}(e; \mathbf{r}_2)|$, thus preserving the relationship stated in (87). \square

There are more variants of sym curl elements. We can add edge continuity of $t^\top \boldsymbol{\tau} t$ and face continuity $\int_f \text{skw}(\Pi_f \boldsymbol{\tau} \times \mathbf{n})$ so that $\boldsymbol{\tau} \times \mathbf{n}$ is continuous. Then we can construct finite element spaces $\mathbb{V}_{k+1}^{\text{sym curl}^+}(\mathbf{r}_1; \mathbb{T})$ and $\mathbb{V}_{k+1}^{\text{sym curl}^+}(\mathbf{r}_1; \mathbb{T})$. We can also relax to $\mathbf{r}_3 \geq \mathbf{r}_2 \ominus 1$ and impose condition

$$\text{sym curl } \boldsymbol{\tau} \in \mathbb{V}_k^{\text{div div}^+}(\mathbf{r}_2, \mathbf{r}_3; \mathbb{S}),$$

which require additional DoFs for $\text{div sym curl } \boldsymbol{\tau} \in \mathbb{V}_{k-1}^{\text{div}}(\mathbf{r}_3; \mathbb{S})$. The div div complex in [35] belongs to this type of variant. Furthermore \mathbf{r}_2 can be relaxed to $\mathbf{r}_2 \geq \mathbf{r}_1 \ominus 1$ but the modification of DoFs will be more involved and the lengthy detail is skipped here.

Notice that the space $\mathbb{V}_{k+1}^{\text{sym curl}}((0, -1, -1)^\top; \mathbb{T})$ constructed in [25] is much simpler as $\mathbb{V}_k^{\text{div div}}(-1; \mathbb{S})$ is used.

APPENDIX A. BUBBLE POLYNOMIAL COMPLEXES

In this section we will develop various bubble polynomial complexes.

A.1. Bubble de Rham complex. We refer to Section 3.1 for the definition of polynomial bubble spaces on faces and tetrahedron. It holds [23, Lemma 3.11]

(90)

$$\begin{aligned} \dim \mathbb{B}_k(T; \mathbf{r}) &= -3 \binom{k+3}{3} + 8 \binom{r^\vee+3}{3} - 6(k+r^e-2r^\vee-1) \binom{r^e+2}{2} \\ &+ 6 \binom{r^e+2}{3} + 12 \binom{k-2r^\vee-1}{3} + 12(r^f+1) \binom{k-2r^\vee+r^e}{2} \\ &+ 4 \binom{k+2-r^f}{3} - 12 \binom{r^\vee+2-r^f}{3} - 12 \binom{k-2r^\vee+r^f}{3}. \end{aligned}$$

A.1.1. Bubble de Rham complex in two dimensions.

Lemma A.1. *Let smoothness vectors $\mathbf{r}_1 \geq -1$, $\mathbf{r}_0 = \mathbf{r}_1 + 1$, and $\mathbf{r}_2 = \mathbf{r}_1 \ominus 1$. Let $f \in \Delta_2(T)$ and $k \geq \max\{2r_1^\vee - 1, 0\}$. Then the bubble de Rham complexes*

$$(91) \quad 0 \xrightarrow{C} \mathbb{B}_{k+2}(f; \mathbf{r}_0) \xrightarrow{\text{curl}_f} \mathbb{B}_{k+1}^{\text{div}_f}(f; \mathbf{r}_1) \xrightarrow{\text{div}_f} \mathbb{B}_k(f; \mathbf{r}_2)/\mathbb{R} \rightarrow 0,$$

$$(92) \quad 0 \xrightarrow{C} \mathbb{B}_{k+2}(f; \mathbf{r}_0) \xrightarrow{\text{grad}_f} \mathbb{B}_{k+1}^{\text{rot}_f}(f; \mathbf{r}_1) \xrightarrow{\text{rot}_f} \mathbb{B}_k(f; \mathbf{r}_2)/\mathbb{R} \rightarrow 0$$

are exact.

Proof. Since complex (92) is only the rotation of complex (91), it suffices to prove the exactness of complex (91).

We refer to [22, Corollary 4.1] for case $r_1^e \geq 0$. Now we assume $r_1^e = -1$. It's easy to see that $\mathbb{B}_{k+1}^{\text{div}_f}(f; \mathbf{r}_1) \cap \ker(\text{div}_f) = \text{curl}_f \mathbb{B}_{k+2}(f; \mathbf{r}_0)$. We will finish the proof of the exactness of complex (91) by checking the dimension identity

$$(93) \quad \dim \mathbb{B}_{k+2}(f; \mathbf{r}_0) + \dim \mathbb{B}_k(f; \mathbf{r}_2)/\mathbb{R} = \dim \mathbb{B}_{k+1}^{\text{div}_f}(f; \mathbf{r}_1).$$

By Lemma 3.5 in [22],

$$\dim \mathbb{B}_{k+2}(f; \mathbf{r}_0) = \dim \mathbb{P}_{k+2}(f) - 3 \binom{r_1^v + 3}{2} - 3(k - 2r_1^v - 1),$$

$$\dim \mathbb{B}_k(f; \mathbf{r}_2) = \dim \mathbb{P}_k(f) - 3 \binom{r_2^v + 2}{2},$$

$$\dim \mathbb{B}_{k+1}^{\text{div}_f}(f; \mathbf{r}_1) = 2 \dim \mathbb{P}_{k+1}(f) - 6 \binom{r_1^v + 2}{2} - 3(k - 2r_1^v).$$

Noting that $\dim \mathbb{P}_{k+2}(f) + \dim \mathbb{P}_k(f) = 2 \dim \mathbb{P}_{k+1}(f) + 1$, we have

$$\begin{aligned} & \dim \mathbb{B}_{k+2}(f; \mathbf{r}_0) + \dim \mathbb{B}_k(f; \mathbf{r}_2)/\mathbb{R} - \dim \mathbb{B}_{k+1}^{\text{div}_f}(f; \mathbf{r}_1) \\ &= 6 \binom{r_1^v + 2}{2} + 3 - 3 \binom{r_1^v + 3}{2} - 3 \binom{r_2^v + 2}{2} = 0. \end{aligned}$$

Thus, (93) follows. \square

Lemma A.2. *Let $\mathbf{r}_0 \geq 0$, $\mathbf{r}_1 = \mathbf{r}_0 - 1$, $\mathbf{r}_2 = \mathbf{r}_1 \ominus 1$, $\mathbf{r}_3 = \mathbf{r}_2 \ominus 1$ be smoothness vectors. Assume \mathbf{r}_2 satisfies (19), and $k \geq \max\{2r_2^v, 1\}$. Then the bubble de Rham complex*

$$(94) \quad 0 \xrightarrow{\subset} \mathbb{B}_{k+2}(\mathbf{r}_0) \xrightarrow{\text{grad}} \mathbb{B}_{k+1}^{\text{curl}}(\mathbf{r}_1) \xrightarrow{\text{curl}} \mathbb{B}_k^{\text{div}}(\mathbf{r}_2) \xrightarrow{\text{div}} \mathbb{B}_{k-1}(\mathbf{r}_3)/\mathbb{R} \rightarrow 0$$

is exact.

Proof. Clearly (94) is a complex, and $\text{grad} \mathbb{B}_{k+2}(\mathbf{r}_0) = \mathbb{B}_{k+1}^{\text{curl}}(\mathbf{r}_1) \cap \ker(\text{curl})$. Then $\dim \text{curl} \mathbb{B}_{k+1}^{\text{curl}}(\mathbf{r}_1) = \dim \mathbb{B}_{k+1}^{\text{curl}}(\mathbf{r}_1) - \dim \mathbb{B}_{k+2}(\mathbf{r}_0)$. On the other side, by the div stability (20), $\dim \mathbb{B}_k^{\text{div}}(\mathbf{r}_2) \cap \ker(\text{div}) = \dim \mathbb{B}_k^{\text{div}}(\mathbf{r}_2) - \dim \mathbb{B}_{k-1}(\mathbf{r}_3)/\mathbb{R}$. Hence we have

$$\begin{aligned} & \dim \mathbb{B}_k^{\text{div}}(\mathbf{r}_2) \cap \ker(\text{div}) - \dim \text{curl} \mathbb{B}_{k+1}^{\text{curl}}(\mathbf{r}_1) = \dim \mathbb{B}_{k+2}(\mathbf{r}_0) - \dim \mathbb{B}_{k+1}^{\text{curl}}(\mathbf{r}_1) \\ & \quad + \dim \mathbb{B}_k^{\text{div}}(\mathbf{r}_2) - \dim \mathbb{B}_{k-1}(\mathbf{r}_3)/\mathbb{R}. \end{aligned}$$

\square Consider $r_0^f \geq 2$. Using the last row of Table 2 in [23], we obtain $\mathbb{B}_k^{\text{div}}(\mathbf{r}_2) \cap \ker(\text{div}) = \text{curl} \mathbb{B}_{k+1}^{\text{curl}}(\mathbf{r}_1)$.

\square Consider $\mathbf{r}_0 = (r_0^v, r_0^e, 1)^\top$ with $r_0^e \geq 4$. Set $\tilde{\mathbf{r}}_0 = (r_0^v, r_0^e, 2)^\top$, $\tilde{\mathbf{r}}_1 = \tilde{\mathbf{r}}_0 - 1$, $\tilde{\mathbf{r}}_2 = \tilde{\mathbf{r}}_1 - 1$ and $\tilde{\mathbf{r}}_3 = \mathbf{r}_3$. By DoFs (21),

$$\dim \mathbb{B}_{k+2}(\mathbf{r}_0) - \dim \mathbb{B}_{k+2}(\tilde{\mathbf{r}}_0) = \sum_{f \in \Delta_2(T)} \dim \mathbb{B}_k(f; \mathbf{r}_0 - 2),$$

$$\dim \mathbb{B}_{k+1}^{\text{curl}}(\mathbf{r}_1) - \dim \mathbb{B}_{k+1}^{\text{curl}}(\tilde{\mathbf{r}}_1) = 3 \sum_{f \in \Delta_2(T)} \dim \mathbb{B}_k(f; \mathbf{r}_1 - 1),$$

and by (18),

$$\dim \mathbb{B}_k^{\text{div}}(\mathbf{r}_2) - \dim \mathbb{B}_k^{\text{div}}(\tilde{\mathbf{r}}_2) = 2 \sum_{f \in \Delta_2(T)} \dim \mathbb{B}_k(f; \mathbf{r}_2).$$

Then it follows from $\mathbf{r}_0 - 2 = \mathbf{r}_1 - 1 = \mathbf{r}_2$ that

$$\begin{aligned} \dim \mathbb{B}_{k+1}^{\text{curl}}(\mathbf{r}_1) - \dim \mathbb{B}_{k+1}^{\text{curl}}(\tilde{\mathbf{r}}_1) &= \dim \mathbb{B}_{k+2}(\mathbf{r}_0) - \dim \mathbb{B}_{k+2}(\tilde{\mathbf{r}}_0) \\ &\quad + \dim \mathbb{B}_k^{\text{div}}(\mathbf{r}_2) - \dim \mathbb{B}_k^{\text{div}}(\tilde{\mathbf{r}}_2). \end{aligned}$$

Since $\mathbb{B}_{k-1}^{L^2}(\mathbf{r}_3) = \mathbb{B}_{k-1}^{L^2}(\tilde{\mathbf{r}}_3)$, we conclude the exactness of the bubble complex (94) beginning with \mathbf{r}_0 from the bubble complex (94) beginning with $\tilde{\mathbf{r}}_0$.

□3 Consider $\mathbf{r}_0 = (r_0^v, 2, 1)^\top$ with $r_0^v \geq 4$. We have

$$\begin{aligned} \dim \mathbb{B}_{k+2}(\mathbf{r}_0) &= -3 \binom{k+5}{3} + 8 \binom{r_1^v+4}{3} + 4 \binom{k+3}{3} - 12 \binom{r_1^v+2}{3} \\ &\quad + 24(k - 2r_1^v), \\ \dim \mathbb{B}_{k+1}^{\text{curl}}(\mathbf{r}_1) &= -9 \binom{k+4}{3} + 24 \binom{r_1^v+3}{3} + 12 \binom{k+3}{3} - 36 \binom{r_1^v+2}{3} \\ &\quad + 18(k - 2r_1^v), \\ \dim \mathbb{B}_k^{\text{div}}(\mathbf{r}_2) &= -9 \binom{k+3}{3} + 24 \binom{r_1^v+2}{3} + 12 \binom{k+2}{3} - 36 \binom{r_1^v+1}{3} \\ &\quad + 18(k - 2r_1^v + 1) + 8 \binom{k-1}{2} - 24 \binom{r_2^v}{2}, \\ \dim \mathbb{B}_{k-1}^{L^2}(\mathbf{r}_3) &= \binom{k+2}{3} - 4 \binom{r_1^v+1}{3} - 1. \end{aligned}$$

Then

$$\dim \mathbb{B}_{k+2}(\mathbf{r}_0) - \dim \mathbb{B}_{k+1}^{\text{curl}}(\mathbf{r}_1) + \dim \mathbb{B}_k^{\text{div}}(\mathbf{r}_2) - \dim \mathbb{B}_{k-1}^{L^2}(\mathbf{r}_3) = 0.$$

□4 The exactness of the bubble complex (94) beginning with $\mathbf{r}_0 = (r_0^v, 3, 1)^\top$ with $r_0^v \geq 6$ can be proved similarly.

□5 Consider $\mathbf{r}_0 = (r_0^v, r_0^e, 0)^\top$ with $r_0^e \geq 2$. Set $\tilde{\mathbf{r}}_0 = (r_0^v, r_0^e, 1)^\top$, $\tilde{\mathbf{r}}_1 = \tilde{\mathbf{r}}_0 - 1$, $\tilde{\mathbf{r}}_2 = \mathbf{r}_2$ and $\tilde{\mathbf{r}}_3 = \mathbf{r}_3$. By DoFs (21) and (17),

$$\begin{aligned} \dim \mathbb{B}_{k+2}(\mathbf{r}_0) - \dim \mathbb{B}_{k+2}(\tilde{\mathbf{r}}_0) &= \sum_{f \in \Delta_2(T)} \dim \mathbb{B}_{k+1}(f; \mathbf{r}_0 - 1), \\ \dim \mathbb{B}_{k+1}^{\text{curl}}(\mathbf{r}_1) - \dim \mathbb{B}_{k+1}^{\text{curl}}(\tilde{\mathbf{r}}_1) &= \sum_{f \in \Delta_2(T)} \dim \mathbb{B}_{k+1}(f; \mathbf{r}_1). \end{aligned}$$

So

$$\dim \mathbb{B}_{k+1}^{\text{curl}}(\mathbf{r}_1) - \dim \mathbb{B}_{k+1}^{\text{curl}}(\tilde{\mathbf{r}}_1) = \dim \mathbb{B}_{k+2}(\mathbf{r}_0) - \dim \mathbb{B}_{k+2}(\tilde{\mathbf{r}}_0).$$

Since $\mathbb{B}_k^{\text{div}}(\mathbf{r}_2) = \mathbb{B}_k^{\text{div}}(\tilde{\mathbf{r}}_2)$ and $\mathbb{B}_{k-1}^{L^2}(\mathbf{r}_3) = \mathbb{B}_{k-1}^{L^2}(\tilde{\mathbf{r}}_3)$, we conclude the exactness of the bubble complex (94) beginning with \mathbf{r}_0 from the bubble complex (94) beginning with $\tilde{\mathbf{r}}_0$.

□6 Consider $\mathbf{r}_0 = (r_0^v, 1, 0)^\top \geq 0$ with $r_0^v \geq 2$. We have

$$\begin{aligned} \dim \mathbb{B}_{k+2}(\mathbf{r}_0) &= -3 \binom{k+5}{3} + 8 \binom{r_0^v+3}{3} + 4 \binom{k+4}{3} - 12 \binom{r_0^v+2}{3} \\ &\quad + 6(k - 2r_0^v + 1), \end{aligned}$$

$$\begin{aligned}
\dim \mathbb{B}_{k+1}^{\text{curl}}(\mathbf{r}_1) &= -9 \binom{k+4}{3} + 24 \binom{r_1^\vee + 3}{3} + 12 \binom{k+3}{3} - 36 \binom{r_1^\vee + 2}{3} \\
&\quad + 18(k - 2r_1^\vee) + 4 \binom{k}{2} - 12 \binom{r_1^\vee}{2}, \\
\dim \mathbb{B}_k^{\text{div}}(\mathbf{r}_2) &= -9 \binom{k+3}{3} + 24 \binom{r_1^\vee + 2}{3} + 12 \binom{k+2}{3} - 36 \binom{r_1^\vee + 1}{3} \\
&\quad + 24(k - 2r_1^\vee + 1) + 8 \binom{k-1}{2} - 24 \binom{r_2^\vee}{2}, \\
\dim \mathbb{B}_{k-1}^{L^2}(\mathbf{r}_3) &= \binom{k+2}{3} - 4 \binom{r_1^\vee + 1}{3} - 1.
\end{aligned}$$

Then

$$\dim \mathbb{B}_{k+2}(\mathbf{r}_0) - \dim \mathbb{B}_{k+1}^{\text{curl}}(\mathbf{r}_1) + \dim \mathbb{B}_k^{\text{div}}(\mathbf{r}_2) - \dim \mathbb{B}_{k-1}^{L^2}(\mathbf{r}_3) = 0.$$

\square The exactness of the bubble complex (94) beginning with $\mathbf{r}_0 = (r_0^\vee, 0, 0)^\top$ with $r_0^\vee \geq 0$ can be proved similarly. \square

A.2. Bubble spaces for tensors. For a tensor space \mathbb{X} with $\mathbb{X} = \mathbb{M}, \mathbb{S}, \mathbb{T}$, define bubble spaces

$$\begin{aligned}
\mathbb{B}_k^{\text{div}}(\mathbf{r}; \mathbb{X}) &:= \{\boldsymbol{\tau} \in \mathbb{B}_k(\mathbf{r}; \mathbb{X}) : \boldsymbol{\tau} \mathbf{n}|_{\partial T} = 0\}, \\
\mathbb{B}_k^{\text{curl}}(\mathbf{r}; \mathbb{X}) &:= \{\boldsymbol{\tau} \in \mathbb{B}_k(\mathbf{r}; \mathbb{X}) : \boldsymbol{\tau} \times \mathbf{n}|_{\partial T} = 0\}, \\
\mathbb{B}_k^{\text{div div}}(\mathbf{r}; \mathbb{X}) &:= \{\boldsymbol{\tau} \in \mathbb{B}_k(\mathbf{r}; \mathbb{X}) : (\mathbf{n}^\top \boldsymbol{\tau} \mathbf{n})|_{\partial T} = 0, \text{tr}_2^{\text{div div}}(\boldsymbol{\tau}) = 0, \\
&\quad (\mathbf{n}_i^\top \boldsymbol{\tau} \mathbf{n}_j)|_e = 0 \text{ for } e \in \Delta_1(T) \text{ and } i, j = 1, 2\}, \\
\mathbb{B}_k^{\text{sym curl}}(\mathbf{r}; \mathbb{X}) &:= \{\boldsymbol{\tau} \in \mathbb{B}_k(\mathbf{r}; \mathbb{X}) : (\mathbf{n} \times \text{sym}(\boldsymbol{\tau} \times \mathbf{n}) \times \mathbf{n})|_{\partial T} = 0, \\
&\quad (\mathbf{n} \cdot \boldsymbol{\tau} \times \mathbf{n})|_{\partial T} = 0, \text{sym curl } \boldsymbol{\tau} \in \mathbb{B}_{k-1}^{\text{div div}}((0, -1, -1)^\top; \mathbb{S})\}, \\
\mathbb{B}_k^{\text{inc}}(\mathbf{r}; \mathbb{X}) &:= \{\boldsymbol{\tau} \in \mathbb{B}_k(\mathbf{r}; \mathbb{X}) : (\mathbf{n} \times \boldsymbol{\tau} \times \mathbf{n})|_{\partial T} = 0, \text{tr}_2^{\text{inc}}(\boldsymbol{\tau}) = 0, \\
&\quad \text{inc } \boldsymbol{\tau} \in \mathbb{B}_{k-2}^{\text{div}}((0, -1, -1)^\top; \mathbb{S})\}.
\end{aligned}$$

A.3. Bubble Hessian complex.

Lemma A.3. Assume the polynomial degree $k \geq \max\{2r^\vee + 2, 3\}$, and the smoothness vector \mathbf{r} satisfy either:

- (1) $r^\vee \geq 2r^e + 1$ and $r^e \geq 2(r^f + 1)$, or
- (2) $r^\vee \geq 0$ and $r^e = r^f = -1$.

Then we have the (div; \mathbb{T}) stability

$$(95) \quad \text{div } \mathbb{B}_{k-1}^{\text{div}}(\mathbf{r}; \mathbb{T}) = \mathbb{B}_{k-2}(\mathbf{r} \ominus 1; \mathbb{R}^3)/\text{RT}.$$

Proof. (1) For case $r^\vee \geq 1$ and $r^e \geq 0$, consider the bubble diagram

$$\begin{array}{ccccc}
& & \mathbb{B}_k^{\text{div}}(\mathbf{r} + 1) & \xrightarrow{\text{div}} & \mathbb{B}_{k-1}(\mathbf{r}) & \longrightarrow & \mathbb{R} \\
& \nearrow^{-2 \text{ vskw}} & & & \nearrow^{\text{tr}} & & \\
\mathbb{B}_k^{\text{curl}}(\mathbf{r} + 1; \mathbb{M}) & \xrightarrow{\text{curl}} & \mathbb{B}_{k-1}^{\text{div}}(\mathbf{r}; \mathbb{M}) & \xrightarrow{\text{div}} & \mathbb{B}_{k-2}(\mathbf{r} \ominus 1; \mathbb{R}^3)/\mathbb{R}^3 & \longrightarrow & 0.
\end{array}$$

For $\mathbf{u} \in \mathbb{B}_{k-2}(\mathbf{r} \ominus 1; \mathbb{R}^3)/\text{RT}$, since $(\mathbf{r}, \mathbf{r} \ominus 1, k-1)$ is div stable, there exists $\boldsymbol{\tau} \in \mathbb{B}_{k-1}^{\text{div}}(\mathbf{r}; \mathbb{M})$ such that $\text{div } \boldsymbol{\tau} = \mathbf{u}$. Noting that $\text{tr } \boldsymbol{\tau} \in \mathbb{B}_{k-1}(\mathbf{r})/\mathbb{R}$ and $(\mathbf{r} + 1, \mathbf{r}, k)$ is div

stable, we have $\text{tr } \boldsymbol{\tau} = \text{div } \boldsymbol{v}$ with $\boldsymbol{v} \in \mathbb{B}_k^{\text{div}}(\boldsymbol{r} + 1) = \mathbb{B}_k(\boldsymbol{r} + 1; \mathbb{R}^3)$. Choose $\boldsymbol{\sigma} = \boldsymbol{\tau} - \frac{1}{2} \text{curl}(\text{mskw } \boldsymbol{v}) \in \mathbb{B}_{k-1}^{\text{div}}(\boldsymbol{r}; \mathbb{M})$. Then $\text{div } \boldsymbol{\sigma} = \text{div } \boldsymbol{\tau} = \boldsymbol{u}$, and by the anticommutativity, $\text{tr } \boldsymbol{\sigma} = \text{tr } \boldsymbol{\tau} - \text{div } \boldsymbol{v} = 0$. Thus, $\boldsymbol{\sigma} \in \mathbb{B}_{k-1}^{\text{div}}(\boldsymbol{r}; \mathbb{T})$, and $\boldsymbol{u} \in \text{div } \mathbb{B}_{k-1}^{\text{div}}(\boldsymbol{r}; \mathbb{T})$.

(2) The case $r^v = 0$ and $r^e = r^f = -1$ can be found in [33, Theorem 4.4]. Now consider case $r^v \geq 1$ and $r^e = r^f = -1$. Notice that

$$\mathbb{B}_{k-1}^{\text{div}}((r^v, 0, -1)^\top; \mathbb{T}) \subseteq \mathbb{B}_{k-1}^{\text{div}}((r^v, -1, -1)^\top; \mathbb{T}).$$

We conclude (95) with $\boldsymbol{r} = (r^v, -1, -1)^\top$ from (95) with $\boldsymbol{r} = (r^v, 0, -1)^\top$. \square

Lemma A.4. *Let $\boldsymbol{r}_0 \geq (4, 2, 1)^\top$, $\boldsymbol{r}_1 = \boldsymbol{r}_0 - 2$, $\boldsymbol{r}_2 = \boldsymbol{r}_1 \ominus 1$, $\boldsymbol{r}_3 = \boldsymbol{r}_2 \ominus 1$. Assume \boldsymbol{r}_2 satisfies the condition in Lemma A.3, and $k \geq 2r_2^v + 2$. Then the bubble Hessian complex*

$$(96) \quad 0 \xrightarrow{\subset} \mathbb{B}_{k+2}(\boldsymbol{r}_0) \xrightarrow{\text{hess}} \mathbb{B}_k^{\text{curl}}(\boldsymbol{r}_1; \mathbb{S}) \xrightarrow{\text{curl}} \mathbb{B}_{k-1}^{\text{div}}(\boldsymbol{r}_2; \mathbb{T}) \xrightarrow{\text{div}} \mathbb{B}_{k-2}(\boldsymbol{r}_3; \mathbb{R}^3)/\text{RT} \rightarrow 0$$

is exact.

Proof. Obviously (96) is a complex, $\mathbb{B}_k^{\text{curl}}(\boldsymbol{r}_1; \mathbb{S}) \cap \ker(\text{curl}) = \text{hess } \mathbb{B}_{k+2}(\boldsymbol{r}_0)$, and

$$\dim \text{curl } \mathbb{B}_k^{\text{curl}}(\boldsymbol{r}_1; \mathbb{S}) = 3 \dim \mathbb{B}_k((\boldsymbol{r}_1)_+) + \dim \mathbb{B}_k^{\text{curl}}(\boldsymbol{r}_1) - \dim \mathbb{B}_{k+2}(\boldsymbol{r}_0).$$

By bubble complex (94),

$$\dim \mathbb{B}_{k+2}(\boldsymbol{r}_0) = 3 \dim \mathbb{B}_{k+1}(\boldsymbol{r}_0 - 1) - \dim \mathbb{B}_k^{\text{div}}(\boldsymbol{r}_1) + \dim \mathbb{B}_{k-1}(\boldsymbol{r}_2) - 1,$$

$$\dim \mathbb{B}_{k+1}(\boldsymbol{r}_0 - 1) = \dim \mathbb{B}_k^{\text{curl}}(\boldsymbol{r}_1) - \dim \mathbb{B}_{k-1}^{\text{div}}(\boldsymbol{r}_2) + \dim \mathbb{B}_{k-2}(\boldsymbol{r}_3) - 1.$$

Noting that $2 \dim \mathbb{B}_k^{\text{curl}}(\boldsymbol{r}_1) = \dim \mathbb{B}_k^{\text{div}}(\boldsymbol{r}_1) + 3 \dim \mathbb{B}_k((\boldsymbol{r}_1)_+)$, we get from the last two equations that

$$\begin{aligned} \dim \mathbb{B}_{k+2}(\boldsymbol{r}_0) &= 3 \dim \mathbb{B}_k((\boldsymbol{r}_1)_+) + \dim \mathbb{B}_k^{\text{curl}}(\boldsymbol{r}_1) \\ &\quad - 3 \dim \mathbb{B}_{k-1}^{\text{div}}(\boldsymbol{r}_2) + \dim \mathbb{B}_{k-1}(\boldsymbol{r}_2) + 3 \dim \mathbb{B}_{k-2}(\boldsymbol{r}_3) - 4. \end{aligned}$$

Then

$$\dim \text{curl } \mathbb{B}_k^{\text{curl}}(\boldsymbol{r}_1; \mathbb{S}) = 3 \dim \mathbb{B}_{k-1}^{\text{div}}(\boldsymbol{r}_2) - \dim \mathbb{B}_{k-1}(\boldsymbol{r}_2) - 3 \dim \mathbb{B}_{k-2}(\boldsymbol{r}_3) + 4.$$

Thanks to the $(\text{div}; \mathbb{T})$ stability (95), we only need to prove $\mathbb{B}_{k-1}^{\text{div}}(\boldsymbol{r}_2; \mathbb{T}) \cap \ker(\text{div}) = \text{curl } \mathbb{B}_k^{\text{curl}}(\boldsymbol{r}_1; \mathbb{S})$. Since $\text{curl } \mathbb{B}_k^{\text{curl}}(\boldsymbol{r}_1; \mathbb{S}) \subseteq \mathbb{B}_{k-1}^{\text{div}}(\boldsymbol{r}_2; \mathbb{T}) \cap \ker(\text{div})$, we will finish the proof by dimension count. According to the $(\text{div}; \mathbb{T})$ stability (95) and $\dim \mathbb{B}_{k-1}^{\text{div}}(\boldsymbol{r}_2; \mathbb{T}) = 3 \dim \mathbb{B}_{k-1}^{\text{div}}(\boldsymbol{r}_2) - \dim \mathbb{B}_{k-1}(\boldsymbol{r}_2)$,

$$\begin{aligned} \dim \mathbb{B}_{k-1}^{\text{div}}(\boldsymbol{r}_2; \mathbb{T}) \cap \ker(\text{div}) &= \dim \mathbb{B}_{k-1}^{\text{div}}(\boldsymbol{r}_2; \mathbb{T}) - 3 \dim \mathbb{B}_{k-2}(\boldsymbol{r}_3) + 4 \\ &= 3 \dim \mathbb{B}_{k-1}^{\text{div}}(\boldsymbol{r}_2) - \dim \mathbb{B}_{k-1}(\boldsymbol{r}_2) - 3 \dim \mathbb{B}_{k-2}(\boldsymbol{r}_3) + 4. \end{aligned}$$

Hence, $\dim \mathbb{B}_{k-1}^{\text{div}}(\boldsymbol{r}_2; \mathbb{T}) \cap \ker(\text{div}) = \dim \text{curl } \mathbb{B}_k^{\text{curl}}(\boldsymbol{r}_1; \mathbb{S})$. \square

A.4. Bubble elasticity complex.

Lemma A.5. *Assume the polynomial degree $k \geq \max\{2r^v, 1\}$, and the smoothness vector \boldsymbol{r} satisfy either:*

- (1) $r^v \geq 2r^e + 1$ and $r^e \geq 2(r^f + 1)$, or
- (2) $r^v \geq 0$ and $r^e = r^f = -1$.

Then we have the $(\text{div}; \mathbb{S})$ stability

$$(97) \quad \text{div } \mathbb{B}_{k+1}^{\text{div}}(\boldsymbol{r}; \mathbb{S}) = \mathbb{B}_k(\boldsymbol{r} \ominus 1; \mathbb{R}^3)/\text{RM}.$$

Proof. (1) For case $r^v \geq 1$ and $r^e \geq 0$, consider the bubble diagram

$$\begin{array}{ccccc} & & \mathbb{B}_{k+2}^{\text{div}}(\mathbf{r} + 1; \mathbb{M}) & \xrightarrow{\text{div}} & \mathbb{B}_{k+1}(\mathbf{r}; \mathbb{R}^3) & \longrightarrow & \mathbb{R}^3 \\ & \nearrow S & & \nearrow -2 \text{ vskw} & & & \\ \mathbb{B}_{k+2}^{\text{curl}}(\mathbf{r} + 1; \mathbb{M}) & \xrightarrow{\text{curl}} & \mathbb{B}_{k+1}^{\text{div}}(\mathbf{r}; \mathbb{M}) & \xrightarrow{\text{div}} & \mathbb{B}_k(\mathbf{r} \ominus 1; \mathbb{R}^3) / \mathbb{R}^3 & \longrightarrow & 0. \end{array}$$

Then follow the proof of the first part of Lemma A.3 to obtain (97).

(2) The case $r^v = 0$ and $r^e = r^f = -1$ can be found in [38, Lemma 3.2]. Now consider case $r^v \geq 1$ and $r^e = r^f = -1$. Notice that

$$\mathbb{B}_{k+1}^{\text{div}}((r^v, 0, -1)^\top; \mathbb{S}) \subseteq \mathbb{B}_{k+1}^{\text{div}}((r^v, -1, -1)^\top; \mathbb{S}).$$

We conclude (97) with $\mathbf{r} = (r^v, -1, -1)^\top$ from (97) with $\mathbf{r} = (r^v, 0, -1)^\top$. \square

Lemma A.6. *Let*

$$\mathbf{r}_0 \geq (2, 1, 0)^\top, \mathbf{r}_1 = \mathbf{r}_0 - 1, \mathbf{r}_2 = \max\{\mathbf{r}_1 \ominus 2, (0, -1, -1)^\top\}, \mathbf{r}_3 = \mathbf{r}_2 \ominus 1.$$

Assume \mathbf{r}_2 satisfies the condition in Lemma A.5, and $k \geq \max\{2r_2^v, 1\}$. Then the bubble elasticity complex

$$(98) \quad 0 \xrightarrow{\subset} \mathbb{B}_{k+4}(\mathbf{r}_0; \mathbb{R}^3) \xrightarrow{\text{def}} \mathbb{B}_{k+3}^{\text{inc}}(\mathbf{r}_1; \mathbb{S}) \xrightarrow{\text{inc}} \mathbb{B}_{k+1}^{\text{div}}(\mathbf{r}_2; \mathbb{S}) \xrightarrow{\text{div}} \mathbb{B}_k(\mathbf{r}_3; \mathbb{R}^3) / \text{RM} \rightarrow 0$$

is exact.

Proof. Obviously (98) is a complex, $\mathbb{B}_{k+3}^{\text{inc}}(\mathbf{r}_1; \mathbb{S}) \cap \ker(\text{inc}) = \text{def } \mathbb{B}_{k+4}(\mathbf{r}_0; \mathbb{R}^3)$, and

$$\dim \text{inc } \mathbb{B}_{k+3}^{\text{inc}}(\mathbf{r}_1; \mathbb{S}) = \dim \mathbb{B}_{k+3}^{\text{inc}}(\mathbf{r}_1; \mathbb{S}) - 3 \dim \mathbb{B}_{k+4}(\mathbf{r}_0).$$

Thanks to the $(\text{div}; \mathbb{S})$ stability (97), we only need to prove $\mathbb{B}_{k+1}^{\text{div}}(\mathbf{r}_2; \mathbb{S}) \cap \ker(\text{div}) = \text{inc } \mathbb{B}_{k+3}^{\text{inc}}(\mathbf{r}_1; \mathbb{S})$. Since $\text{inc } \mathbb{B}_{k+3}^{\text{inc}}(\mathbf{r}_1; \mathbb{S}) \subseteq \mathbb{B}_{k+1}^{\text{div}}(\mathbf{r}_2; \mathbb{S}) \cap \ker(\text{div})$, we will finish the proof by dimension count.

We first consider case $r_1^f = -1, 0$. By DoFs (61),

$$\dim \mathbb{B}_{k+3}^{\text{inc}}(\mathbf{r}_1; \mathbb{S}) = 3 \dim \mathbb{B}_{k+4}(\mathbf{r}_0) + \dim \mathbb{B}_{k+1}^{\text{div}}(\mathbf{r}_2; \mathbb{S}) \cap \ker(\text{div}).$$

This indicates $\dim \text{inc } \mathbb{B}_{k+3}^{\text{inc}}(\mathbf{r}_1; \mathbb{S}) = \dim \mathbb{B}_{k+1}^{\text{div}}(\mathbf{r}_2; \mathbb{S}) \cap \ker(\text{div})$, as required.

Next consider case $r_1^f \geq 1$. By bubble complex (94),

$$\begin{aligned} \dim \mathbb{B}_{k+4}(\mathbf{r}_0) &= 3 \dim \mathbb{B}_{k+3}(\mathbf{r}_1) - 3 \dim \mathbb{B}_{k+2}(\mathbf{r}_1 - 1) + \dim \mathbb{B}_{k+1}(\mathbf{r}_2) - 1, \\ \dim \mathbb{B}_{k+3}(\mathbf{r}_1) &= 3 \dim \mathbb{B}_{k+2}(\mathbf{r}_1 - 1) - \dim \mathbb{B}_{k+1}^{\text{div}}(\mathbf{r}_2) + \dim \mathbb{B}_k(\mathbf{r}_3) - 1. \end{aligned}$$

Combining the last two equations yields

$$\begin{aligned} \dim \text{inc } \mathbb{B}_{k+3}^{\text{inc}}(\mathbf{r}_1; \mathbb{S}) &= 6 \dim \mathbb{B}_{k+3}(\mathbf{r}_1) - 3 \dim \mathbb{B}_{k+4}(\mathbf{r}_0) \\ &= 3 \dim \mathbb{B}_{k+1}^{\text{div}}(\mathbf{r}_2) - 3 \dim \mathbb{B}_{k+1}(\mathbf{r}_2) - 3 \dim \mathbb{B}_k(\mathbf{r}_3) + 6. \end{aligned}$$

Noting that $\dim \mathbb{B}_{k+1}^{\text{div}}(\mathbf{r}_2; \mathbb{S}) = 3 \dim \mathbb{B}_{k+1}^{\text{div}}(\mathbf{r}_2) - 3 \dim \mathbb{B}_{k+1}(\mathbf{r}_2)$, we get from (97) that

$$\dim \text{inc } \mathbb{B}_{k+3}^{\text{inc}}(\mathbf{r}_1; \mathbb{S}) = \dim \mathbb{B}_{k+1}^{\text{div}}(\mathbf{r}_2; \mathbb{S}) \cap \ker(\text{div}).$$

Therefore, $\text{inc } \mathbb{B}_{k+3}^{\text{inc}}(\mathbf{r}_1; \mathbb{S}) = \mathbb{B}_{k+1}^{\text{div}}(\mathbf{r}_2; \mathbb{S}) \cap \ker(\text{div})$. \square

A.5. Bubble divdiv complex.

Lemma A.7. *Let*

$$\mathbf{r}_0 \geq (1, 0, 0)^\top, \quad \mathbf{r}_1 = \mathbf{r}_0 - 1, \quad \mathbf{r}_2 = \max\{\mathbf{r}_1 \ominus 1, (0, -1, -1)^\top\}, \quad \mathbf{r}_3 = \mathbf{r}_2 \ominus 2.$$

Assume \mathbf{r}_2 satisfies the condition in Lemma A.5, $\mathbf{r}_2 \ominus 1$ satisfies (19), and $k \geq \max\{2r_2^\vee + 1, 3\}$. We have the following exact bubble divdiv complex

$$(99) \quad 0 \xrightarrow{\subset} \mathbb{B}_{k+2}(\mathbf{r}_0; \mathbb{R}^3) \xrightarrow{\text{dev grad}} \mathbb{B}_{k+1}^{\text{sym curl}^+}(\mathbf{r}_1; \mathbb{T}) \\ \xrightarrow{\text{sym curl}} \mathbb{B}_k^{\text{div div}^+}(\mathbf{r}_2; \mathbb{S}) \xrightarrow{\text{div div}} \mathbb{B}_{k-2}(\mathbf{r}_3)/\mathbb{P}_1(T) \rightarrow 0,$$

where

$$\mathbb{B}_{k+1}^{\text{sym curl}^+}(\mathbf{r}_1; \mathbb{T}) := \{\boldsymbol{\tau} \in \mathbb{B}_{k+1}^{\text{sym curl}}(\mathbf{r}_1; \mathbb{T}) : \text{sym curl } \boldsymbol{\tau} \in \mathbb{B}_k^{\text{div div}^+}(\mathbf{r}_2; \mathbb{S})\}, \\ \mathbb{B}_k^{\text{div div}^+}(\mathbf{r}_2; \mathbb{S}) := \{\boldsymbol{\tau} \in \mathbb{B}_k^{\text{div div}}(\mathbf{r}_2; \mathbb{S}) : \boldsymbol{\tau} \mathbf{n}|_{\partial T} = 0\}.$$

Proof. By the definition of the bubble spaces, we can see that (99) is a complex, and $\mathbb{B}_{k+1}^{\text{sym curl}^+}(\mathbf{r}_1; \mathbb{T}) \cap \ker(\text{sym curl}) = \text{dev grad } \mathbb{B}_{k+2}(\mathbf{r}_0; \mathbb{R}^3)$.

We first prove $\text{div div } \mathbb{B}_k^{\text{div div}^+}(\mathbf{r}_2; \mathbb{S}) = \mathbb{B}_{k-2}(\mathbf{r}_3)/\mathbb{P}_1(T)$. When $r_2^f \geq 1$, we have $\mathbb{B}_k^{\text{div div}^+}(\mathbf{r}_2; \mathbb{S}) = \mathbb{B}_k(\mathbf{r}_2; \mathbb{S})$, then apply the bubble complex (94) to get

$$\text{div div } \mathbb{B}_k^{\text{div div}^+}(\mathbf{r}_2; \mathbb{S}) = \text{div div } \mathbb{B}_k(\mathbf{r}_2; \mathbb{S}) = \text{div div } \mathbb{B}_k(\mathbf{r}_2; \mathbb{M}) \\ = \text{div}(\mathbb{B}_{k-1}(\mathbf{r}_2 - 1; \mathbb{M})/\mathbb{R}^3) = \mathbb{B}_{k-2}(\mathbf{r}_3)/\mathbb{P}_1(T).$$

When $r_2^f = -1, 0$, we follow the proof of Lemma 4.12 and Corollary 4.13 to acquire $\text{div div } \mathbb{B}_k^{\text{div div}^+}(\mathbf{r}_2; \mathbb{S}) = \mathbb{B}_{k-2}(\mathbf{r}_3)/\mathbb{P}_1(T)$.

We next prove $\text{sym curl } \mathbb{B}_{k+1}^{\text{sym curl}^+}(\mathbf{r}_1; \mathbb{T}) = \mathbb{B}_k^{\text{div div}^+}(\mathbf{r}_2; \mathbb{S}) \cap \ker(\text{div div})$.

□ First consider $\mathbf{r}_0 \geq (2, 1, 0)^\top$. Let $\boldsymbol{\sigma} \in \mathbb{B}_k^{\text{div div}^+}(\mathbf{r}_2; \mathbb{S}) \cap \ker(\text{div div})$. Then $\text{div } \boldsymbol{\sigma} \in \mathbb{B}_{k-1}^{\text{div}}(\mathbf{r}_2 \ominus 1; \mathbb{R}^3) \cap \ker(\text{div})$. By the bubble complex (94), $\text{div } \boldsymbol{\sigma} = \text{curl } \mathbf{v}$ with $\mathbf{v} \in \mathbb{B}_k^{\text{curl}}(\mathbf{r}_2; \mathbb{R}^3)$. That is $\boldsymbol{\sigma} - \text{mskw } \mathbf{v} \in \mathbb{B}_k^{\text{div}}(\mathbf{r}_2; \mathbb{M}) \cap \ker(\text{div})$. Apply the bubble complex (94) again to get $\boldsymbol{\sigma} - \text{mskw } \mathbf{v} = \text{curl } \boldsymbol{\tau}$ with $\boldsymbol{\tau} \in \mathbb{B}_{k+1}^{\text{curl}}(\mathbf{r}_1; \mathbb{M})$. By the symmetry of $\boldsymbol{\sigma}$, we have $\boldsymbol{\sigma} = \text{sym curl } \boldsymbol{\tau} = \text{sym curl}(\text{dev } \boldsymbol{\tau})$, where $\text{dev } \boldsymbol{\tau} \in \mathbb{B}_{k+1}^{\text{sym curl}^+}(\mathbf{r}_1; \mathbb{T})$.

□ Then consider $\mathbf{r}_0 = (r_0^\vee, 0, 0)^\top$ with $r_0^\vee \geq 1$. Let $\hat{\mathbf{r}}_1 = (\max\{r_1^\vee, 1\}, 0, -1)^\top \geq (1, 0, -1)^\top$. We have $\mathbf{r}_1 \leq \hat{\mathbf{r}}_1$ and $\hat{\mathbf{r}}_1 \ominus 1 = \mathbf{r}_2$. Thus, we conclude the result from

$$\text{sym curl } \mathbb{B}_{k+1}^{\text{sym curl}^+}(\hat{\mathbf{r}}_1; \mathbb{T}) \subseteq \text{sym curl } \mathbb{B}_{k+1}^{\text{sym curl}^+}(\mathbf{r}_1; \mathbb{T}) \subseteq \mathbb{B}_k^{\text{div div}^+}(\mathbf{r}_2; \mathbb{S}) \cap \ker(\text{div div})$$

$$\text{and } \text{sym curl } \mathbb{B}_{k+1}^{\text{sym curl}^+}(\hat{\mathbf{r}}_1; \mathbb{T}) = \mathbb{B}_k^{\text{div div}^+}(\mathbf{r}_2; \mathbb{S}) \cap \ker(\text{div div}). \quad \square$$

Lemma A.8. *Under the same assumption of Lemma A.7, we have the following exact bubble divdiv complex*

$$(100) \quad 0 \xrightarrow{\subset} \mathbb{B}_{k+2}(\mathbf{r}_0; \mathbb{R}^3) \xrightarrow{\text{dev grad}} \mathbb{B}_{k+1}^{\text{sym curl}}(\mathbf{r}_1; \mathbb{T}) \\ \xrightarrow{\text{sym curl}} \mathbb{B}_k^{\text{div div}}(\mathbf{r}_2; \mathbb{S}) \xrightarrow{\text{div div}} \mathbb{B}_{k-2}(\mathbf{r}_3)/\mathbb{P}_1(T) \rightarrow 0.$$

Proof. When $r_2^f \geq 0$, the complex (100) is exactly the complex (99). Then we focus on the proof for the case $r_2^f = -1$. By the definition of the bubble spaces, we can see that (100) is a complex, and $\mathbb{B}_{k+1}^{\text{sym curl}}(\mathbf{r}_1; \mathbb{T}) \cap \ker(\text{sym curl}) = \text{dev grad } \mathbb{B}_{k+2}(\mathbf{r}_0; \mathbb{R}^3)$.

Since $\operatorname{div} \operatorname{div} \mathbb{B}_k^{\operatorname{div} \operatorname{div}^+}(\mathbf{r}_2; \mathbb{S}) \subseteq \operatorname{div} \operatorname{div} \mathbb{B}_k^{\operatorname{div} \operatorname{div}}(\mathbf{r}_2; \mathbb{S}) \subseteq \mathbb{B}_{k-2}(\mathbf{r}_3)/\mathbb{P}_1(T)$, by complex (99), we have

$$\operatorname{div} \operatorname{div} \mathbb{B}_k^{\operatorname{div} \operatorname{div}}(\mathbf{r}_2; \mathbb{S}) = \operatorname{div} \operatorname{div} \mathbb{B}_k^{\operatorname{div} \operatorname{div}^+}(\mathbf{r}_2; \mathbb{S}) = \mathbb{B}_{k-2}(\mathbf{r}_3)/\mathbb{P}_1(T).$$

Thanks to (35i) and (73l) we have

$$\dim \mathbb{B}_k^{\operatorname{div} \operatorname{div}}(\mathbf{r}_2; \mathbb{S}) - \dim \mathbb{B}_{k+1}^{\operatorname{sym} \operatorname{curl}}(\mathbf{r}_1; \mathbb{T}) = \dim \mathbb{B}_k^{\operatorname{div} \operatorname{div}^+}(\mathbf{r}_2; \mathbb{S}) - \dim \mathbb{B}_{k+1}^{\operatorname{sym} \operatorname{curl}^+}(\mathbf{r}_1; \mathbb{T}).$$

Finally, apply the exactness of complex (99) to get

$$\mathbb{B}_k^{\operatorname{div} \operatorname{div}}(\mathbf{r}_2; \mathbb{S}) \cap \ker(\operatorname{div} \operatorname{div}) = \operatorname{sym} \operatorname{curl} \mathbb{B}_{k+1}^{\operatorname{sym} \operatorname{curl}}(\mathbf{r}_1; \mathbb{T}).$$

□

REFERENCES

- [1] S. Amstutz and N. Van Goethem. The incompatibility operator: from Riemann’s intrinsic view of geometry to a new model of elasto-plasticity. In *Topics in Applied Analysis and Optimisation*, pages 33–70. Springer, 2019. 2
- [2] J. Argyris, I. Fried, and D. Scharpf. The TUBA family of plate elements for the matrix displacement method. *Aero. J. Roy. Aero. Soc.*, 72:701–709, 1968. 2
- [3] D. N. Arnold. *Finite element exterior calculus*. Society for Industrial and Applied Mathematics (SIAM), Philadelphia, PA, 2018. 1
- [4] D. N. Arnold, G. Awanou, and R. Winther. Finite elements for symmetric tensors in three dimensions. *Math. Comp.*, 77(263):1229–1251, 2008. 42
- [5] D. N. Arnold, J. Douglas, Jr., and C. P. Gupta. A family of higher order mixed finite element methods for plane elasticity. *Numer. Math.*, 45(1):1–22, 1984. 2
- [6] D. N. Arnold, R. S. Falk, and R. Winther. Differential complexes and stability of finite element methods. II. The elasticity complex. In *Compatible spatial discretizations*, volume 142 of *IMA Vol. Math. Appl.*, pages 47–67. Springer, New York, 2006. 4
- [7] D. N. Arnold, R. S. Falk, and R. Winther. Finite element exterior calculus, homological techniques, and applications. *Acta Numer.*, 15:1–155, 2006. 1, 10
- [8] D. N. Arnold, R. S. Falk, and R. Winther. Finite element exterior calculus: from Hodge theory to numerical stability. *Bull. Amer. Math. Soc. (N.S.)*, 47(2):281–354, 2010. 1
- [9] D. N. Arnold and K. Hu. Complexes from complexes. *Found. Comput. Math.*, 21(6):1739–1774, 2021. 1, 3, 4, 5, 6, 9, 10, 11
- [10] D. N. Arnold and R. Winther. Mixed finite elements for elasticity. *Numer. Math.*, 92(3):401–419, 2002. 4
- [11] I. N. Bernšteĭn, I. M. Gelfand, and S. I. Gelfand. Differential operators on the base affine space and a study of g -modules. In *Lie groups and their representations (Proc. Summer School, Bolyai János Math. Soc., Budapest, 1971)*, pages 21–64, 1975. 4
- [12] D. Boffi, F. Brezzi, and M. Fortin. *Mixed finite element methods and applications*, volume 44 of *Springer Series in Computational Mathematics*. Springer, Heidelberg, 2013. 14
- [13] J. H. Bramble and M. Zlámal. Triangular elements in the finite element method. *Math. Comp.*, 24:809–820, 1970. 2
- [14] C. Chen, L. Chen, X. Huang, and H. Wei. Geometric decomposition and efficient implementation of high order face and edge elements. *Commun. Comput. Phys.*, 35(4):1045–1072, 2024. 12
- [15] L. Chen, J. Hu, and X. Huang. Multigrid methods for Hellan–Herrmann–Johnson mixed method of Kirchhoff plate bending problems. *J. Sci. Comput.*, 76(2):673–696, 2018. 1
- [16] L. Chen and X. Huang. Decoupling of mixed methods based on generalized Helmholtz decompositions. *SIAM J. Numer. Anal.*, 56(5):2796–2825, 2018. 1
- [17] L. Chen and X. Huang. Finite elements for divdiv-conforming symmetric tensors. *arXiv preprint arXiv:2005.01271*, 2020. 2, 6
- [18] L. Chen and X. Huang. Discrete Hessian complexes in three dimensions. In *The virtual element method and its applications*, volume 31 of *SEMA SIMAI Springer Ser.*, pages 93–135. Springer, Cham, 2022. 29
- [19] L. Chen and X. Huang. A finite element elasticity complex in three dimensions. *Math. Comp.*, 91(337):2095–2127, 2022. 2, 6, 34, 40, 42, 43
- [20] L. Chen and X. Huang. Finite elements for div- and divdiv-conforming symmetric tensors in arbitrary dimension. *SIAM J. Numer. Anal.*, 60(4):1932–1961, 2022. 20, 24

- [21] L. Chen and X. Huang. Finite elements for div div conforming symmetric tensors in three dimensions. *Math. Comp.*, 91(335):1107–1142, 2022. 2, 6, 37, 44, 45, 46, 47
- [22] L. Chen and X. Huang. Finite element complexes in two dimensions (in Chinese). *Sci. Sin. Math.*, 54:1–34, 2024. 2, 3, 12, 13, 41, 50
- [23] L. Chen and X. Huang. Finite element de Rham and Stokes complexes in three dimensions. *Math. Comp.*, 93(345):55–110, 2024. 2, 3, 6, 11, 12, 13, 14, 15, 22, 49, 50
- [24] L. Chen and X. Huang. $H(\text{div})$ -conforming finite element tensors with constraints. *Results Appl. Math.*, 2024. 3, 14, 15, 16, 18, 20
- [25] L. Chen and X. Huang. A new div-div-conforming symmetric tensor finite element space with applications to the biharmonic equation. *Math. Comp.*, 2024. 1, 37, 49
- [26] S. H. Christiansen. On the linearization of Regge calculus. *Numer. Math.*, 119(4):613–640, 2011. 2
- [27] S. H. Christiansen, J. Gopalakrishnan, J. Guzmán, and K. Hu. A discrete elasticity complex on three-dimensional Alfeld splits. *Numer. Math.*, 156(1):159–204, 2024. 2, 6, 31
- [28] S. H. Christiansen, J. Hu, and K. Hu. Nodal finite element de Rham complexes. *Numer. Math.*, 139(2):411–446, 2018. 15
- [29] P. G. Ciarlet, L. Gratie, and C. Mardare. Intrinsic methods in elasticity: a mathematical survey. *Discrete Contin. Dyn. Syst.*, 23(1-2):133–164, 2009. 2
- [30] M. Eastwood. A complex from linear elasticity. In *The Proceedings of the 19th Winter School “Geometry and Physics” (Srní, 1999)*, pages 23–29, 2000. 4, 10
- [31] M. D. Gunzburger. Navier-stokes equations for incompressible flows: finite-element methods. In *Handbook of computational fluid mechanics*, pages 99–157. Elsevier, 1996. 14
- [32] R. Hiptmair and J. Xu. Nodal auxiliary space preconditioning in $h(\text{curl})$ and $h(\text{div})$ spaces. *SIAM Journal on Numerical Analysis*, 45(6):2483–2509, 2007. 9
- [33] J. Hu and Y. Liang. Conforming discrete Gradgrad-complexes in three dimensions. *Math. Comp.*, 90(330):1637–1662, 2021. 2, 6, 29, 53
- [34] J. Hu, Y. Liang, and R. Ma. Conforming finite element divdiv complexes and the application for the linearized Einstein–Bianchi system. *SIAM J. Numer. Anal.*, 60(3):1307–1330, 2022. 2, 6, 37
- [35] J. Hu, Y. Liang, R. Ma, and M. Zhang. New conforming finite element divdiv complexes in three dimensions. *arXiv preprint arXiv:2204.07895*, 2022. 2, 6, 24, 28, 49
- [36] J. Hu, T. Lin, and Q. Wu. A construction of C^r conforming finite element spaces in any dimension. *Found. Comput. Math.*, <https://doi.org/10.1007/s10208-023-09627-6>, 2023. 2
- [37] J. Hu, R. Ma, and M. Zhang. A family of mixed finite elements for the biharmonic equations on triangular and tetrahedral grids. *Sci. China Math.*, 64(12):2793–2816, 2021. 2, 6, 24
- [38] J. Hu and S. Zhang. A family of symmetric mixed finite elements for linear elasticity on tetrahedral grids. *Sci. China Math.*, 58(2):297–307, 2015. 20, 21, 54
- [39] K. E. Iverson. A programming language. In *Proceedings of the May 1-3, 1962, spring joint computer conference*, pages 345–351, 1962. 5
- [40] C. Johnson and B. Mercier. Some equilibrium finite element methods for two-dimensional elasticity problems. *Numer. Math.*, 30(1):103–116, 1978. 2
- [41] M.-J. Lai and L. L. Schumaker. Trivariate C^r polynomial macroelements. *Constructive Approximation*, 26(1):11–28, 2007. 2
- [42] L. Li. *Regge Finite Elements with Applications in Solid Mechanics and Relativity*. PhD thesis, University of Minnesota, 2018. 2
- [43] M. Neilan. Discrete and conforming smooth de Rham complexes in three dimensions. *Math. Comp.*, 84(295):2059–2081, 2015. 14, 15
- [44] D. Pauly and W. Zulehner. The divDiv-complex and applications to biharmonic equations. *Appl. Anal.*, 99(9):1579–1630, 2020. 1, 9, 11
- [45] A. Pechstein and J. Schöberl. Tangential-displacement and normal-normal-stress continuous mixed finite elements for elasticity. *Math. Models Methods Appl. Sci.*, 21(8):1761–1782, 2011. 1
- [46] A. S. Pechstein and J. Schöberl. The TDNNs method for Reissner-Mindlin plates. *Numer. Math.*, 137(3):713–740, 2017. 1
- [47] V. Quenneville-Belair. *A New Approach to Finite Element Simulations of General Relativity*. ProQuest LLC, Ann Arbor, MI, 2015. Thesis (Ph.D.)—University of Minnesota. 1
- [48] R. Stenberg. A nonstandard mixed finite element family. *Numer. Math.*, 115(1):131–139, 2010. 18
- [49] N. Van Goethem. The non-Riemannian dislocated crystal: a tribute to Ekkehart Kröner (1919–2000). *J. Geom. Mech.*, 2(3):303–320, 2010. 2
- [50] A. Ženíšek. Interpolation polynomials on the triangle. *Numer. Math.*, 15:283–296, 1970. 2

- [51] A. Ženíšek. Tetrahedral finite $C^{(m)}$ -elements. *Acta Univ. Carolinae—Math. et Phys.*, 15(1-2):189–193, 1974. [2](#)
- [52] M. Wang and J. Xu. The Morley element for fourth order elliptic equations in any dimensions. *Numer. Math.*, 103(1):155–169, 2006. [2](#), [37](#)
- [53] M. Wang and J. Xu. Minimal finite element spaces for $2m$ -th-order partial differential equations in R^n . *Math. Comp.*, 82(281):25–43, 2013. [2](#), [37](#)
- [54] S. Wu and J. Xu. Nonconforming finite element spaces for $2m$ th order partial differential equations on \mathbb{R}^n simplicial grids when $m = n + 1$. *Math. Comp.*, 88(316):531–551, 2019. [2](#)
- [55] S. Zhang. A family of 3D continuously differentiable finite elements on tetrahedral grids. *Appl. Numer. Math.*, 59(1):219–233, 2009. [2](#)
- [56] S. Zhang. A family of differentiable finite elements on simplicial grids in four space dimensions. *Math. Numer. Sin.*, 38(3):309–324, 2016. [2](#)

DEPARTMENT OF MATHEMATICS, UNIVERSITY OF CALIFORNIA AT IRVINE, IRVINE, CA 92697, USA
Email address: chenlong@math.uci.edu

SCHOOL OF MATHEMATICS, SHANGHAI UNIVERSITY OF FINANCE AND ECONOMICS, SHANGHAI 200433, CHINA
Email address: huang.xuehai@sufe.edu.cn